

# Performance-Based Specifications of Fiber-Reinforced Concrete with Adapted Rheology to Enhance Performance and Reduce Steel-Reinforcement in Structural Members



June 2020  
Final Report

Project number TR201806  
MoDOT Research Report number cmr 20-006

## PREPARED BY:

Kamal H. Khayat, PhD, P.Eng.

Missouri University of Science and Technology

## PREPARED FOR:

Missouri Department of Transportation

Construction and Materials Division, Research Section

## TECHNICAL REPORT DOCUMENTATION PAGE

<b>1. Report No.</b> cmr 20-006	<b>2. Government Accession No.</b>	<b>3. Recipient's Catalog No.</b>	
<b>4. Title and Subtitle</b> Performance-Based Specifications of Fiber-Reinforced Concrete with Adapted Rheology to Enhance Performance and Reduce Steel-Reinforcement in Structural Members		<b>5. Report Date</b> May May 2020 Published: June 2020	
		<b>6. Performing Organization Code</b>	
<b>7. Author(s)</b> Kamal H. Khayat, PhD, P.Eng. <a href="http://orcid.org/0000-0003-1431-0715">http://orcid.org/0000-0003-1431-0715</a>		<b>8. Performing Organization Report No.</b> Project #00061652	
<b>9. Performing Organization Name and Address</b> Center for Transportation Infrastructure and Safety/NUTC Program Missouri University of Science and Technology 220 Engineering Research Lab 500 W. 16 <sup>th</sup> St. Rolla, MO 65409		<b>10. Work Unit No.</b>	
		<b>11. Contract or Grant No.</b> MoDOT project # TR201806	
<b>12. Sponsoring Agency Name and Address</b> Missouri Department of Transportation (SPR-B) Construction and Materials Division P.O. Box 270 Jefferson City, MO 65102		<b>13. Type of Report and Period Covered</b> Final Report (December 1, 2017-May 1, 2020)	
		<b>14. Sponsoring Agency Code</b>	
<b>15. Supplementary Notes</b> Conducted in cooperation with the U.S. Department of Transportation, Federal Highway Administration. MoDOT research reports are available in the Innovation Library at <a href="https://www.modot.org/research-publications">https://www.modot.org/research-publications</a> .			
<b>16. Abstract</b> The main objective of this research is to propose novel materials for the construction and retrofitting of bridges, including Economical Crack-Free High-Performance Concrete (Eco-Bridge-Crete, or EBC) and Fiber-Reinforced Super-Workable Concrete (FR-SWC). The project seeks to optimize the coupled effect of fiber characteristics, expansive agent (EA), saturated lightweight sand (LWS), and external moist curing on mechanical properties, shrinkage, and corrosion resistance of such classes of high-performance concrete. The project also aims to replace steel reinforcement in flexural members with steel fibers partially. In Task I, Eco-Bridge-Crete mixture design was optimized to reduce drying and restrained expansion and secure high mechanical properties. Eco-Bridge-Crete mixtures were optimized using various shrinkage mitigating strategies, including the use of different contents of CaO-based EA, LWS, and steel fibers as well as different moist curing conditions. The study revealed some synergistic effects among the EA, LWS, and fiber contents and external curing that led to lower shrinkage and restrained expansion and greater strength. The combined use of EA, along with LWS, was shown to reduce concrete conductivity and improve corrosion resistance. Overall, the use of synthetic fibers, EA along with LWS, increased moist curing duration, and concrete cover depth was identified as suitable strategies for improving the corrosion resistance of Eco-Bridge-Crete mixtures. In Task II, the structural performance of reinforced concrete beams cast with FR-SWC mixtures made with different fiber types and reinforcing steel densities was evaluated. The testing involved casting of beam elements with different steel reinforcement densities (0.4 to 0.8 in.2 of steel area in the tension zone).			
<b>17. Key Words</b> Bridge; Cracking; Corrosion resistance; Durability; Eco-Bridge-Crete; Expansive admixture; Flexural strength; Shrinkage; Steel reinforcement; Structural performance		<b>18. Distribution Statement</b> No restrictions. This document is available through the National Technical Information Service, Springfield, VA 22161.	
<b>19. Security Classif. (of this report)</b> Unclassified.	<b>20. Security Classif. (of this page)</b> Unclassified.	<b>21. No. of Pages</b> 147	<b>22. Price</b>

**Performance-Based Specifications of Fiber-Reinforced Concrete  
with Adapted Rheology to Enhance Performance and Reduce  
Steel-Reinforcement in Structural Members**

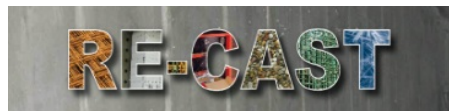
Project Number: TR201806

Final Report

Investigator

Dr. Kamal H. Khayat, Professor, P.Eng., Missouri S&T

May 2020



## **COPYRIGHT**

Authors herein are responsible for the authenticity of their materials and for obtaining written permissions from publishers or individuals who own the copyright to any previously published or copyrighted material used herein.

## **DISCLAIMER**

The opinions, findings, and conclusions expressed in this document are those of the investigators. They are not necessarily those of the Missouri Department of Transportation, U.S. Department of Transportation, or Federal Highway Administration. This information does not constitute a standard or specification.

## **ACKNOWLEDGMENTS**

The authors would like to acknowledge the many individuals and organizations that made this research project possible. First and foremost, the author would like to acknowledge the financial support of the Missouri Department of Transportation (MoDOT) as well as the RE-CAST (Research on Concrete Applications for Sustainable Transportation) Tier-1 University Transportation Center (UTC) at Missouri University of Science and Technology (Missouri S&T). The author would like to acknowledge the valuable cooperation of the following individuals for their great help in conducting the experimental work: Kavya Vallurupalli, Kamran Aghae, Jingjie Wei, and Yucun Gu (Ph.D. students), as well as Dr. Ahmed Abdelrazik (post-doctoral fellow). The support of Dr. Nima Farzadnia, Research Engineer of the Center for Infrastructure Engineering Studies (CIES) and Jason Cox, Senior Research Specialist at the CIES, is greatly appreciated.

## ABSTRACT

The main objective of this research is to propose novel materials for the construction and retrofitting of bridges, including Economical Crack-Free High-Performance Concrete (Eco-Bridge-Crete, or EBC) and Fiber-Reinforced Super-Workable Concrete (FR-SWC). The project seeks to optimize the coupled effect of fiber characteristics, expansive agent (EA), saturated lightweight sand (LWS), and external moist curing on mechanical properties, shrinkage, and corrosion resistance of such classes of high-performance concrete. The project also aims to replace steel reinforcement in flexural members with steel fibers partially.

In Task I, Eco-Bridge-Crete mixture design was optimized to reduce drying and restrained expansion and secure high mechanical properties. Eco-Bridge-Crete mixtures were optimized using various shrinkage mitigating strategies, including the use of different contents of CaO-based EA, LWS, and steel fibers as well as different moist curing conditions. The study revealed some synergistic effects among the EA, LWS, and fiber contents and external curing that led to lower shrinkage and restrained expansion and greater strength. A statistical factorial design was employed to prepare 25 concrete mixtures to derive statistical models to predict the performance of Eco-Bridge-Crete given key input factors that included the EA, LWS, and fiber contents and moist curing duration. The modeled response parameters included drying shrinkage, restrained expansion, and compressive and flexural strengths. Optimized Eco-Bridge-Crete mixtures exhibited low drying shrinkage of 300  $\mu$ strain after 16 weeks (112 days) of drying. A total of 16 mixtures were prepared to evaluate the synergistic effect of LWS, EA, and fiber (steel and synthetic) on the viscoelastic properties of Eco-Bridge-Crete and FR-SWC. Selected Eco-Bridge-Crete mixtures were also used to evaluate the corrosion resistance of Eco-Bridge-Crete prepared with steel and synthetic fibers. Eight beam specimens with reinforcing bars embedded

at cover depths of 1, 1.5, and 2 in. were tested for corrosion resistance. The samples were prepared with 1 and 7 days of moist curing. The concrete was also tested to determine sorptivity and bulk resistivity. The combined use of EA, along with LWS, was shown to reduce concrete conductivity and improve corrosion resistance. The optimized Eco-Bridge-Crete containing a ternary combination of 5% EA and 25% LWS replacements and 0.5% steel fibers developed significantly higher corrosion resistance compared to the FRC with only EA or LWS. Overall, the use of synthetic fibers, EA along with LWS, increased moist curing duration, and concrete cover depth was identified as suitable strategies for improving the corrosion resistance of Eco-Bridge-Crete mixtures.

In Task II, the structural performance of reinforced concrete beams cast with FR-SWC mixtures made with different fiber types and reinforcing steel densities was evaluated. The testing involved casting of beam elements with different steel reinforcement densities (0.4 to 0.8 in.<sup>2</sup> of steel area in the tension zone). FR-SWC beams made with double hooked-end macro fibers (5D) showed significant savings of up to 60%, 40%, and 25% when considering design criteria dealing with maximum crack width, allowable deflection, and ultimate load, respectively. The optimized FR-SWC beams made with micro-macro steel fibers showed significant savings up to 70% of the steel reinforcing bars when considering the maximum crack width design criteria.

**Keywords:** Bridge; Cracking; Corrosion resistance; Durability; Eco-Bridge-Crete; Expansive admixture; Flexural strength; Shrinkage; Steel reinforcement; Structural performance

## EXECUTIVE SUMMARY

This research project was undertaken to enhance the performance of a novel class of fiber-reinforced concrete (FRC) that can be used for infrastructure construction, namely Economical and Crack-Free High-Performance Concrete (Eco-Bridge-Crete, or EBC) for bridge deck construction and replacement as well as Fiber-Reinforced Super-Workable Concrete (FR-SWC) that can be used for the infrastructure construction. The project is a continuation of the MoDOT/RE-CAST TR2015-03 entitled “*Economical and Crack-Free High-Performance Concrete for Pavement and Transportation Infrastructure Construction*” and MoDOT/RE-CAST TR2015-05 entitled “*Performance of Fiber-Reinforced Self-Consolidating Concrete (FR-SCC) for Repair of Bridge Sub-Structures and Fiber-Reinforced Super-Workable Concrete (FR-SWC) for Infrastructure Construction*” that were completed by the principal investigator and his team at Missouri S&T. The performance-based specifications proposed for the FR-SWC and Eco-Bridge-Crete that were further developed in this project are summarized in **Table 1**.

**Table 1 – Performance-based specifications for FR-SWC and Eco-Bridge-Crete**

Fiber-Reinforced Super-Workable Concrete	
Slump flow	$22 \pm 2$ in.
Modified J-Ring diameter (diameter/height, D/a)	$20 \pm 2$ in. (> 12)
Compressive strength at 56 days (continuous moist curing)	$\geq 6000$ psi
Drying shrinkage after 120 days (28 days of moist curing)	$\leq 500$ $\mu$ strain
Durability (corrosion, frost durability)	High
Eco-Bridge-Crete	
Binder content	$\leq 590$ lb/yd <sup>3</sup>
Slump (without fibers)	$4 \pm 1$ in.
Slump (with fibers)	$7 \pm 1$ in.
Compressive strength at 56 days (continuous moist curing)	$\geq 5000$ psi
Drying shrinkage after 120 days (7 days of moist curing)	$\leq 350$ $\mu$ strain
Durability (corrosion, frost and abrasion resistance)	High

The Eco-Bridge-Crete and FR-SWC mixtures were further optimized to reduce shrinkage and increase tensile strength and ductility. The investigation involved the evaluation of the benefits of using saturated lightweight sand (LWS) for internal curing, expansive agent (EA) for shrinkage compensation, and fibers to reduce shrinkage and enhance strength and corrosion resistance of reinforcing bars of structural concrete that can be used in bridge construction and rehabilitation. The project also aimed to partially replace steel reinforcement in structural beams with steel fibers.

The project comprised of two main tasks: Task-I) optimization for Eco-Bridge-Crete and FR-SWC; and Task II) structural performance of FR-SWC made with different fiber types and reinforcing steel densities. A brief description of the experimental and key findings is presented below.

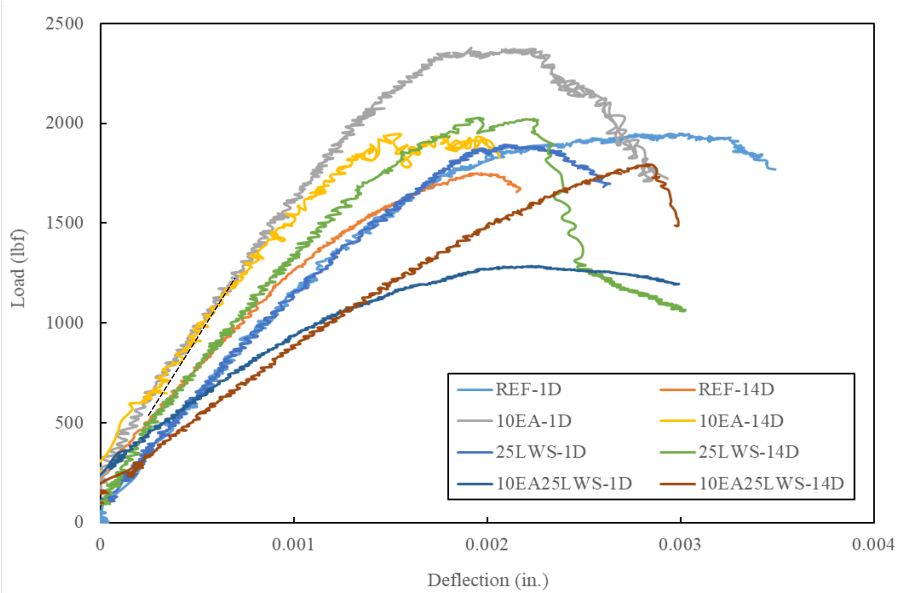
## **Task I: Materials performance optimization for Eco-Bridge-Crete and FR-SWC**

### ***Task I-A: Optimization for Eco-Bridge-Crete and FR-SWC***

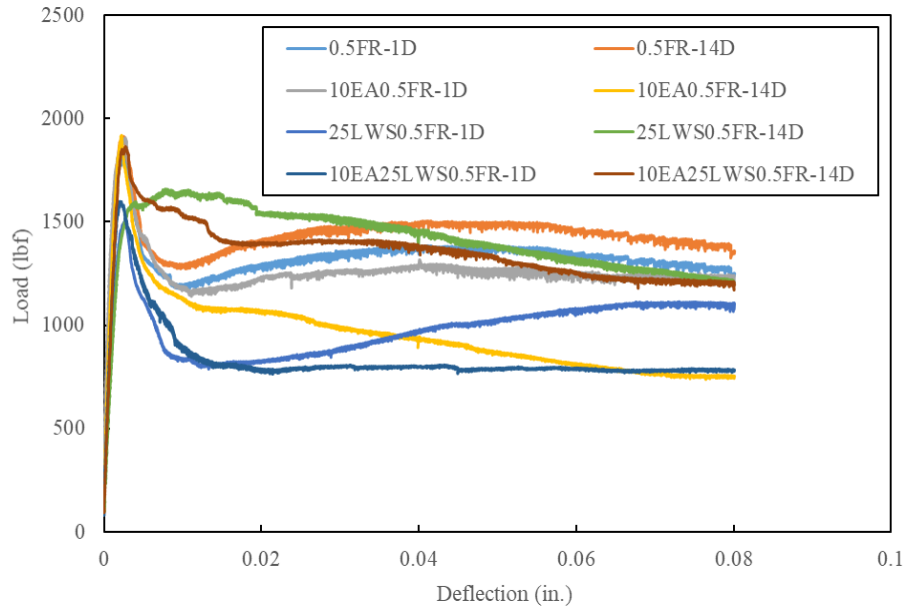
In this task, a factorial design approach was employed to quantify the effect of different test parameters on the performance of a reference Eco-Bridge-Crete that was designed to meet the performance criteria elaborated in **Table 1**. In total, 25 mixtures were prepared, including 16 mixtures to establish the factorial design, four central point mixtures, and five validation mixtures. Statistical models were developed to predict the performance of the reference Eco-Bridge-Crete, given the contents of EA, LWS, and steel fiber and the duration of moist curing. The modeled responses included compressive and flexural strengths, drying shrinkage, and restrained expansion.



**Figure 1** illustrates some of the 25 mixtures used to develop the statistical models. The figure shows the variations of flexural load vs. deflection of selected Eco-Bridge-Crete mixtures made with and without fibers and to 1 and 14 days of moist curing. The results show the high ductility of the FRC (**Figure 1-b**) compared to the mixture made without any fibers (**Figure 1-a**).



(a)



(b)

**Figure 1 – Load vs. deflection curve of Eco-Bridge-Crete subjected to 1 and 14 days of moist curing and made a) without fibers, and b) with fibers**

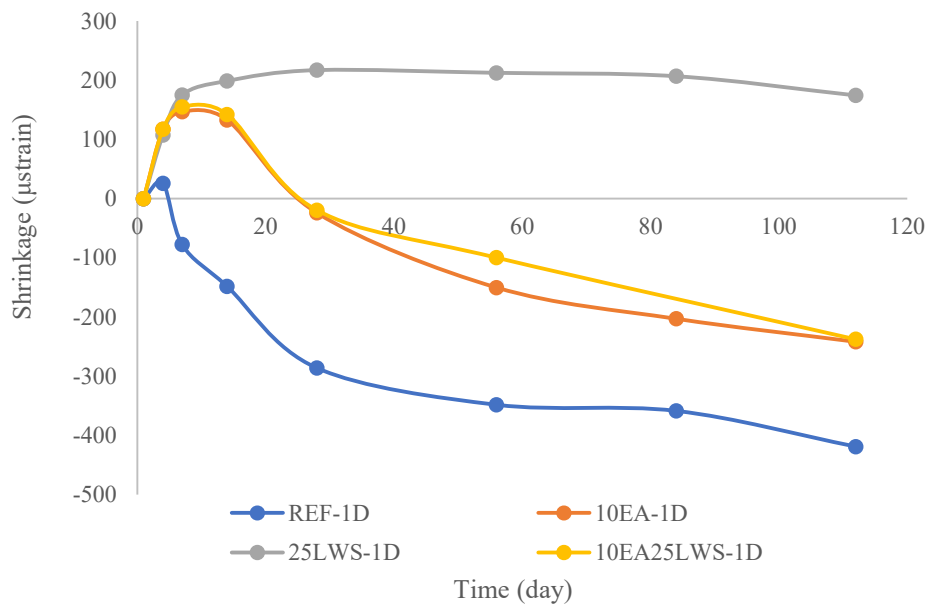
**Note:** Mixtures are denoted by EA, LWS, and FR content (10EA25LWS0.5FR refers to 10% EA, by binder mass, 25% LWS, by sand volume, and 0.5% fiber volume).

As noted in **Figure 1-a**, the flexural strength of the non-FRC containing 10% EA or 25% LWS can be 17% and 23%, respectively, greater than the reference mixture made without any EA or LWS. **Figure 1-b** shows that the inclusion of fibers and extension in moist curing from 1 to 14 days increased the flexural strength. The residual strengths at L/600 and L/150 varied from 335 to 1515 psi and 310 to 1180 psi, respectively. The maximum residual strength was obtained by the 25LWS0.5FR-14D mixture that was 270% greater than the non-FRC subjected to 1-day moist curing (REF-1D), and 140% more than the reference FRC with 14 days of moist curing (0.5FR-14D). This improvement highlights the importance of curing that can enhance the bond with fibers and hence flexural performance.

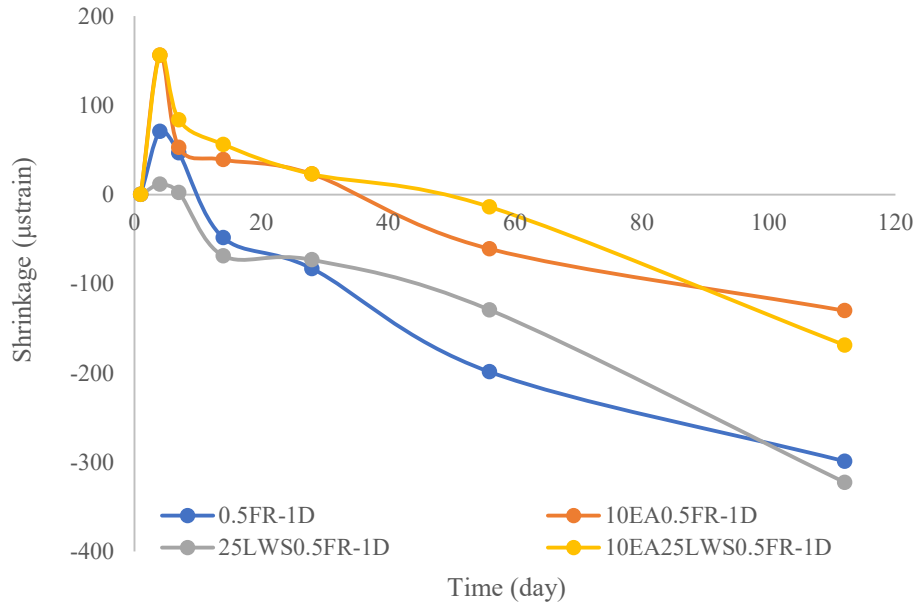
**Figure 2** compares the drying shrinkage of selected mixtures made with and without steel fibers. The results show that the addition of 10% EA increased the early expansion of the non-FRC by

up to 465%. This initial expansion resulted in a shrinkage reduction of 180  $\mu$ strain at 112 days. The best performance was secured by the 25LWS-1D mixture made with 25% LWS. In this case, the internal curing significantly reduced shrinkage where following early expansion, almost no shrinkage was recorded (i.e., complete shrinkage compensation). According to **Figure 2-b**, the addition of 0.5% of steel fibers restricted the initial expansion and final shrinkage by 26% and 23%, respectively. Favorable shrinkage mitigation can be achieved using 10% EA in addition to 0.5% steel fibers.

Data from the 25 investigated Eco-Bridge-Crete mixtures were used to derive statistical models to predict the performance of the concrete given four key input factors that can affect shrinkage and mechanical properties: EA, LWS, and fiber contents and duration of moist curing. The derived models are reported in **Table 2**. The statistical models are interpreted by illustrating trade-offs among the four input factors on the modeled responses.



(a)



(b)

**Figure 2 – Shrinkage of a) non-fiber and b) fiber-reinforced Eco-Bridge-Crete mixtures subjected to 1-day moist curing**

Figures 3 and 4 show contour diagrams of the variations of the 56-day compressive and flexural strengths and 56-day drying shrinkage and restrained expansion. The combined use of EA, LWS, and fiber is shown to increase flexural strength by as much as 35%. The curing duration is shown to have the most significant influence on reducing shrinkage, while the LWS and EA contents can significantly reduce shrinkage.

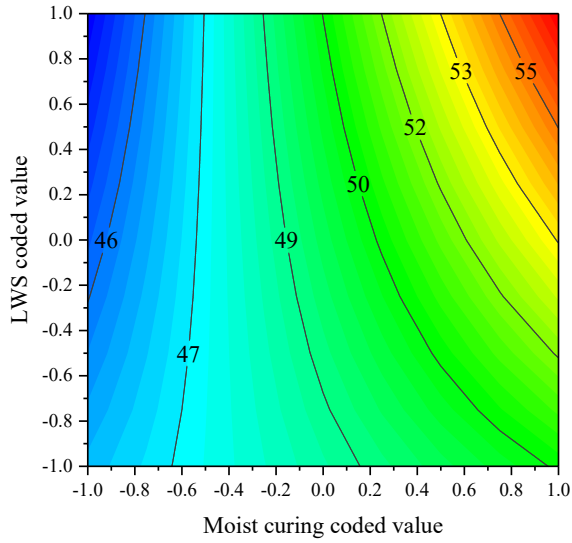
The analysis of the contour diagrams indicates a substantial benefit/collective role of internal and external curing on the mitigation of drying shrinkage and restrained expansion. For example, Figure 4-a shows that the increase in LWS from coded values of -1 to +1 (0 to 25%) in concrete subjected to a moist curing duration of -0.6 (approximately 3.5 days) can lead to shrinkage reduction of 145 µstrain after 56 days; the latter value corresponds to no net drying shrinkage after 56 days due to the initial expansion and shrinkage compensation effect of the EA.

The increase in fiber content from coded values of -1 to +1 (0 to 0.5%) is also shown increase the 56-day flexural strength from 6.5 to 8.4 MPa (940 to 1235 psi) for concrete made with LWS coded value of -0.5 (approximately 6%), and EA and MC coded values of 0 (6% and 7.5 days, respectively).

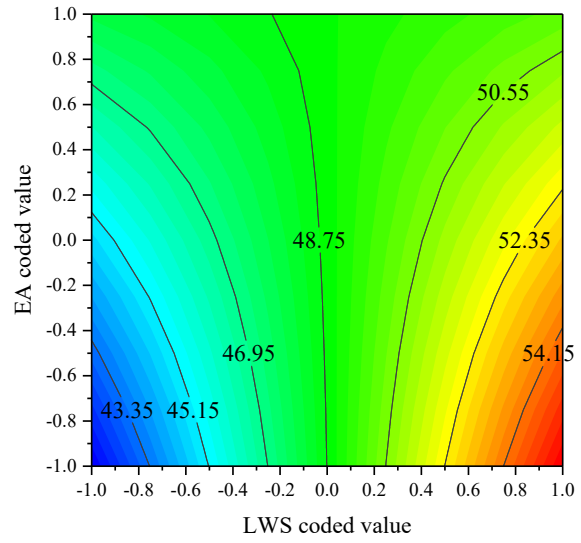
**Table 2 – Derived statistical models**

Parameters and interactions	28-day compressive, MPa	56-day compressive, MPa	56-day flexural, MPa	7-day shrinkage, $\mu$ strain	56-day shrinkage, $\mu$ strain	7-day expansion, $\mu$ strain	56-day expansion, $\mu$ strain
Intercept	44.15	42.88	7.96	112.2	-30.8	60.7	-12.4
EA	-2.98	-2.13	1.18	27.1	-	15.6	-
LWS	-8.91	-3.94	0.54	20.8	73.4	-	27.8
MC	7.95	3.89	-	38.9	66.5	21.0	40.9
Fiber	-6.93	-2.11	1.08	-	-	-	-
EA*LWS	-	-	-0.94	-	-62.8	-	-25.5
EA*MC	-	-	-	-	-	-9.6	-
LWS*MC	-	-	-	-	-	-	16.1
EA*Fiber	-	2.05	-	-	37.7	-11.0	-
LWS*Fiber	-3.19	-1.79	-0.9	-	-44.9	-13.9	-26.4
EA*LWS*Fiber	5.08	3.6	-2.0	29.5	-50.4	19.5	-26.4
LWS*MC*Fiber	-	-2.03	-	-	-	-	-

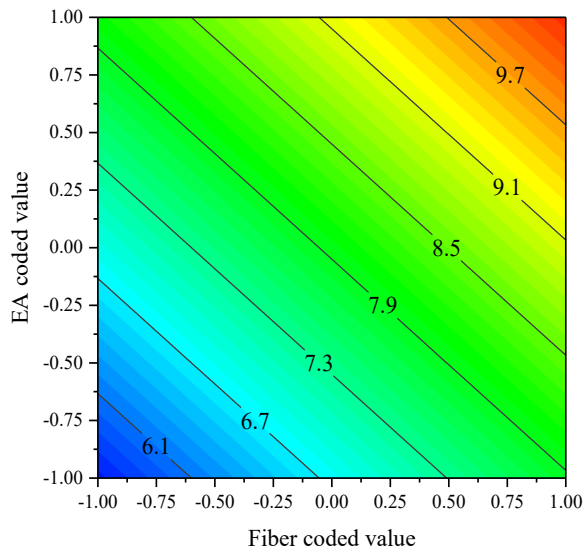
**Note:** (-) denotes that the effect of parameter is less or not significant. 1MPa = 145 psi.



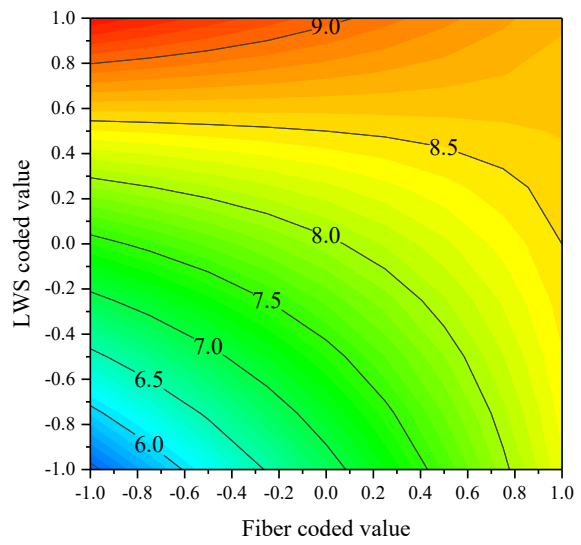
(a) EA and Fiber coded values as -1, -1



(b) Fiber and MC coded values as -1, 1

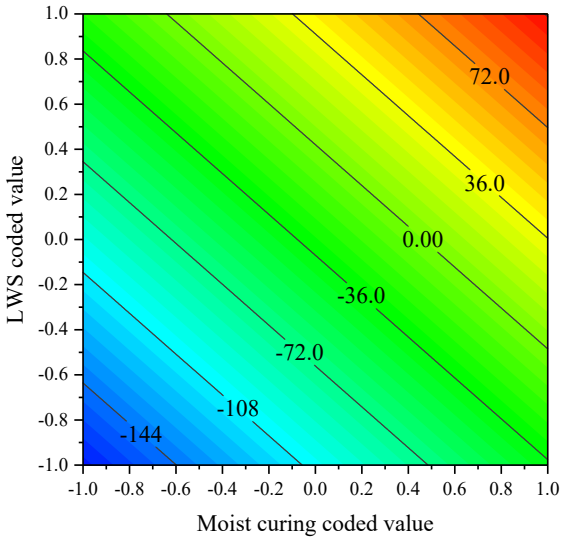


(c) LWS and MC coded values as 0, 0

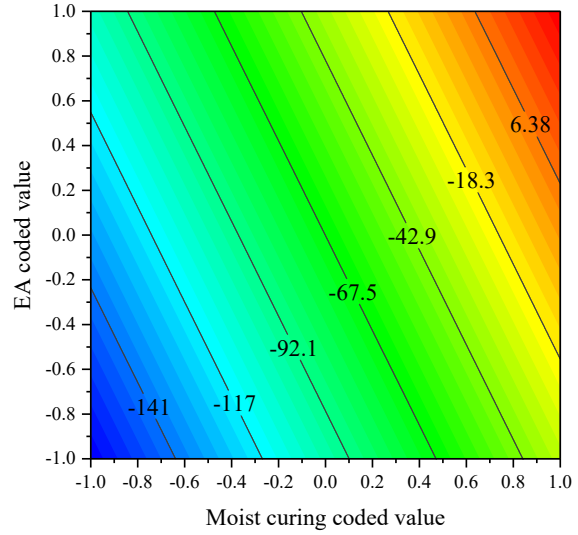


(d) EA and MC coded values as 0, 0

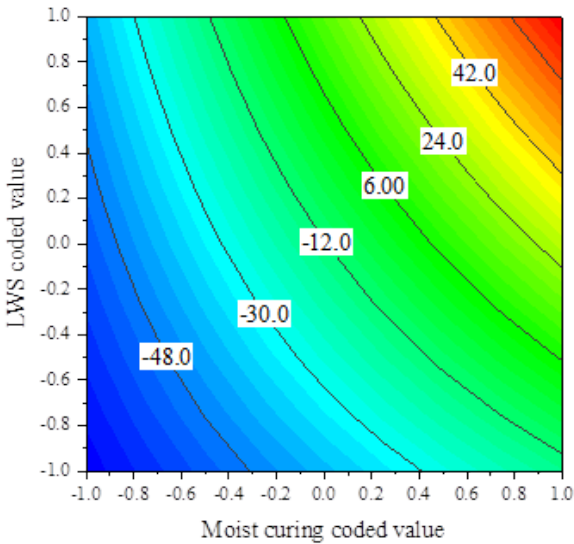
**Figure 3 – Contour diagrams of effects of EA, LWS, moist curing (MC) and Fiber content on 56-day compressive strength (a) and (b), 56-day flexural strength (c) and (d)**



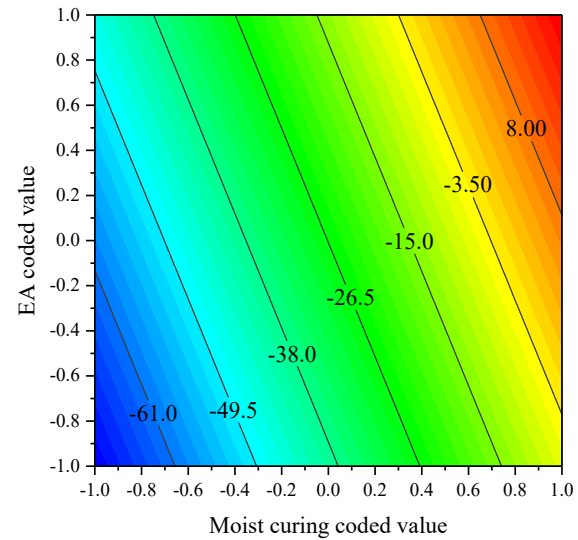
(a) EA, Fiber coded values as 0, 0



(b) LWS and Fiber coded values as -0.5, 0



(c) EA and Fiber coded values as 0, 0



(d) LWS and Fiber coded values as -0.5, 0

**Figure 4 – Contour diagrams of effects of EA, LWS, moist curing (MC) and Fiber content on 56-day drying shrinkage (a) and (b), 56-day restrained expansion (c) and (d)**

***Task I-B: Viscoelastic properties of FR-SWC and Eco-Bridge-Crete mixtures made with different fibers and shrinkage mitigating strategies***

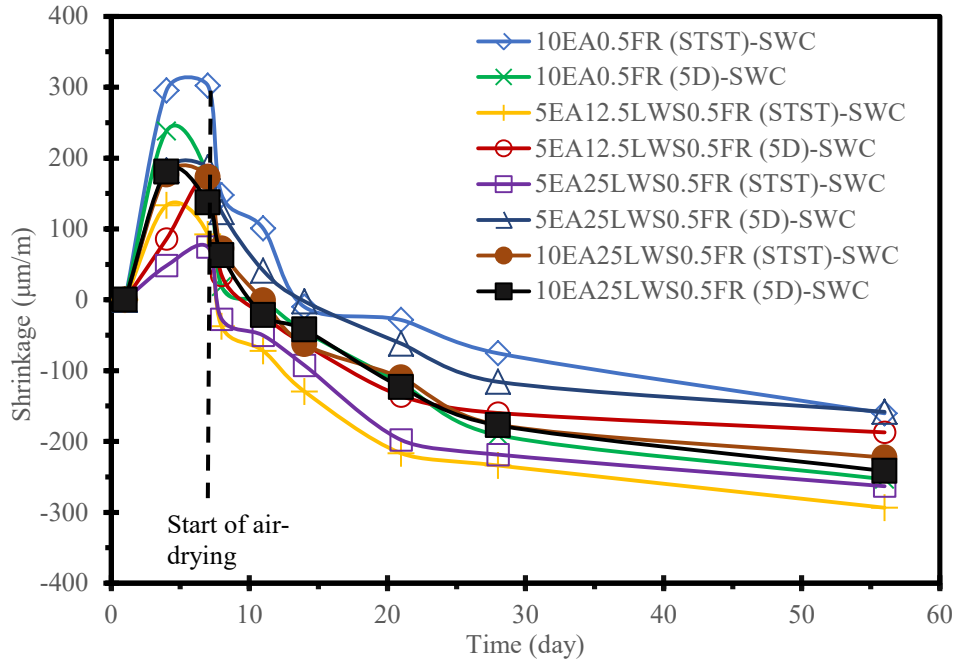
Four optimized EA-LWS-fiber systems having high overall desirability values based on the synergetic effects of the four input factors were selected from Task I-A to evaluate the performance of Eco-Bridge-Crete as well as FR-SWC that were recommended in MoDOT/RE-

CAST TR2015-03 and TR2015-05, respectively. The mixtures were prepared with two types of steel fibers and one type of synthetic fiber. The fibers included macro hooked-end steel fibers (ST), micro straight steel fibers, macro 5D steel fibers with double hooked ends, and polyethylene blend synthetic fibers (PLP). The synthetic fibers and macro hooked-end steel fibers were incorporated in the Eco-Bridge-Crete mixtures. A hybrid system of micro-macro steel fibers (STST) and the 5D steel fibers (5D) were used for the FR-SWC mixtures.

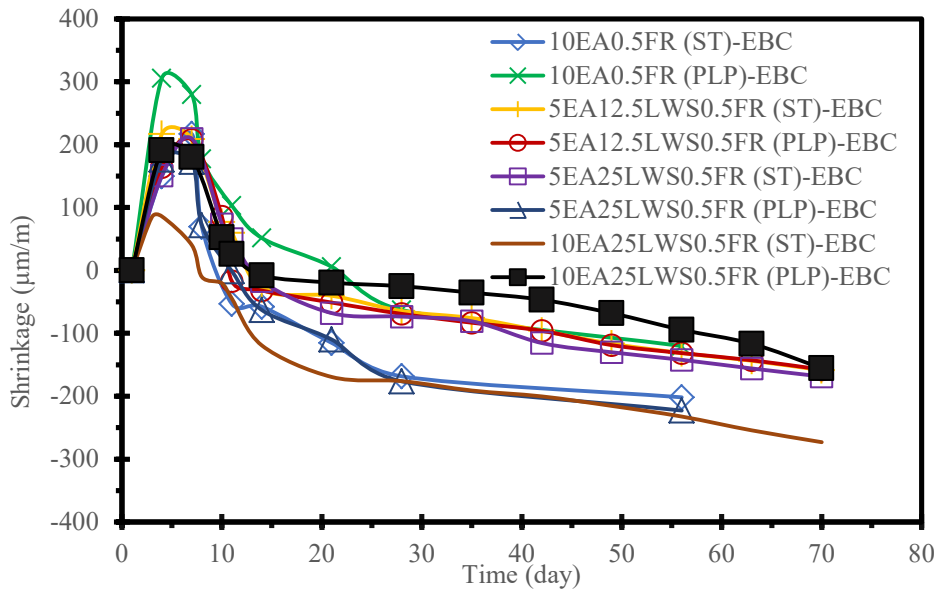
The mixtures were evaluated to determine their workability (unit weight, air content, slump, slump flow, passing ability [modified J-Ring test], and stability [surface settlement test]), drying shrinkage, and restrained expansion. All of the investigated mixtures had adequate workability, including high passing ability and resistance to the surface settlement of the FR-SWC. The results showed that the synergetic effect of the combination of shrinkage reducing materials, including LWS and EA, coupled with fibers, was useful in reducing shrinkage.

**Figure 5** shows the drying shrinkage of the FR-SWC and EBC mixtures made with 0.5% STST and 5D steel fibers, and ST and PLP fibers, respectively. The mixtures made with EA exhibited initial expansion. For the FR-SWC mixtures, the maximum early expansion was obtained by the mixtures containing 10% EA (10EA0.5FR (STST)-SWC and 10EA0.5FR (5D)-SWC). The lowest drying shrinkage was recorded by the 5EA25LWS0.5FR (5D)-SWC mixture. The incorporation of the 5D fibers reduced the drying shrinkage by 45% at 56 days compared with the counterpart mixtures made with the STST fibers. This reflects the effectiveness of the higher content of LWS in extending cement hydration and possibly the better performance of the 5D fibers in inhibiting drying shrinkage of the FR-SWC.





a) FR-SWC mixtures with 0.5% STST and 5D



b) Eco-Bridge-Crete mixtures with 0.5% PLP and ST

**Figure 5 – Drying shrinkage of FR-SWC and EBC mixtures**

For the EBC mixtures, the maximum early expansion was obtained by mixtures containing 10% EA (10EA0.5FR (PLP)-EBC). The lowest shrinkage was recorded by the 10EA25LWS0.5FR

(PLP)-EBC mixture. The incorporation of the PLP fibers reduced drying shrinkage by 55% at 70 days, as compared with the counterpart mixtures with the ST fibers. This shows the effectiveness of the PLP fibers in inhibiting shrinkage of the FR-EBC.

Comparing to the drying shrinkage results with those of mechanical properties, it can be concluded that the synthetic PLP fibers were more effective in restraining drying shrinkage of the EBC mixtures, while the ST fibers improved the flexural properties significantly.

***Task I-C: Corrosion resistance of reinforcing bars of optimized Eco-Bridge-Crete***

In this task, Eco-Bridge-Crete mixtures were prepared with either synthetic or steel fibers to evaluate the corrosion resistance of reinforcing bars embedded at cover depths of 1, 1.5, and 2 inches. The investigated mixtures were selected to emphasize the influence of fiber type, moist curing type and duration, as well as the effect of EA and LWS on corrosion resistance. For each mixture, concrete samples measuring  $25 \times 8 \times 3.5$  in. were prepared with nine reinforcing bars embedded at different cover depths (three bars at each cover depth). The corrosion testing was conducted on the beam samples following 90 days of air drying. The time of cracking due to corrosion was identified as the time at which there was a considerable increment in electrical current. The time of cracking was used as an indicator of the corrosion resistance of the concrete. A lower electrical current was observed as the cover depth increased from 1 to 1.5 and 2 inches.

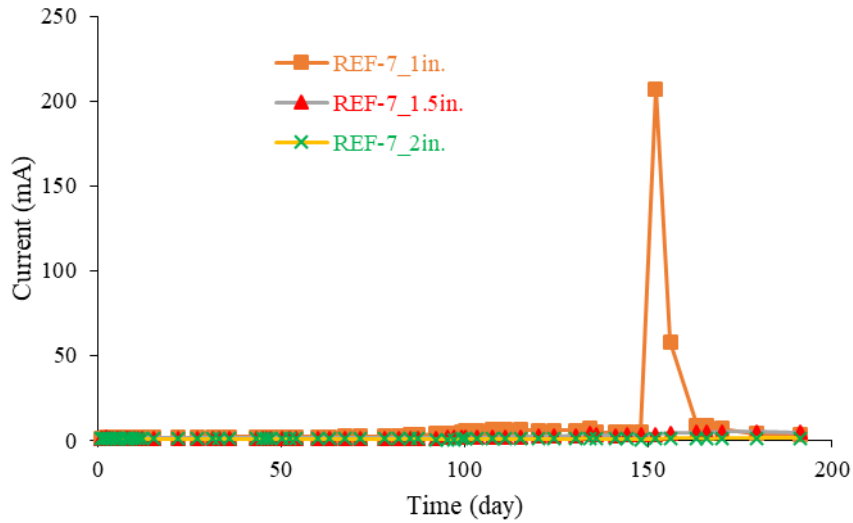
None of the investigated mixtures exhibited signs of corrosion when a sufficient cover of 2 in. was provided over the reinforcing bars. This was also the case for a cover of 1.5 in., in exception of the 5EA0.5FR-1 mixture. For beams with 1 in. cover, all of the eight tested mixtures exhibited a sudden increase in current during the 200-day test period. The two mixtures that had the shortest onset to corrosion were the 5EA0.5FR-1 and 25LWS0.5FR-1 mixtures, where the first

peak in current occurred after approximately 50 days. Both mixtures received only 1 day of moist curing, with the latter one also prepared with 25% of LWS.

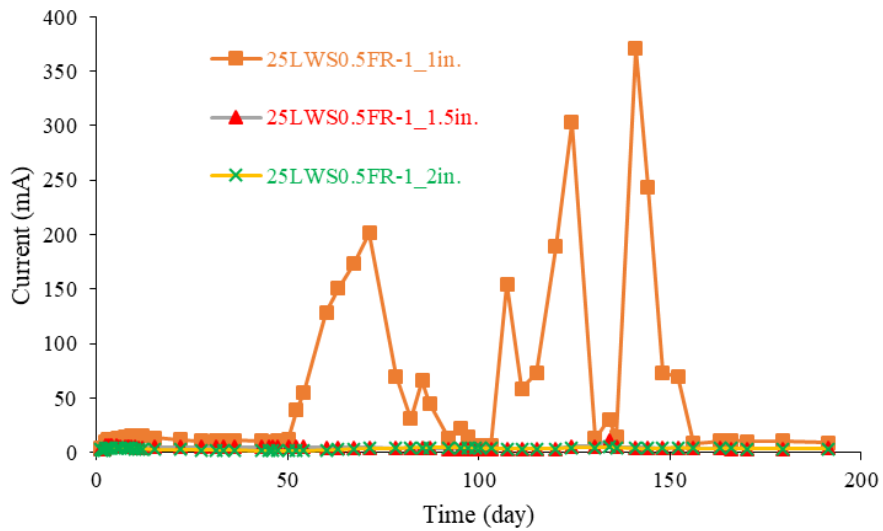
Typical variations in electrical current with time of testing (200 days) for reinforcing bars embedded a cover depth of 1 in. are shown in **Figure 6** for two of the investigated mixtures. The results show that the increase in electrical resistivity of the concrete with the increase in moisture-curing duration. The combined use of EA and LWS was more effective in improving corrosion resistance compared to the use of either the EA or LWS. The use of synthetic fibers instead of steel fibers, EA along with LWS, and increase in moist curing duration were found to be effective strategies for improving corrosion resistance of EBC mixtures. **Table 3** summarizes the overall effect of the investigated parameters on the corrosion resistance of the Eco-Bridge-Crete mixtures.

**Table 3 – Influence of investigated parameter on corrosion resistance**

Increase in parameter	Corrosion resistance	Comment
Cover depth	Increase	Increase in concrete electrical resistance
Moist curing duration	Increase	Decrease in capillary porosity
Use of fibers	Decrease with steel fibers No effect with synthetic fibers	Decrease as a result of fiber corrosion Synthetic fibers do not contribute to corrosion
LWS content	Increase	Decrease in capillary porosity Especially effective when used in combination with EA and fibers 7 days of moist curing without LWS led to higher corrosion resistance than 1 d of moist curing and 25% LWS
EA content	Increase/decrease	Increase when used in combination with LWS and fibers Decrease otherwise



(a)



(b)

**Figure 6 – Average current variations of reinforcing bars embedded at 1, 1.5, and 2 in. of cover depths for a) REF-7 and b) 25LWS0.5FR-1 mixtures**

**Task II: Structural performance of FR-SWC made with different fiber types and reinforcing steel densities**

In Task II, the structural performance of FR-SWC made with different steel fiber types was investigated to determine the potential savings of reinforcing steel due to the use of steel fibers.

Three types of steel fibers were used in this task: hooked-end fibers measuring 1.2 in. in length,

double hooked-end macro fibers (5D fiber) measuring 2.4 in. in length, and straight fibers measuring 0.5 in. in length. The testing involved the casting of reinforced concrete beam elements with areas of steel reinforcement varying between 0.4 and 0.8 in.<sup>2</sup> in the tension zone. In total, 10 reinforced concrete beams were cast to evaluate the flexural strength of optimized super workable concrete (SWC) made with and without fiber reinforcement. The beams measured 8 ft in length and 8 × 12 in. in cross-section. The results of the 10 beams were compared with the mean of six other beams cast in MoDOT/RE-CAST TR2015-05.

For beams made with the lower steel reinforcement, the combination of macro-micro steel fibers increased the ultimate load in a more significant way than in beams made with a higher level of reinforcing bars compared to beams made with the non-fibrous SWC and the same level of reinforcement. The ultimate loads for beams made with the lowest and highest steel reinforcement levels and macro-micro steel fibers were 25 and 41 kips, respectively, compared to 21 and 40 kips, respectively, for the non-fibrous SWC beams. The use of the 5D fibers, which has double hooked ends, increased the ultimate load significantly for beams made with both low and high areas of steel reinforcement compared to beams made with the non-fibrous SWC. The ultimate loads for the FR-SWC beams made with relatively low and high reinforcing steel and 5D fibers were 29 and 50 kip, respectively, compared to 21 and 40 kips, respectively, for the non-fibrous SWC beams.

The use of FR-SWC can lead to a potential saving in steel reinforcement.

**Figure 7** shows the load-crack width relationship of the investigated beams. The use of fibers had a significant effect on reducing crack width. The fibers helped increase the residual loads at small crack openings (<0.02 in.) and prevented a sudden increase in crack width and crack propagation beyond that limit compared to the non-fibrous SWC beams.

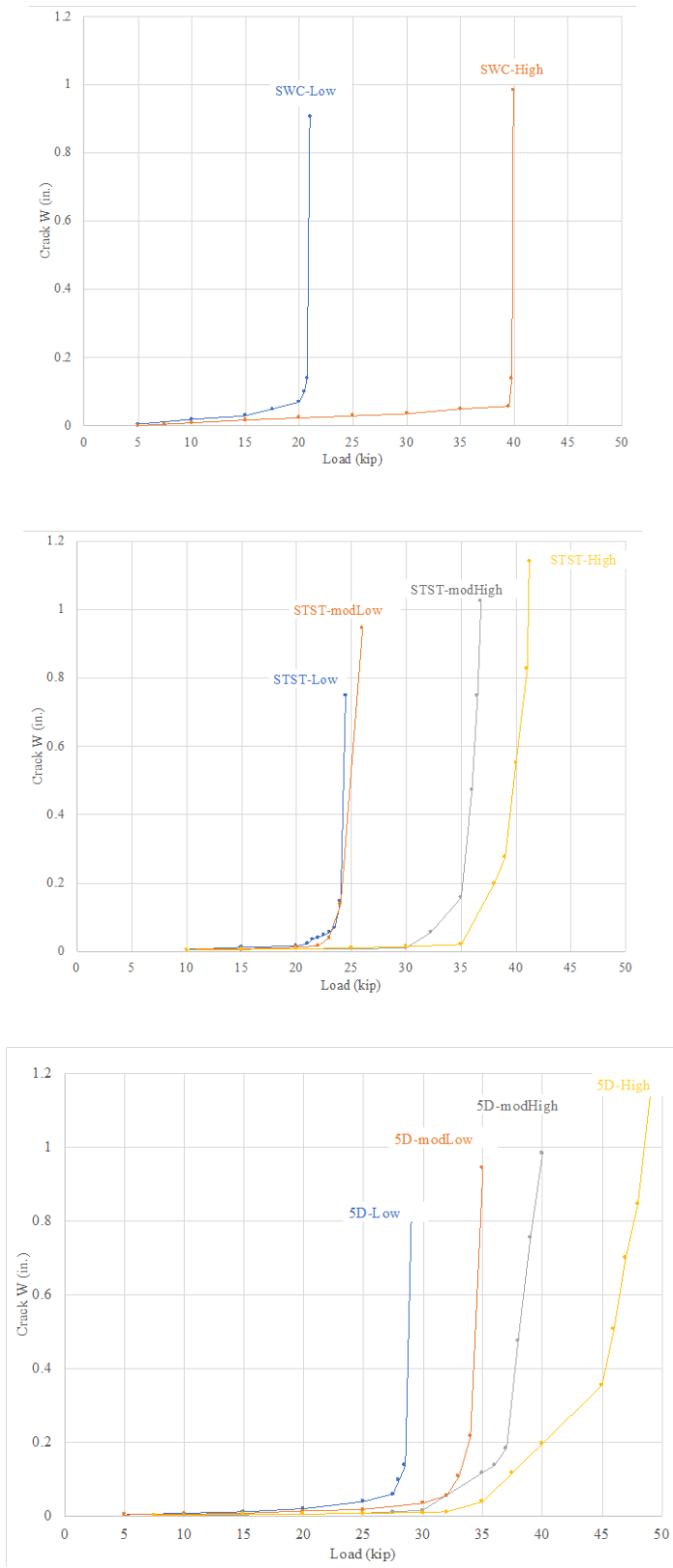


**Figure 7 – Load-crack width relationship for 10 tested beams (Low, modLow, modHigh, and High denote beams with 2 #4, 2 #4 + 1 #3, 2 #4 + 1 #5, and 1 #4 + 2 #5, respectively)**

For both the fibrous and non-fibrous SWC beams, the maximum crack width at failure was directly proportional to the reinforcing bar density, which indicates that replacing the number of steel bars with steel fibers can help in reducing crack width. For beams with low steel reinforcement, the crack width increased from 0.15 to 0.8 in. with an increase in loading from 23 to 25 kips for the FR-SWC beams made with STST fibers. Such increase was 26 to 28 kips for the beams made with 5D fibers.

**Figure 8** summarizes the savings that can be achieved with the use of FR-SWC compared to SWC in flexural elements given different design criteria. The optimized FR-SWC beams made with micro-macro steel fibers showed significant savings up to 70% of the steel reinforcing bars when considering the maximum crack width design criteria. Beams made with the 5D fibers showed significant savings of up to 60%, 40%, and 25% when considering design criteria dealing with maximum crack width, allowable deflection, and ultimate load, respectively.

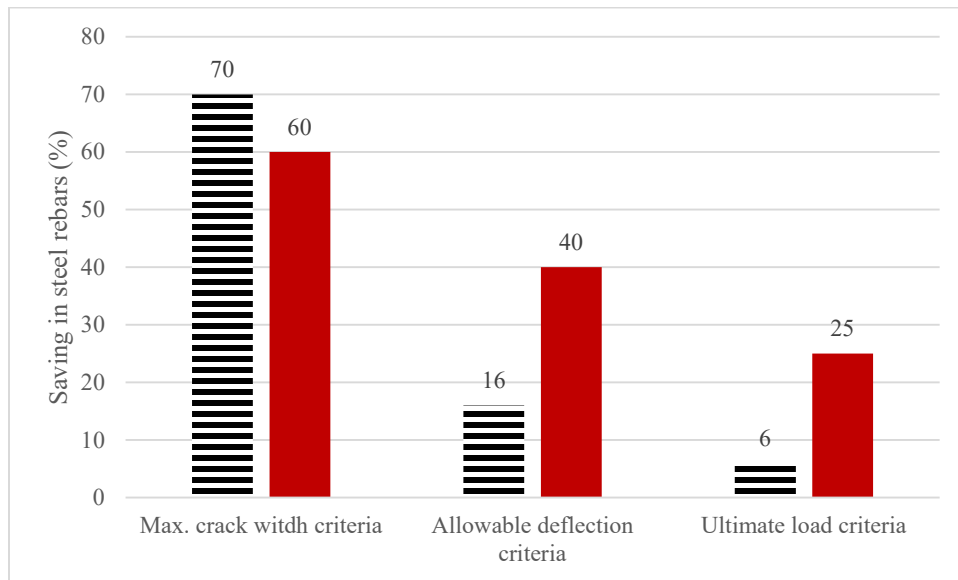


**Figure 8 – Savings in steel reinforcement bars with FR-SWC**

# CONTENTS

COPYRIGHT.....	iii
DISCLAIMER.....	iii
ACKNOWLEDGMENTS.....	iii
ABSTRACT.....	iv
EXECUTIVE SUMMARY.....	vi
CONTENTS.....	xxiii
LIST OF FIGURES.....	xxv
LIST OF TABLES.....	xxviii
1. INTRODUCTION.....	1
1.1 Problem statement.....	1
1.2 Research objectives.....	5
1.3 Research methodology.....	5
2. EXPERIMENTAL PROGRAM.....	8
2.1 Materials.....	8
2.1.1. Cementitious materials.....	8
2.1.2 Chemical admixtures.....	9
2.1.3. Aggregates.....	9
2.1.4. Fibers.....	10
2.2 Experimental program.....	11
2.2.1 Task I - Optimization for Eco-Bridge-Crete and FR-SWC.....	11
2.2.2 Task II: Structural performance of FR-SWC made with different fiber types and reinforcing steel densities.....	17
2.3 Mixing and test methods.....	19
2.3.1 Mixing procedure and curing – Task I: Optimization for Eco-Bridge-Crete and FR-SWC.....	19
2.3.2 Test methods - Task I: Optimization for Eco-Bridge-Crete and FR-SWC.....	20
2.3.3 Casting and curing of flexural reinforced concrete beams.....	28
2.3.4 Reinforced concrete beam testing.....	30
3. TEST RESULTS AND DISCUSSION.....	32
3.1 Task I: Optimization for Eco-Bridge-Crete and FR-SWC.....	32
3.1.1 Task I-A: Optimization for Eco-Bridge-Crete mixtures.....	32



3.1.2 Task I-B: Performance of selected FR-SWC and Eco-Bridge-Crete mixtures made with different fibers .....	53
3.1.3 Task I-C: Corrosion resistance of reinforcing bars of optimized Eco-Bridge-Crete....	58
3.2 Task II: Structural performance of FR-SWC made with different fiber types and reinforcing steel densities.....	69
<p>The work presented in this task involved the testing of 10 reinforced concrete beam elements cast with FR-SWC mixtures made with STST and 5D fibers that are elaborated in Table 1-1. The beams were cast with different densities of steel reinforcement to determine the potential savings of reinforcing steel due to fiber use, as elaborated in Figure 2-3. ....</p>	
3.2.1 Load-deflection and toughness analysis .....	70
3.2.2 Load-deflection curve analysis.....	70
3.2.3 Crack width analysis.....	73
3.2.4 Load and strength analysis .....	77
4. SUMMARY AND CONCLUSIONS.....	83
<p>Synergistic effect of LWS, EA, fiber, and moist curing on performance of Eco-Crete-Bridge .....</p>	
	83
<p>Viscoelastic properties of FR-SWC and Eco-Bridge-Crete mixtures made with different fibers and shrinkage mitigating strategies .....</p>	
	85
<p>Evaluation of corrosion resistance.....</p>	
	86
<p>Structural performance of Eco-Bridge-Crete .....</p>	
	87
REFERENCES .....	89
Appendix-A.....	92
Appendix-B.....	104
Appendix-C.....	110

## LIST OF FIGURES

Figure 1 – Load vs. deflection curve of Eco-Bridge-Crete subjected to 1 and 14 days of moist curing and made a) without fibers, and b) with fibers .....	ix
Figure 2 – Shrinkage of a) non-fiber and b) fiber-reinforced Eco-Bridge-Crete mixtures subjected to 1-day moist curing .....	xi
Figure 3 – Contour diagrams of effects of EA, LWS, moist curing (MC) and Fiber content on 56-day compressive strength (a) and (b), 56-day flexural strength (c) and (d).....	xiii
Figure 4 – Contour diagrams of effects of EA, LWS, moist curing (MC) and Fiber content on 56-day drying shrinkage (a) and (b), 56-day restrained expansion (c) and (d).....	xiv
Figure 5 – Drying shrinkage of FR-SWC and EBC mixtures .....	xvi
Figure 6 – Average current variations of reinforcing bars at 1, 1.5, and 2 in. of cover depths for a) REF-7 and b) 25LWS0.5FR-1 mixtures .....	xix
Figure 7 – Load-crack width relationship for 10 tested beams (Low, modLow, modHigh, and High denote beams with 2 #4, 2 #4 + 1 #3, 2 #4 + 1 #5, and 1 #4 + 2 #5, respectively) .....	xxi
Figure 8 – Savings in steel reinforcement bars with FR-SWC .....	xxii
Figure 1-1 – Field implementation of flowable FRC with adapted rheology for construction of a bridge deck near Taos, Missouri .....	1
Figure 2-1 Particle size distribution of cementitious materials ( $\mu\text{m}$ ) .....	8
Figure 2-2 – Aggregate grain size distribution .....	10
Figure 2-3 – Flexural testing of full-scale monolithic beams .....	18
Figure 2-4 – (a) J-Ring test and (b) surface settlement test .....	20
Figure 2-5 – Test setup for compressive strength .....	21
Figure 2-6 – Test setup for flexural strength measurement of beam specimens .....	22
Figure 2-7 – Drying shrinkage measurement (a) drying shrinkage and (b) restrained expansion .....	22
Figure 2-8 – Schematic of the test setup for measuring the corrosion resistance of embedded reinforcing bar in concrete .....	23
Figure 2-9 – Custom made corrosion test sample molds with epoxy-coated bars at ends .....	25
Figure 2-10 – Dimensions of the concrete samples for the corrosion test.....	25
Figure 2-11 – Corrosion test setup: a) placement of samples to form a sealed salt tank, and b) stainless-steel mesh cut and weaved with tinned Cu wire .....	26
Figure 2-12 – Four panels each with 5 V power supply and 1 $\Omega$ shunt resistors .....	27
Figure 2-13 – Testing apparatus for bulk resistivity (right) and sorptivity (right) .....	27
Figure 2-14 – Four reinforcing bar configurations .....	28
Figure 2-15 – Strain gauges attached at the middle of the bottom reinforcing bars .....	29
Figure 2-16 – Formwork and cast beams.....	30
Figure 2-17 – Curing of beams and cylinders and occupying samples .....	30
Figure 2-18 – Beams testing and crack monitoring .....	31
Figure 3-1– Load vs. deflection of a) non- fiber mixtures and b) fiber-reinforced mixtures .....	38
Figure 3-2 – Shrinkage of a) non-fiber Eco-Bridge-Crete, b) fiber-reinforced Eco-Bridge-Crete mixtures subjected to 1-day moist curing .....	40
Figure 3-3 – Shrinkage of a) non- fiber Eco-Bridge-Crete and b) fiber-reinforced mixtures subjected to 14 day-moist curing .....	41

Figure 3-4 – (a) Restrained expansion of non- fiber Eco-Bridge-Crete, and (b) fiber-reinforced mixtures subjected to 1-day moist curing .....	42
Figure 3-5 – (a) Restrained expansion of non-fiber Eco-Bridge-Crete, and (b) fiber-reinforced mixtures subjected to 14 days moist curing.....	43
Figure 3-6 – Contour diagrams of effects of EA, LWS, Moist curing (MC) and Fiber content on 56-day compressive strength (a) and (b), 56-day flexural strength (c) and (d) .....	47
Figure 3-7 – Contour diagrams of effects of EA, LWS, Moist curing (MC) and Fiber content on 56-day drying shrinkage (a) and (b), 56-day restrained expansion (c) and (d).....	49
Figure 3-8 – Drying shrinkage of FR-SWC mixtures containing 0.5% micro-macro steel fiber (STST) and 5D steel fiber (5D) .....	55
Figure 3-9 – Drying shrinkage of Eco-Bridge-Crete mixtures made with 0.5% macro synthetic fiber (PLP) and macro steel fiber (ST) .....	56
Figure 3-10 – Restrained expansion test results on FR-SWC mixtures containing 0.5% micro-macro steel fiber (STST) and 5D steel fiber (5D).....	57
Figure 3-11 – Restrained expansion test results of Eco-Bridge-Crete mixtures including 0.5% macro synthetic fiber (PLP) and macro steel fiber (ST).....	58
Figure 3-12 – Average current variations of reinforcing bars at 1, 1.5, and 2 in. of cover depths for a) REF-7 and b) 25LWS0.5FR-1 mixtures .....	61
Figure 3-13 – Influence of fiber content and type on current variation with time for reinforcing bars at 1 in. cover depth .....	63
Figure 3-14 – Influence of moist curing duration on current variation with time for reinforcing bars at 1 in. cover depth .....	65
Figure 3-15 – Influence of moist curing type on current variation with time for reinforcing bars at 1 in. cover depth.....	66
Figure 3-16 – Influence of the EA and/or LWS on current variation with time for reinforcing bars at 1 in. cover depth.....	68
Figure 3-17 – Testing Beams #1 to #5.....	71
Figure 3-18 – Testing Beams #6 to #10.....	72
Figure 3-19 – Load vs. strain values in concrete and steel reinforcing bars for FR-SWC made with STST fibers (Beam #4).....	73
Figure 3-20 – Load-deflection curves for 10 investigated beams.....	75
Figure 3-21 – Load-crack width relationship for 10 tested beams (Low, modLow, modHigh, and High denote beams with 2 #4, 2 #4 + 1 #3, 2 #4 + 1 #5, and 1 #4 + 2 #5, respectively) .....	76
Figure 3-22 – Load at crack width 0.016 in. (0.4 mm) vs. area of steel reinforcing bars.....	78
Figure 3-23 – Load at def = 0.5 in. (L/200) vs. area of steel reinforcing bars.....	79
Figure 3-24 – Ultimate load vs. area of steel reinforcing bars.....	79
Figure 3-25 – Toughness at crack width 0.016 in. (0.4 mm) vs. area of steel reinforcing bars ...	80
Figure 3-26 – Toughness at def = 0.5 in. (L/200) vs. area of steel reinforcing bars .....	80
Figure 3-27 – Toughness at def = 1.5 in. (max) vs. area of steel reinforcing bars .....	81
Figure 3-28 – Savings in steel reinforcement bars with FR-SWC.....	82
Figure A-1 – Flexural strength results of Mixtures used for experimental design .....	95
Figure A-2 – Drying shrinkage used for statistic design for mixtures.....	98
Figure A-3 – Drying shrinkage used for statistic design for mixtures (Validation Points) .....	99

Figure A-4 – Restrained expansion used for statistic design for mixtures .....	102
Figure A-5 – Restrained expansion used for statistic design for mixtures (Validation Points)..	103
Figure B-1 – Contour diagrams based on statistic model .....	109
Figure C-1 – Current variation with exposure to chlorides for REF-7 mixture with reinforcing bars at cover depths at (a) 1 in. (b) 1.5 in. and (c) 2 in. ....	111
Figure C-2 – Current variation with exposure to chlorides for 5EA0.5FR(PLP)-7 mixture with reinforcing bars at cover depths at (a) 1 in. (b) 1.5 in. and (c) 2 in. ....	112
Figure C-3 – Current variation with exposure to chlorides for 5EA25LWS0.5FR-7 mixture with reinforcing bars at cover depths at (a) 1 in. (b) 1.5 in. and (c) 2 in. ....	113
Figure C-4 – Current variation with exposure to chlorides for 5EA25LWS0.5FR-1 mixture with reinforcing bars at cover depths at (a) 1 in. (b) 1.5 in. and (c) 2 in. ....	114
Figure C-5 – Current variation with exposure to chlorides for 0.5FR-7 mixture with reinforcing bars at cover depths at (a) 1 in. (b) 1.5 in. and (c) 2 in. ....	115
Figure C-6 – Current variation with exposure to chlorides for 25LWS0.5FR-1 mixture with reinforcing bars at cover depths at (a) 1 in. (b) 1.5 in. and (c) 2 in. ....	116
Figure C-7 – Current variation with exposure to chlorides for 5EA0.5FR-7 mixture with reinforcing bars at cover depths at (a) 1 in. (b) 1.5 in. and (c) 2 in. ....	117
Figure C-8 – Current variation with exposure to chlorides for 5EA0.5FR-1 mixture with reinforcing bars at cover depths at (a) 1 in. (b) 1.5 in. and (c) 2 in. ....	118

## LIST OF TABLES

Table 1 – Performance-based specifications for FR-SWC and Eco-Bridge-Crete.....	vi
Table 2 – Derived statistical models.....	xii
Table 3 – Influence of investigated parameter on corrosion resistance.....	xviii
Table 1-1 – Mixture designs of Eco-Bridge-Crete from MoDOT/RE-CAST TR2015-03.....	2
Table 1-2 – Properties of optimized Eco-Bridge-Crete mixtures.....	2
Table 1-3 – Mixture designs of SWC and FR-SWC from MoDOT/RE-CAST TR2015-05.....	3
Table 1-4 – Workability of reference SWC and FR-SWC mixtures.....	3
Table 1-5 – Mechanical properties of optimized FR-SWC mixtures.....	4
Table 2-1 – Physical and chemical characteristics of cementitious materials and EA.....	9
Table 2-2 – Characteristics of chemical admixtures.....	9
Table 2-3 – Fiber types and characteristics.....	11
Table 2-4 – Coded and actual values of investigated parameters.....	12
Table 2-5 – Factorial design involving 25 mixtures evaluated in Task I-A.....	12
Table 2-6 – Mixture compositions of Eco-Bridge-Crete considered in the factorial design.....	13
Table 2-7 – Experimental program of Task I-A.....	13
Table 2-8 – Test properties used to evaluate mixtures prepared in Task I-B.....	15
Table 2-9 – Mixture compositions of 16 Eco-Bridge Crete and FR-SWC mixtures.....	16
Table 2-10 – Mixture proportions used for corrosion resistance testing.....	17
Table 2-11 – Scope of testing of reinforced concrete beams.....	18
Table 3-1 – Fresh properties of selected Eco-Bridge-Crete mixtures.....	32
Table 3-2 – Compressive strength results of the 25 Eco-Bridge-Crete mixtures.....	34
Table 3-3 – Flexural strength results of Eco-Bridge-Crete at 56 days.....	36
Table 3-4 – Derived statistical models.....	44
Table 3-5 – Derived statistical models (based on coded values).....	45
Table 3-6 – Relative effect of four parameters on the different properties.....	50
Table 3-7 – Performance optimization and significant levels to estimate overall desirability.....	51
Table 3-8 – Seven mixtures with high overall desirability values and four selected mixtures with different desirability values.....	52
Table 3-9 – Fresh properties of FR-SWC and Eco-Bridge-Crete mixtures.....	54
Table 3-10 – Combinations of parameters selected for corrosion testing.....	59
Table 3-11 – Measured properties of the investigated mixtures: Time of cracking due to corrosion (first peak in current), sorptivity and bulk resistivity.....	60
Table 3-12 – Mixtures compared to investigate the influence of test parameters.....	62
Table 3-13 – Influence of investigated parameter on corrosion resistance.....	69
Table 3-14 – Fresh and hardened properties of FR-SWC mixture.....	70
Table 4-1 – Relative effect of four parameters on the different properties.....	84
Table 4-2 – Influence of investigated parameter on corrosion resistance.....	87

# 1. INTRODUCTION

## 1.1 Problem statement

This investigation builds on the findings of two major studies completed by the principal investigator and his team at Missouri S&T that were funded by the Missouri Department of Transportation (MoDOT) and the RE-CAST (Research on Concrete Applications for Sustainable Transportation) Tier-1 University Transportation Center (UTC) at Missouri University of Science and Technology (Missouri S&T). The first study (TR2015-03) is entitled “Economical and Crack-Free High-Performance Concrete for Pavement and Transportation Infrastructure Construction”, and the second one (TR2015-05) is entitled “Performance of Fiber-Reinforced Self-Consolidating Concrete (FR-SCC) for Repair of Bridge Sub-Structures and Fiber-Reinforced Super-Workable Concrete (FR-SWC) for Infrastructure Construction”. Both projects involved the optimization of the concrete mixtures to reduce shrinkage/cracking and increase tensile strength to increase the service life of concrete infrastructure. The outcome of the latter project was used for the replacement of a two-span concrete bridge at Route M/J over Route 50 near Taos, Missouri, by MoDOT (**Figure 1-1**).



**Figure 1-1 – Field implementation of flowable FRC with adapted rheology for construction of a bridge deck near Taos, Missouri**

The mixture designs of an Eco-Bridge-Crete recommended in the TR2015-03 study are reported in **Table 1-1**. The mixtures differed in terms of binder composition, which included 60% slag cement and 5% silica fume substitutions in one mixture and 20% slag cement and 35% Class C fly ash in the other mixture. Both mixtures were prepared with 25% lightweight sand (LWS) and no fiber. The main characteristics of the mixtures are reported in **Table 1-2**. The air-entrained mixtures had slump values of 4.3 to 4.0 in. and 56-day compressive strengths of 6820 and 6380 psi, respectively. The mixtures had low drying shrinkage values of 210 and 270  $\mu$ strain after 120 days of drying following 7 days of moist curing.

**Table 1-1 – Mixture designs of Eco-Bridge-Crete from MoDOT/RE-CAST TR2015-03**

Mixture	Type I/II cement, pcy	FA, pcy	Slag, pcy	SF, pcy	Water, pcy	C. agg. 3/8", pcy	C. agg. 1", pcy	Sand, pcy	LWS, pcy	HRWR, fl oz/yd <sup>3</sup>	AEA, fl oz/yd <sup>3</sup>
350-60SL-5SF-25LWS	206.5	-	354	29.5	236	784	1096	944	314	32	0.44
350-20SL-35FA-25LWS	265.5	206.5	118	-	236	784	1096	944	314	27	0.36

**Table 1-2 – Properties of optimized Eco-Bridge-Crete mixtures**

Mixture		350-60SL-5SF-25LWS	350-20SL-35FA-25LWS
Slump, in.		4.3	4.0
Compressive strength, psi	28 days	6090	5370
	56 days	6820	6380
Splitting tensile strength, psi	28 days	455	390
	56 days	460	435
Flexural strength, psi	28 days	870	830
	91 days	900	885
Toughness, lbf-in.	28 days	47	46
Drying shrinkage, $\mu$ strain	120 days	210	270

The mixture designs of a Super-Workable Concrete (SWC) and two FR-SWC mixtures made with two types of steel fibers that were recommended in the TR2015-05 investigation are reported in **Table 1-3**. The two steel fiber types included a double hooked end long fiber (5D fiber) or a combination of macro hooked-end steel fiber and micro straight steel fiber (STST). The workability characteristics of the mixtures are reported in **Table 1-4**. The air-entrained mixtures can develop high passing ability and stability achieved. **Table 1-5** summarizes the mechanical properties of moist-cured samples as well as drying shrinkage after 120 days of the SWC and FR-SWC mixtures that were moist-cured for 28 days before drying.

**Table 1-3 – Mixture designs of SWC and FR-SWC from MoDOT/RE-CAST TR2015-05**

Mixture	Type I/II cement, pcy	FA, pcy	EA, pcy	Water, pcy	C. agg. ½", pcy	Sand, pcy	Fibers, pcy			VMA, fl oz/yd <sup>3</sup>	HRWR, fl oz/yd <sup>3</sup>	AEA, fl oz/yd <sup>3</sup>
							Macro 1.2 in.	Micro 0.5 in.	5D 2.55 in.			
SWC	448	192	0	265	1433	1433	-	-	-	65	45	1.16
FR-SWC 1	430	185	32	265	1348	1470	-	-	67	65	47	1.29
FR-SWC 2	430	185	32	265	1225	1588	54	13	-	65	47	1.06

**Table 1-4 – Workability of reference SWC and FR-SWC mixtures**

Mixture	Fiber type	V <sub>f</sub> , %	Unit weight, lb/ft <sup>3</sup>	Air, %	Slump flow, in.	Modified J-Ring (D/a)	VSI	Surface settlement, %	Bleeding, %
SWC	-	-	133.0	7.8	22.4	21.7	0	0	0.16
FR-SWC 1	5D	0.5	139.7	8.5	20.0	14.8	0	0.13	0
FR-SWC 2	STST	0.5	141.6	7.5	21.5	15	0	0.39	0

The study proved that the use of EA can mitigate shrinkage and early-age cracking of the concrete. The incorporation of EA in FRC can develop an internal compressive pre-stressing effect, so-called “chemically pre-stressing,” in the matrix, which can enhance mechanical properties. However, the effectiveness of using EA to compensate for shrinkage is significantly influenced by the availability of water necessary for the chemical reaction leading to expansion. Such water is provided through the mixture design and/or external source (i.e., moist curing) as



well as internal curing. The use of LWS has shown a significant benefit to provide internal curing and enhance cement hydration along with forming new hydration products via pozzolanic reaction of supplementary cementitious materials. Proper use of fibers was shown to increase flexural strength, and flexural toughness in monolith beams cast using FRC vs. those that were cast using regular concrete. As such, the incorporation of fibers can replace a portion of the steel reinforcing bars without reducing flexural strength. The use of fibers can also improve flexural performance, crack resistance, and ductility that can enhance the resilience of the structural system. The use of fibers can enable partially or complete substituting of welded wire mesh reinforcement (such as shear reinforcement in beams and roof elements). This reduces the need for manufacturing, detailing, and placing of reinforcement cages and leads to improvement of construction efficiency. Furthermore, the element thickness and the structure self-weight can be reduced since minimum cover requirements do not hold anymore.

**Table 1-5 – Mechanical properties of optimized FR-SWC mixtures**

Mixture		SWC	FR-SWC 1	FR-SWC 2
Compressive strength, psi	28 days	5500	6060	6050
	56 days	6425	7250	7170
Splitting tensile strength, psi	28 days	400	740	620
	56 days	415	775	690
Flexural strength, psi	28 days	629	703	785
	56 days	680	755	840
Toughness, lbf-in.	28 days	6.1	110	130
	56 days	6.7	115	140
First crack stress, psi	28 days	397	1390	910
	56 days	430	1,500	980
Residual stress, psi	28 days	0	930	680
	56 days	0	1,000	735
Elastic modulus, ksi	28 days	3750	3770	4150
	56 days	4050	4,140	4200
Drying shrinkage, $\mu$ strain	120 days	600	460	450

## **1.2 Research objectives**

The proposed project aimed to optimize the fiber characteristics-EA-LWS-moist curing system to enhance the restrained shrinkage cracking and transport properties of Eco-Bridge-Crete and FR-SWC mixtures developed in MoDOT/RE-CAST TR2015-03 and TR2015-05, respectively. The project also aimed to partially replace steel reinforcement in structural members by means of steel fibers. The following objectives were as follows:

- Development of a prediction model to predict the performance of Eco-Bridge-Crete given the EA, LWS, and fiber contents and moist curing conditions.
- Optimization of fiber characteristics-EA-LWS-moist curing system and fiber type to reduce drying shrinkage and restrained expansion for Eco-Bridge-Crete and FR-SWC.
- Evaluation of corrosion resistance of Eco-Bridge-Crete mixtures.
- Appraisal of the degree of enhancement in flexural properties of fiber-reinforced flexural elements due to partial replacement of the steel reinforcement with fibers in FR-SWC.

## **1.3 Research methodology**

The research project includes two tasks to fulfill the objectives of the study: Task-I) optimization for Eco-Bridge-Crete and FR-SWC; and Task II) structural performance of FR-SWC made with different fiber types and reinforcing steel densities. The scope of the work of these tasks is elaborated below.

### **Task I: Optimization for Eco-Bridge-Crete and FR-SWC**

#### ***Task I-A: Factorial design for mixture optimization of Eco-Bridge-Crete***

In this task, the effect of CaO-based EA, LWS, and moist curing regime on the performance Eco-Bridge-Crete was evaluated. The target performance included fresh properties, compressive

strength, flexural strength, drying shrinkage, and restrained expansion. A factorial design approach was employed to quantify the effect of different test parameters and contents. In total, 25 mixtures were cast, including 16 mixtures used for the factorial design, four central point mixtures, and five validation mixtures. Statistical models were developed to predict the performance of Eco-Bridge-Crete, given the EA, LWS, and fiber contents and the duration of moist curing. These models were used to quantify the effect of the test parameters and contents investigated on mechanical properties, drying shrinkage, and restrained expansion.

The main effects of these four factors (EA, LWA, moist curing, and fiber content), and two-way interactions, three-way interactions, four-way interaction of the factors, were first developed to fit the statistical models. Based on the above factorial design, models for the different properties were simplified and obtained.

***Task I-B: Performance of FR-SWC and Eco-Bridge-Crete mixtures made with different fibers***

In this task, 16 optimized concrete mixtures were investigated to determine the combined effect of EA, LWA, moist curing, and fiber content and type on viscoelastic properties. The testing included four mixtures representing Eco-Bridge-Crete and FR-SWC from MoDOT/RE-CAST TR2015-03 and TR2015-05 that were modified with four optimized EA-LWS-fiber systems from Task I-A. Three types of fibers were used: two steel fiber types and one type of synthetic fiber. The mixtures were evaluated to determine the unit weight, air content, slump/slump flow, passing ability (modified J-Ring test) in the case of the FR-SWC, stability (surface settlement), drying shrinkage, and restrained expansion. All concrete samples received 7 days of moist curing followed by air curing.

### ***Task I-C: Corrosion resistance of reinforcing bars using various Eco-Bridge-Crete***

This task dealt with the assessment of corrosion resistance of reinforcing bars embedded in proven Eco-Bridge-Crete mixtures prepared with steel and synthetic fibers. Eight corrosion test specimens with a size of  $25 \times 3.5 \times 8$  in. and embedded reinforcing bars at cover depths of 1, 1.5, and 2 in. were cast. For all the mixtures, water-to-binder ratio (w/b) was 0.40, and samples were prepared with 1 and 14 days of moist curing. The concrete was also tested to determine the effect of fiber type, internal and external curing, and EA content and their combinations on sorptivity and bulk resistivity.

### **Task II: Structural performance of FR-SWC made with different fiber types and reinforcing steel densities**

In Task II, the structural performance of FR-SWC made with and without the optimized EA-fiber systems was investigated to determine the potential savings of reinforcing steel due to the use of steel fibers. The testing involved the casting of beam elements with different steel reinforcement densities (0.4 to 0.8 in.<sup>2</sup> steel area in the tension zone).

In total, 10 reinforced concrete beams were cast to evaluate the flexural strength of optimized SWC mixtures with and without fiber reinforcement. The results were compared with six other beams cast in MoDOT/RE-CAST TR2015-05 with different tension steel area. The beams measured 8 ft. in length with a cross-section of 8 × 12 inches. The structural performance of the beams under different serviceability and ultimate design criteria were analyzed to evaluate savings that can be achieved when using different types of steel fibers.

## 2. EXPERIMENTAL PROGRAM

### 2.1 Materials

#### 2.1.1. Cementitious materials

Type I/II ordinary portland cement (OPC) was used in this study. Class C fly ash (FA) was employed for the SWC and FR-SWC. For preparing the Eco-Bridge-Crete mixtures, a slag cement (SL) was used in addition to the FA. **Figure 2-1** shows the particle size distribution of the cementitious materials. Type G (CaO-based) expansive agent (EA) was used to compensate for drying shrinkage, where the hydration of CaO and formation of calcium hydroxide ( $\text{Ca}(\text{OH})_2$ ) crystals can lead to expansion. **Table 2-1** presents the physical and chemical properties of the cementitious materials.

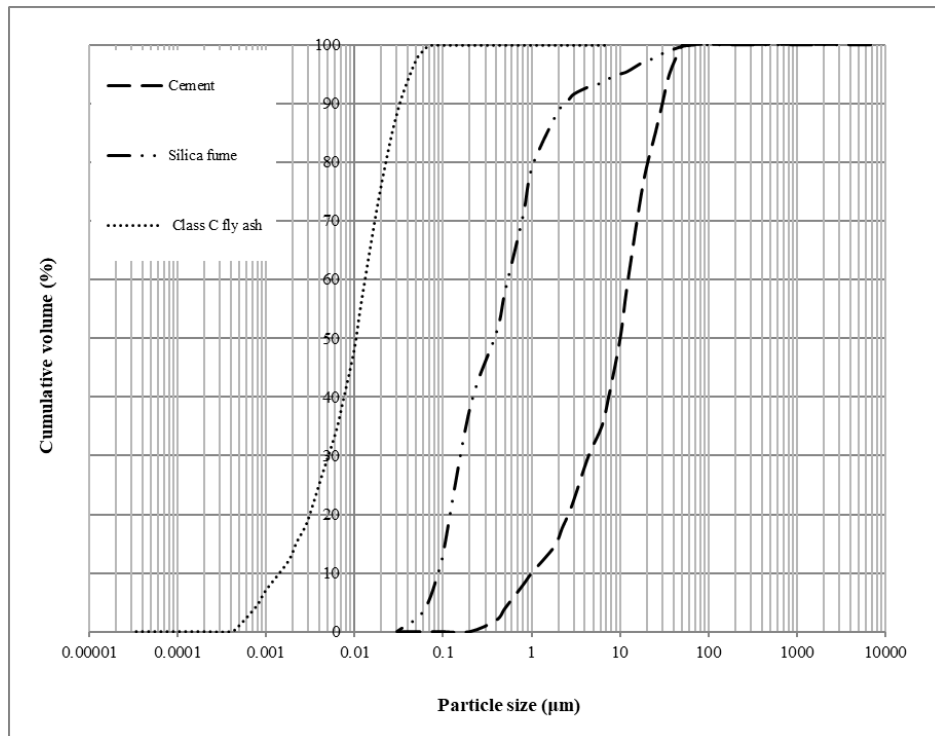


**Figure 2-1** Particle size distribution of cementitious materials ( $\mu\text{m}$ )

**Note:** SL-slag cement, FA-Class C fly ash, OPC-ordinary portland cement

**Table 2-1 – Physical and chemical characteristics of cementitious materials and EA**

	OPC	Class C FA	Slag	Type G EA
SiO <sub>2</sub> , %	18.7	40.4	36.2	12.6
Al <sub>2</sub> O <sub>3</sub> , %	4.04	19.8	7.7	5.7
Fe <sub>2</sub> O <sub>3</sub> , %	3.56	6.3	0.7	1.9
CaO, %	65.9	24.4	44.2	82.6
MgO, %	1.7	3.5	7.6	0.1
SO <sub>3</sub>	2.4	1.0	1.7	-
Na <sub>2</sub> O eq., %	0.97	0.90	0.92	0.9
CaCO <sub>3</sub> , %	3.3	-	-	-
Blaine surface area, m <sup>2</sup> /kg	390	490	590	-
Density	3.14	2.71	2.86	3.1
LOI, %	1.5	-	-	-

### 2.1.2 Chemical admixtures

A polycarboxylate-based high-range water reducer (HRWR) and a synthetic resin type air-entraining agent (AEA) were incorporated in the SWC and FR-SWC and Eco-Bridge-Crete to increase flowability and improve the air void system, respectively. A cellulose-based viscosity-modifying admixture (VMA) was employed to enhance the stability of the SWC and FR-SWC mixtures. **Table 2-2** shows the characteristics of these chemical admixtures.

**Table 2-2 – Characteristics of chemical admixtures**

	Solid content (%)	Specific gravity
HRWR	23.0	1.05
AEA	12.5	1.01
VMA	1.5	1.00

### 2.1.3. Aggregates

Continuously graded natural sand was procured from Capital Sullivan Quarry in MO. The sand has a fineness modulus of 2.6, a specific gravity of 1.83, and a surface saturated dry (SSD) water absorption value of 0.36%. Lightweight sand (LWS) with SSD specific gravity, water absorption and desorption of 1.83, 23.5%, and 70.3%, respectively, was utilized. The LWS was employed for internal curing and to mitigate autogenous and drying shrinkage. In order to prepare Eco-

Bridge-Crete mixtures, crushed limestone aggregate with nominal maximum aggregate sizes of 3/8 and 1 in. were utilized. Crushed limestone aggregate with a nominal maximum aggregate size of 1/2 in. was used to prepare the SWC and FR-SWC mixtures. The coarse aggregates were procured from the Capital Sullivan Quarry in MO. The specific gravities of the 3/8, 1/2, and 1 in. aggregates were 2.51, 2.67, and 2.72, respectively. Their SSD water absorptions were 1.16%, 0.77%, and 1%, respectively.

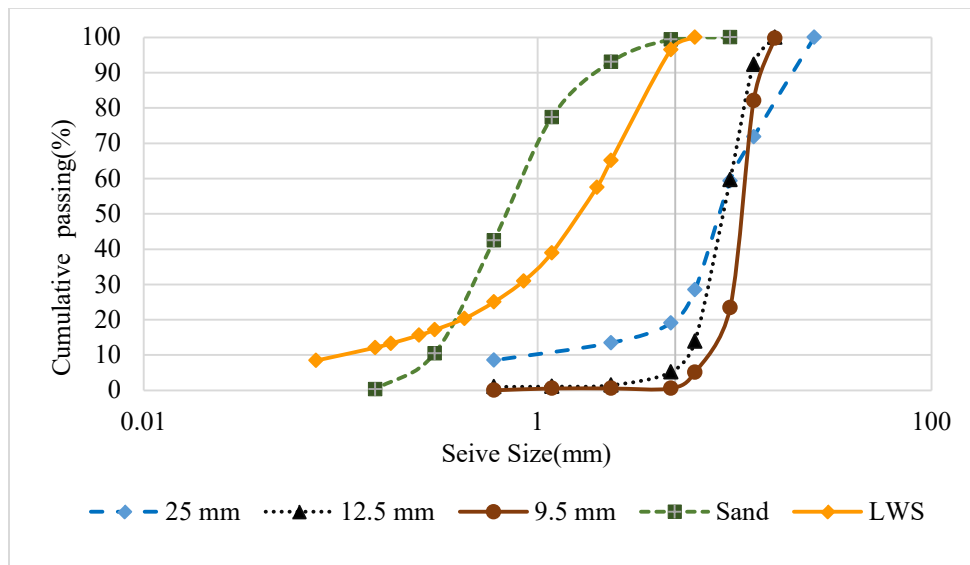






**Figure 2-2 - Aggregate grain size distribution**

#### 2.1.4. Fibers

As shown in **Table 2-3**, four types of fibers were used, including macro hooked-end steel fibers (ST), micro straight steel fibers, macro 5D steel fibers with double hooked ends, and polyethylene blend synthetic fibers (PLP). The synthetic fibers and macro hooked-end steel fibers were incorporated in the Eco-Bridge-Crete mixtures. A hybrid system of micro-macro steel fibers (STST) and the 5D steel fibers (5D) were used for the FR-SWC mixtures.

**Table 2-3 – Fiber types and characteristics**

	ST	5D	STST		PLP
Fiber type	Macro Steel	Macro Steel	80% Macro Steel	20% Micro Steel	Propylene
Shape	Hook 	Hook 	Hook 	Straight 	Monofilament 
Color	Silver	Grey	Silver	Golden	Transp.
Cross-section	Cir.	Cir.	Cir.	Cir.	Rec.
Specific gravity	7.85	7.85	7.85	7.85	0.92
Length, in.	1.2	2.4	1.2	0.5	2.0
Eq. diameter, in.	0.02	0.04	0.02	0.02	0.02
Aspect ratio	55	65	55	65	74
Modulus of elasticity, ksi	29,000	30,500	29,000	29,000	1,400
Tensile strength, ksi	160-188	168	160-188	160-188	87-94

## 2.2 Experimental program

### 2.2.1 Task I - Optimization for Eco-Bridge-Crete and FR-SWC

#### *Task I-A: Factorial design optimization for Eco-Bridge-Crete*

The effect of CaO-based EA, LWS, and fiber contents and initial moist curing of the Eco-Bridge-Crete on compressive and flexural strengths, drying shrinkage, and restrained expansion was evaluated. The mixtures were based on the results of the factorial design used to evaluate the individual and coupled effects of each of the four modeled parameters on concrete performance.

**Table 2-4** presents the coded and actual values of these three parameters that were considered in the factorial design. The -1 and +1 coded values correspond to the minimum and maximum values of each parameter, respectively. **Table 2-5** presents the 25 combinations of input parameters that were considered in the factorial design. The FRC mixtures tested were prepared with the STST fibers comprising of 20% micro and 80% macro steel fibers. The main effects of these four factors (EA, LWA, moist curing, and fiber content), and two-way interactions, three-



way interactions, four-way interaction of the factors, were first developed to fit the statistical models. Statistical models that presented a significant effect on the modeled responses were obtained.

**Table 2-4 – Coded and actual values of investigated parameters**

Test parameter	Coded factor		
	-1	0	1
CaO-based EA (%)	0	6	12
LWS (%)	0	12.5	25
Fiber (%)	0	0.25	0.5
Moist curing (day)	1	7	14

**Table 2-5 – Factorial design involving 25 mixtures evaluated in Task I-A**

Type	No of mixtures	Coded Value				Absolute value			
		EA	LWA	Moist curing	Fiber	EA (%)	LWS (%)	Moist curing (day)	Fiber (%)
Factorial Design	1	-1	-1	-1	-1	0	0	1	0
	2	1	-1	-1	-1	10	0	1	0
	3	-1	1	-1	-1	0	25	1	0
	4	1	1	-1	-1	10	25	1	0
	5	-1	-1	1	-1	0	0	14	0
	6	1	-1	1	-1	10	0	14	0
	7	-1	1	1	-1	0	25	14	0
	8	1	1	1	-1	10	25	14	0
	9	-1	-1	-1	1	0	0	1	0.5
	10	1	-1	-1	1	10	0	1	0.5
	11	-1	1	-1	1	0	25	1	0.5
	12	1	1	-1	1	10	25	1	0.5
	13	-1	-1	1	1	0	0	14	0.5
	14	1	-1	1	1	10	0	14	0.5
	15	-1	1	1	1	0	25	14	0.5
	16	1	1	1	1	10	25	14	0.5
Central Points	17	0	0	0	0	5	12.5	7	0.25
	18	0	0	0	0	5	12.5	7	0.25
	19	0	0	0	0	5	12.5	7	0.25
	20	0	0	0	0	5	12.5	7	0.25
Validation points	21	2/3	-1/3	1	-1	6.67	8.33	14	0
	22	2/3	-1/3	1	-1	6.67	8.33	14	0
	23	-1/3	1/3	-1/3	1	3.33	8.33	4.67	0.5
	24	-1/3 1/3	1/3	-1/3	1	3.33	8.33	4.67	0.5

Type	No of mixtures	Coded Value				Absolute value			
		EA	LWA	Moist curing	Fiber	EA (%)	LWS (%)	Moist curing (day)	Fiber (%)
	25	1	2/3	1	1/3	10	16.67	14	0.17

**Table 2-6** presents the mixture design proportion of the Eco-Bridge-Crete mixtures prepared for the factorial design in Task I-A. The first eight mixtures represent 16 mixture combinations, with the only difference being the duration of the initial moist curing (1 and 14 days); the rest of the mixtures that are identified with (\*) represent the central and validation point mixtures.

**Table 2-6 – Mixture compositions of Eco-Bridge-Crete considered in the factorial design**

Mixture	OPC, pcy	FA, pcy	SL, pcy	Sand, pcy	1", pcy	3/8", pcy	EA, %	LWS, %	FR, %
REF	265	205	119	1253	1096	783	0	0	0
10EA	238	184	105	1253	1096	783	10	0	0
25LWS	265	205	119	940	1096	783	0	25	0
0.5FR	265	205	119	1253	640	1164	0	0	0.5
10EA25LWS	238	184	105	940	1096	783	10	25	0
10EA0.5FR	238	184	105	1253	640	1164	10	0	0.5
25LWS0.5FR	265	205	119	940	640	1164	0	25	0.5
5EA12.5LWS0.25FR	251	194	112	1096	867	975	5	12.5	0.25
10EA25LWS0.5FR*	238	184	105	940	640	1164	10	25	0.5
3EA8LWS0.5FR*	256	200	113	1150	640	1164	3.3	8.3	0.5
7EA8LWS*	248	192	111	1150	1096	783	6.7	8.3	0
10EA17LWS0.2FR*	239	186	105	1045	940	913	10	16.7	0.17

**Note:** \* denotes mixtures corresponding to central and validation points.

**Table 2-7** shows the experimental program that was used to evaluate the 25 concrete mixtures that were investigated in Task I-A.

**Table 2-7 – Experimental program of Task I-A**

Property	Test
Workability	Unit weight (ASTM C138), air content (ASTM C231), and slump (ASTM C143)
Mechanical properties	Compressive strength (ASTM C39) at 28 and 56 days
	Flexural strength and toughness of FRC (ASTM C1609) at 56 days
Viscoelastic properties	Drying shrinkage (ASTM C 157) and restrained expansion (ASTM C806)

In this task, a factorial design model was developed to predict the performance of Eco-Bridge-Crete, given the modeled parameters of the EA, LWS, and fiber contents and moist curing. The models were used to quantify the effect of the test parameters and contents of the investigated responses that are elaborated in **Table 2-7**. The coded and actual values of the different test parameters were shown in **Table 2-5**.

The main effects of the four investigated factors (EA, LWA, moist curing, fiber content), and their two-way interactions, three-way interactions, and four-way interactions were developed to fit the statistical models. The parameter effects corresponding to the different properties were analyzed, and factorial design models that consider the most significant parameters were established.

#### **Task I-B: Performance of FR-SWC and Eco-Bridge-Crete made with different fiber types**

A total of 16 mixtures were cast to evaluate the effect of different fiber types on the performance of Eco-Bridge-Crete and FR-SWC. The performance of mixtures was evaluated using a wide range of properties, as indicated in **Table 2-8**. The testing program included four mixtures representing Eco-Bridge-Crete and FRC-SWC that are based on MoDOT/RE-CAST TR2015-03 and TR2015-05 that were modified with the four optimized EA-LWS-fiber systems from Task I-A. The concrete was subjected to 7 days of moist curing followed by air curing. In the case of the FR-SWC, two steel fibers were used (STST combination and 5D). For the Eco-Crete-Bridge mixtures, the ST steel fiber and the synthetic (PLP) fiber were used. **Table 2-9** shows the selected concrete mixtures that were modified and tested in this task.

**Table 2-8 – Test properties used to evaluate mixtures prepared in Task I-B**

Property	Test
Workability	Unit weight (ASTM C138), air content (ASTM C231), slump (ASTM C143), slump flow (ASTM C1611), passing ability (Modified J-Ring test), and stability (Surface settlement test)
Viscoelastic properties	Drying shrinkage (ASTM C 157) and restrained expansion (ASTM C806)

**Table 2-9 – Mixture compositions of 16 Eco-Bridge Crete and FR-SWC mixtures**

Mixture	Cement, pcy	Fly-ash, pcy	Slag, pcy	EA, pcy	Sand, pcy	LWS, pcy	Agg. 1", pcy	Agg. 1/2", pcy	Agg. 3/8", pcy	Water, pcy	Fibers (pcy)				VMA, fl oz/yd <sup>3</sup>	HRWR, fl oz/yd <sup>3</sup>	AEA, fl oz/yd <sup>3</sup>
											Macro, 1.2 in.	Micro, 0.5 in.	5D, 2.4 in.	PLP, 2 in.			
10EA0.5FR (STST)-SWC	386	167	-	61.5	1470	-	-	1347	-	264	49.6	16.5	-	-	80.1	38.8	7.75
10EA-0.5FR (5D)-SWC	386	167	-	61.5	1470	-	-	1347	-	264	-	-	66.15	-	80.1	38.8	7.75
5EA12.5LWS0.5FR (STST)-SWC	408	176	-	31.0	1286	129	-	1347	-	264	49.6	16.5	-	-	80.1	38.8	7.75
5EA12.5LWS0.5FR (5D)-SWC	408	176	-	31.0	1286	129	-	1347	-	264	-	-	66.15	-	80.1	38.8	7.75
5EA25LWS0.5FR (STST)-SWC	408	176	-	31.0	1102	258	-	1347	-	264	49.6	16.5	-	-	80.1	38.8	7.75
5EA25LWS0.5FR (5D)-SWC	408	176	-	31.0	1102	258	-	1347	-	264	-	-	66.15	-	80.1	38.8	7.75
10EA25LWS0.5FR (STST)-SWC	386	167	-	61.5	1102	258	-	1347	-	264	49.6	16.5	-	-	80.1	38.8	7.75
10EA25LWS0.5FR (5D)-SWC	386	167	-	61.5	1102	258	-	1347	-	264	-	-	66.15	-	80.1	38.8	7.75
10EA0.5FR (ST)-EBC	239	186	106	59.0	1254	-	1075	-	770	236	66.15	-	-	-	-	30.2	3.9
10EA-0.5FR (PLP)-EBC	239	186	106	59.0	1254	-	1075	-	770	236	-	-	-	7.5	-	30.2	3.9
5EA12.5LWS0.5FR (ST)-EBC	253	196	112	29.5	1097	110	1075	-	770	236	66.15	-	-	-	-	30.2	3.9
5EA12.5LWS0.5FR (PLP)-EBC	253	196	112	29.5	1097	110	1075	-	770	236	-	-	-	7.5	-	30.2	3.9
5EA25LWS0.5FR (ST)-EBC	253	196	112	29.5	941	220	1075	-	770	236	66.15	-	-	-	-	30.2	3.9
5EA25LWS0.5FR (PLP)-EBC	253	196	112	29.5	941	220	1075	-	770	236	-	-	-	7.5	-	30.2	3.9
10EA25LWS0.5FR (ST)-EBC	239	186	106	59.0	941	220	1075	-	770	236	66.15	-	-	-	-	30.2	3.9
10EA25LWS0.5FR (PLP)-EBC	239	186	106	59.0	941	220	1075	-	770	236	-	-	-	7.5	-	30.2	3.9

### Task I-C: Corrosion resistance of reinforcing bars in optimized Eco-Bridge-Crete

This task dealt with the assessment of corrosion resistance of reinforcing bars embedded in proven Eco-Bridge-Crete mixtures prepared with steel and synthetic fibers. Eight corrosion test beams measuring 25 × 3.5 × 8 in. were prepared. Reinforcing bars were embedded to secure cover depths of 1, 1.5, and 2 in. from a salt tank. The mixture proportions of the investigated Eco-Bridge-Crete are shown in **Table 2-10**. The w/b was set at 0.42. The beams were subjected to 1 or 7 days of moist curing. The concrete was also tested to evaluate water sorptivity and bulk electrical resistivity to evaluate transport properties affecting corrosion resistance.

**Table 2-10 – Mixture proportions used for corrosion resistance testing**

Mixture	OPC, pcy	FA, pcy	SL, pcy	Sand, pcy	1", pcy	3/8", pcy	EA, %	LWS, %	FR, %
REF <sup>a</sup>	265	205	119	1253	1096	783	0	0	0
0.5FR <sup>a</sup>	265	205	119	1253	640	1164	0	0	0.5
25LWS0.5FR <sup>b</sup>	265	205	119	940	640	1164	0	25	0.5
5EA0.5FR <sup>a,b</sup>	251	194	113	1253	640	1164	5	0	0.5
5EA25LWS0.5FR <sup>a,b</sup>	251	194	113	940	640	1164	5	25	0.5
5EA0.5FR (PLP) <sup>a</sup>	251	194	113	1253	640	1164	5	0	0.5

<sup>a</sup> indicates mixtures subjected to 7 days of moist curing

<sup>b</sup> indicates mixtures subjected to 1 day of moist curing

### 2.2.2 Task II: Structural performance of FR-SWC made with different fiber types and reinforcing steel densities

In total, 10 reinforced concrete beams were cast to evaluate the flexural strength of optimized SWC mixtures made with and without fiber reinforcement. The beams measured 8 ft. in length and 8 × 12 in. in cross-section. **Table 2-11** presents the scope of the work undertaken to determine possible savings in tensile reinforcement stemming from the use of steel fibers. The testing involved the casting of reinforced concrete beam elements with areas of steel reinforcement varying between 0.4 and 0.8 in.<sup>2</sup> in the tension zone to determine the potential

savings of reinforcing steel due to steel fiber use, as shown in **Figure 2-3**. As illustrated in **Table 2-11**, six beams prepared with three #4 reinforcing bars that were tested in the MoDOT/RE-CAST TR2015-05 project are also included in the analysis.

**Table 2-11 – Scope of testing of reinforced concrete beams**

Reinforcing bar combinations	2#4	2#4 + 1#3	3#4	2#4 + 1#5	2#5 + 1#4
FR-SWC 2 (0.5% STST)	Beam 1	Beam 2	2 beams (TR2015-05)	Beam 3	Beam 4
SWC (no fibers)	Beam 5	-	2 beams (TR2015-05)	-	Beam 6
FR-SWC 1 (0.5% 5D)	Beam 7	Beam 8	2 beams (TR2015-05)	Beam 9	Beam 10

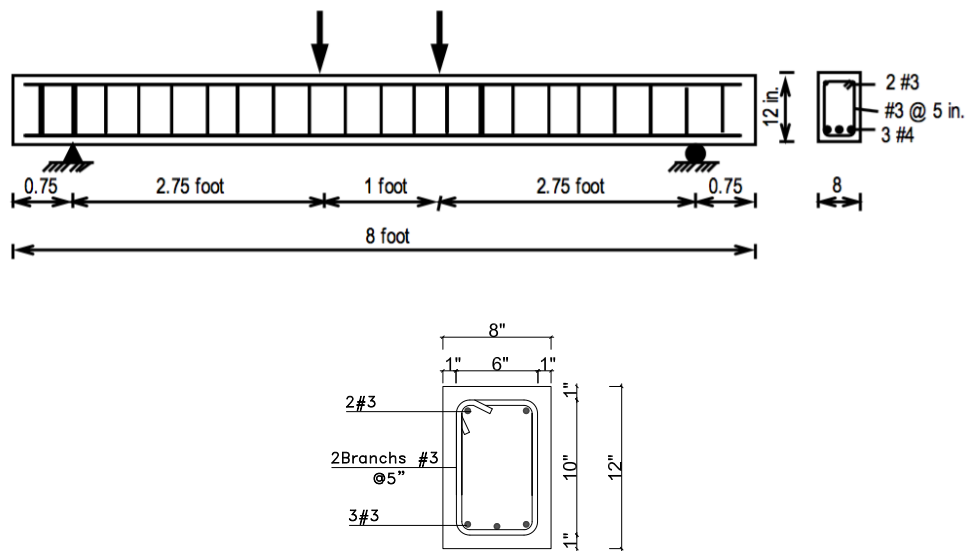


**Figure 2-3 – Flexural testing of full-scale monolithic beams**

The mixture proportions of the investigated SWC and FR-SWC mixtures are based on those proposed in the MoDOT/RE-CAST TR2015-05 project, which are reported in **Table 1-1**. The mixtures were prepared with 30% Class C fly ash substitution and a Type G EA corresponding to 5% of the binder mass. The w/b was set at 0.42 to enhance durability. Continuously graded crushed limestone aggregate with a nominal maximum size of aggregate (MSA) of ½ in. was

used. A polycarboxylate-based HRWR with good workability retention characteristics was used. A synthetic resin-based AEA was used for air entrainment. A polysaccharide VMA was used to enhance stability. For the FR-SWC mixtures, two types of fibers were used that included; a combination of micro and macro steel fibers (STST) and a 2.55 in. - hooked end steel fibers (5D). Fibers were introduced at a fiber volume of 0.5% (67 lb./yd<sup>3</sup>).

## **2.3 Mixing and test methods**

### **2.3.1 Mixing procedure and curing – Task I: Optimization for Eco-Bridge-Crete and FR-SWC**

Concrete mixtures evaluated in Task I was prepared using a 4.2 ft<sup>3</sup> capacity drum mixer. The mixing procedure was as follows:

1. Homogenize sand and pre-soaked lightweight sand (if it is applicable) for 30 seconds.
2. Add coarse aggregate, fibers (if it is applicable), half of the water mixed with AEA, and mix for 2 minutes. The fibers and water added gradually to the mixer while it was turning.
3. Incorporate binders (and EA if it is applicable) and continue mixing for 1 minute.
4. Include the remaining half of the mixing water mixed with the HRWR (and VMA if applicable) and mix for 3 minutes.
5. Turn off the mixture for 2 minutes to adjust the HRWR dosage to secure targeted fluidity.
6. Remix the concrete for an additional 2 minutes.

Different curing regimes in this project. However, all the samples were demolded after 24 hours and cured in the water tank at  $73 \pm 3$  °F before transferring them to the curing chamber with a temperature of  $73 \pm 3$  °F and a relative humidity of  $50\% \pm 4\%$ . In Task I-A, samples



were kept 1, 7, and 14 days in the curing tank. In Task I-C, all the samples were subjected to 6 days of moist curing, and in Task I-D, 1- and 14-day moist curing was applied.

### 2.3.2 Test methods - Task I: Optimization for Eco-Bridge-Crete and FR-SWC

#### Fresh properties

The workability tests, including fluidity, passing ability, and stability, were evaluated. The unit weight and air content of the Eco-Bridge-Crete and FR-SWC mixtures were measured according to ASTM C138 (2017) and ASTM C231 (2017), respectively. The slump of Eco-Bridge-Crete and slump flow of FR-SWC were measured according to ASTM C143 (2015) and ASTM C1611 (2018). The passing ability of the FR-SWC was measured using the modified J-Ring test shown in **Figure 2-4-a**. The stability of Eco-Bridge-Crete and FR-SWC mixtures was measured using a surface settlement test that is shown in **Figure 2-4-b**.



(a)



(b)

**Figure 2-4** – (a) J-Ring test and (b) surface settlement test

#### Mechanical properties

The compressive strength of concrete was determined at 28 and 56 days using 4×8 in. cylinder samples, according to ASTM C39 (2010). The samples were maintained in a lime-saturated

solution for 6 days (after demolding) and then kept in the curing chamber with conditions mentioned in Section 2.3.1 until the time of testing. All cylinders were capped before the testing using a high-strength Sulphur capping compound, according to ASTM C 617 (2015). The loading rate was controlled to secure compressive stress of  $35 \pm 7$  psi/sec during the experiment (Figure 2-5).



**Figure 2-5 – Test setup for compressive strength**

The flexural strength testing was conducted on prismatic samples measuring 3×3×16 in. with a span length of 12 in. according to ASTM C1609 (2012). The loading rate was maintained at displacement control of 0.0035 in./min until the failure of beam samples. **Figure 2-6** shows the test set-up for this test. The flexural strength was calculated as follows:

$$F = PL/bd^2$$

where F is the strength (psi); P is the load (lbf), L is the span (in.), b is the average width of the sample (in.), and d is the average depth of the sample (in.). The residual strength was calculated using the above equation and the residual loads at deflections of L/600 and L/150.



**Figure 2-6 – Test setup for flexural strength measurement of beam specimens**

### **Viscoelastic properties**

**Figure 2-7** shows the drying shrinkage and restrained expansion measurement setups. Drying shrinkage (ASTM C157) was determined on prismatic specimens measuring  $3 \times 3 \times 11.25$  in. using a digital type extensometer. The restrained expansion test was performed on  $3 \times 3 \times 10$  in. prisms, according to ASTM C878. After demolding at 24 h, the prismatic samples were immersed in water for 6 days. The samples were then stored in a temperature and humidity-controlled room at  $73 \pm 3$  °F and  $50\% \pm 4\%$  relative humidity. Shrinkage and expansion were then measured until the stabilization of shrinkage readings.

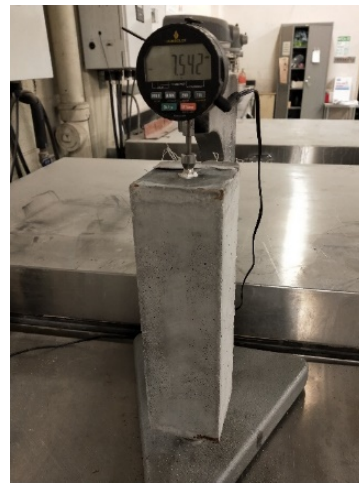


**Figure 2-7 – Drying shrinkage measurement (a) drying shrinkage and (b) restrained expansion**

## Corrosion resistance

The corrosion test setup included a salt tank (5% NaCl solution) with each side made of concrete samples with reinforcing bars embedded at different cover depths and stainless-steel mesh placed inside the tank, as shown in **Figure 2-8**. The electrical connection was made between the embedded reinforcing bars and the stainless-steel mesh using a 5V power supply and 1Ω shunt resistors.

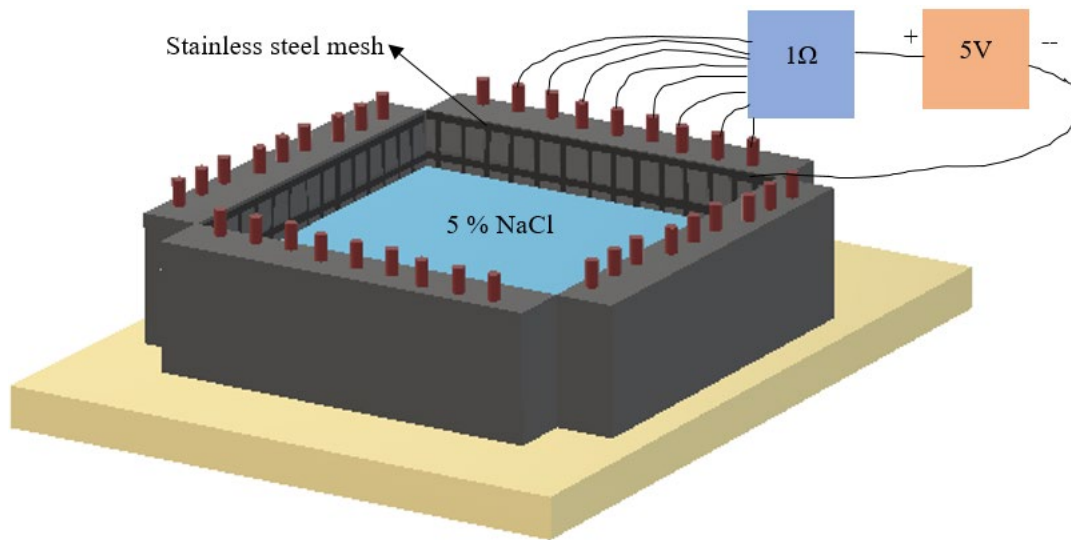


**Figure 2-8 – Schematic of the test setup for measuring the corrosion resistance of embedded reinforcing bar in concrete**

In the corrosion setup, the stainless-steel mesh acts as a cathode, and the reinforcing bar act as an anode and the voltage drop across the 1Ω resistors is recorded over time. The voltage difference between the reinforcing bar and stain steel mesh accelerates the movement  $\text{Cl}^-$  towards the anode, i.e., the reinforcing bar. When the sufficient  $\text{Cl}^-$  reach the reinforcing bar, the passive layer on the reinforcing bar surface (formed due to the high alkaline environment of the concrete) gets depassivated/destroyed, resulting in an oxidation reaction at the reinforcing bar (conversion from Fe to  $\text{Fe}^{+2}$ ). At the cathode, i.e., steel mesh, the reduction reaction occurs, resulting in the formation of  $\text{OH}^-$ . The  $\text{Fe}^{+2}$  formed at the reinforcing bar move into the solution, while the  $\text{OH}^-$

move towards the anode.  $\text{Fe}^{+2}$  and  $\text{OH}^-$  react to form corrosion products (Raupach, 1996). The corrosion products formed have 2-4 times higher volume than the reacted Fe (Ahmad, 2003; Bazant, 1979). This causes a volume expansion and exerts tensile stress on the surrounding concrete. As a result, the concrete cover cracks when the tensile stress exerted by the corrosion products exceeds the tensile strength of the concrete. The cracking reduces the resistance of concrete cover and increases the current between the reinforcing bar and stainless-steel mesh.

During the corrosion test, the variation of the current across each reinforcing bar and the steel mesh was monitored over time. The time of cracking due to corrosion was identified as the time at which there is a considerable increment in the current. The time of cracking was used as an indicator of the corrosion resistance. Additionally, the time of cracking also be used to estimate the service life of the concrete structure (El Maaddawy and Soudki, 2007).

The preparation procedure for the salt tanks involved the following steps: 1) cutting the No. 4 reinforcing bars in 10 in. in length; 2) wire brushing to remove the rusted layer; 3) drilling and tapping of the reinforcing bars at one end and fitting with coarse-thread stainless-steel screw and nut for making an electrical connection; and 4) epoxy coating both ends to prevent corrosion of the edges, as shown in **Figure 2-9**. The reinforcing bars were then placed into a custom-made mold (also shown in **Figure 2-9**) to make the concrete samples with the cover depths of 1, 1.5, and 2 in., as shown in **Figure 2-10**. The casting of the beam specimens was carried out two layers vibrating each layer for 10-15 sec using an external vibration on a vibrating table vibrator as per ASTM C192. After demolding, the samples were moist cured for 1 or 7 days depending on the specimen and then subjected to the drying at  $50\% \pm 4\%$  relative humidity and curing temperature of  $73 \pm 3$  °F for 90 days; i.e., until the start of the corrosion test.



**Figure 2-9 – Custom made corrosion test sample molds with epoxy-coated bars at ends**

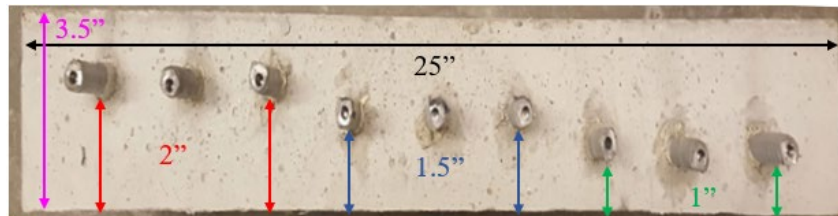
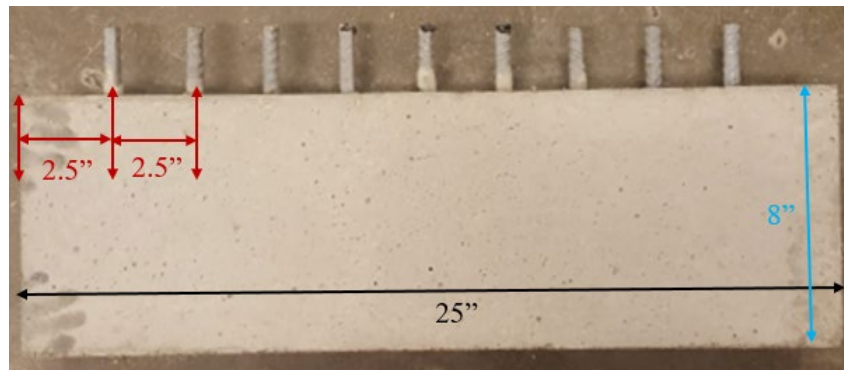
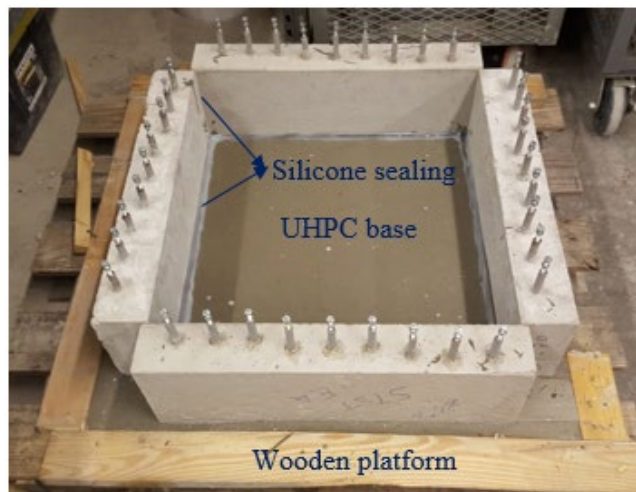


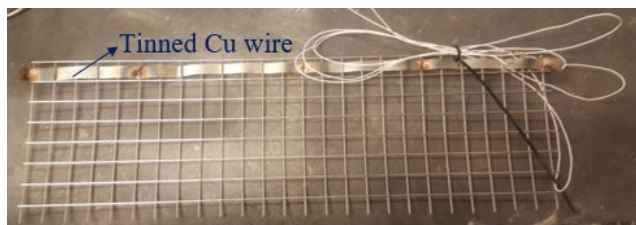
**Figure 2-10 – Dimensions of the concrete samples for the corrosion test**

The assembling process of the salt tanks involved placing of the concrete samples on a wooden platform, filling the base with ultra-high-performance concrete (UHPC) and sealing the joints with silicone to prevent water leakage, as shown in **Figure 2-11-a**. The UHPC was moist cured for 24 hours by covering the salt tanks with damp burlap and plastic sheet. Later, the UHPC base and the outer surfaces of the tank were coated with a waterproofing agent to minimize the

influence of the environment on the corrosion test results. The stainless-steel mesh of 0.92 in. opening and steel wire diameter of 0.08 in. was cut in the dimensions of 24 × 8 in. to place in the salt tanks. The mesh was weaved with tinned copper wire to maintain uniform charge distribution across the mesh during the corrosion test, as shown in **Figure 2-11-b**.



(a)



(b)

**Figure 2-11 – Corrosion test setup: a) placement of samples to form a sealed salt tank, and b) stainless-steel mesh cut and weaved with tinned Cu wire**

The electrical connections were established between the embedded reinforcing bars (anode) and the steel meshes (cathode) using 18-gauge electrical wire and panels with 5V power supply and 1  $\Omega$  shunt resistors shown in **Figure 2-12**. The tanks were saturated with water for 5 days before the addition of NaCl (5% by mass). The voltage drop across the shunt resistors was measured one to two times a day in the first two weeks and one to two times a week thereafter, and the

current values were computed according to Ohm's law. The tanks were cleaned after every 30 to 40 days, and the salt water was replaced. In the meantime, water was added to the salt tanks every week to compensate for evaporated water, and the tanks were covered with plastic sheets to minimize evaporation loss.

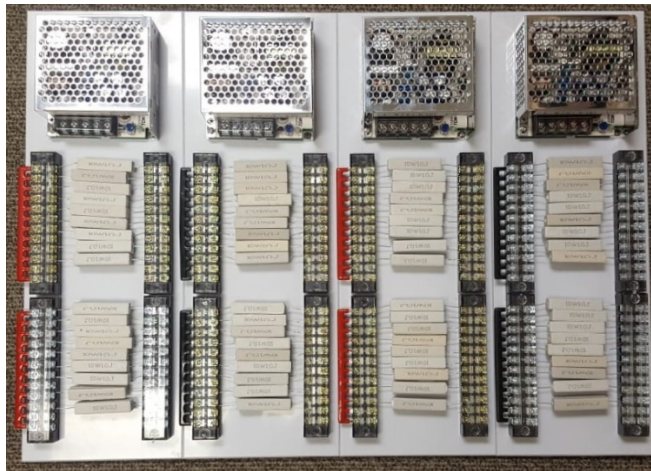


**Figure 2-12 – Four panels each with 5 V power supply and 1 Ω shunt resistors**

### **Transport properties**

The electrical resistivity measurement was used to classify concrete based on the corrosion rate. The electrical resistivity was determined on saw-cut cylindrical samples at the age of 28 days. The measurement of electrical resistivity was determined using the two-electrode method ASTM 1760 (2012), as shown in **Figure 2-13**.

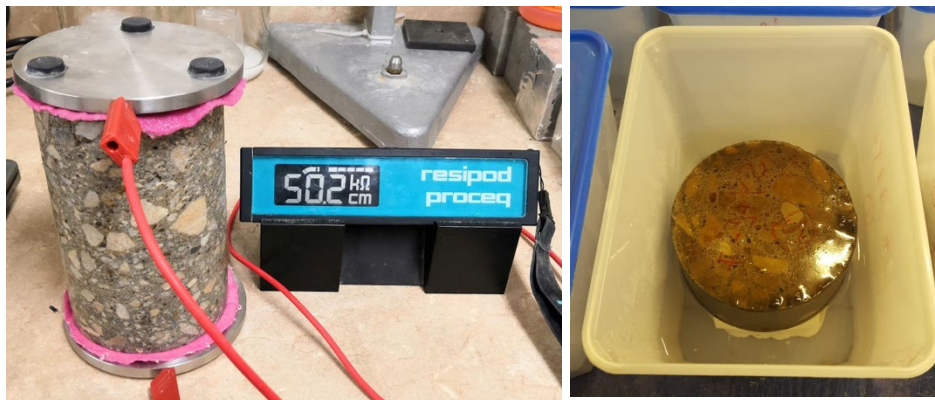


**Figure 2-13 – Testing apparatus for bulk resistivity (left) and sorptivity (right)**



The sorptivity of concrete was determined in compliance with ASTM C1585 (2011). The test consisted of measuring the increase in the mass of a disc specimen cut in three-disc specimens measuring 2 inches. The specimens were placed in the environmental chamber at a temperature of 122°F and relative humidity of 80% for 3 days. After 3 days, each sample was placed inside a sealable container and stored at  $73 \pm 3$  °F for at least 15 days until an equilibrium mass is reached. Prior to absorption testing, the side surfaces of the samples were sealed with aluminum tape, and the top surface was covered with plastic wrap. This was done to prevent the drying of the sample from these surfaces.

### 2.3.3 Casting and curing of flexural reinforced concrete beams

Concrete having the specified mixture composition presented in **Table 2-12** was procured from a local ready-mix plant to cast 10 reinforced concrete beams (**Table 2-11**). As shown in **Figure 2-14**, four top reinforcing bar configurations of 2#4, 2#4 + 1#3, 2#4 + 1#5, and 2#5 + 1#4 were employed.

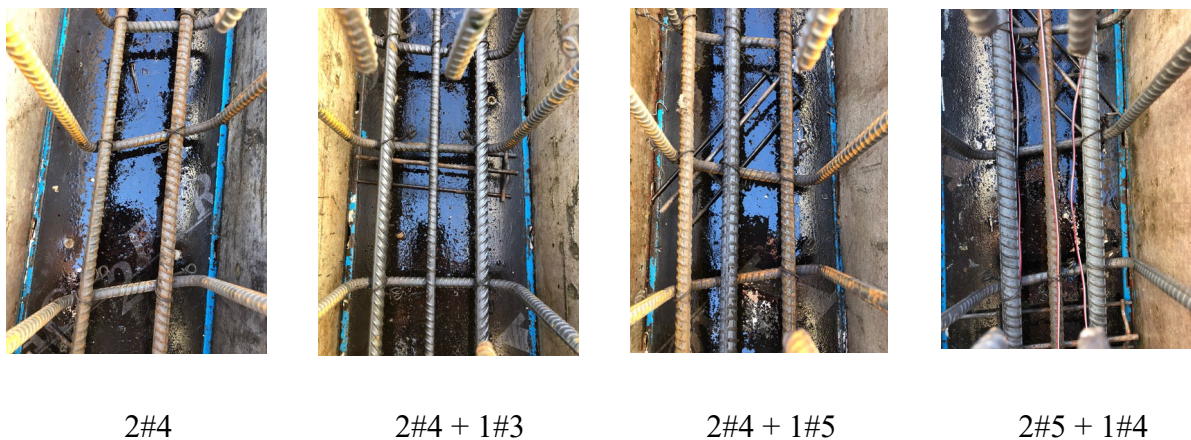


**Figure 2-14 – Four reinforcing bar configurations**

Electrical type strain gauges were attached to the surface of the bottom steel reinforcing bars to monitor the tensile strain in the reinforcing bars during flexural testing. The surface of the steel

bars was first ground to remove all of the ribs and to produce a smooth surface. It was then cleaned using alcohol, and strain gauges were attached to the surface of the reinforcing bars using glue. The number of strain gauges was equal to the number of steel bars. **Figure 2-15** shows three strain gauges attached to three reinforcing bars.



**Figure 2-15 – Strain gauges attached at the middle of the bottom reinforcing bars**

**Figure 2-16** shows the formwork used to cast the beams made of FR-SWC mixtures. The formwork was steel type with spaced vertical ribs, stiff enough to prevent any deformation during casting of concrete. The concrete was cast in one layer and manually consolidated using 1.5 in. steel rods. No bleeding was observed that resulted in the well-finished surface. The beams were cast outdoors and covered using wet burlap and plastic sheets for 24 hours. The beams and occupying samples (**Figure 2-17**) were then demolded and transferred indoors. Beams continued to cure using wet burlap and plastic sheets for 45 days when concrete reached the targeted strength.



**Figure 2-16 – Formwork and cast beams**



**Figure 2-17 – Curing of beams and cylinders and occupying samples**

#### **2.3.4 Reinforced concrete beam testing**

**Figure 2-18** shows the test setup for the beams as well as the crack monitoring during beam testing. A loading system with hydraulic jacks and a load cell of 500 kips (maximum capacity) closed-loop MTS actuator was used to test beams under four-point bending. The beam supported at two points 5 in. from both ends and loaded in the middle using two-point loads separated by 12 inches. Every steel reinforcing bar was instrumented using a strain gauge at the mid-span. The test was paused every 5 kips loading to monitor the maximum crack width until reaching peak load or 1-in. deflection. After reaching a peak load or deflection of 1 in., the test was paused at every deflection of 0.5 in. to monitor the maximum crack width. The test was stopped when

beams reached a deflection of 3 in. or at failure. The beam was considered to fail when the unloading stress reaches 50% of the peak load.



**Figure 2-18 - Beams testing and crack monitoring**

### 3. TEST RESULTS AND DISCUSSION

#### 3.1 Task I: Optimization for Eco-Bridge-Crete and FR-SWC

##### 3.1.1 Task I-A: Optimization for Eco-Bridge-Crete mixtures

As shown in **Table 2-6**, 25 concrete mixtures were prepared to establish statistical models for mechanical properties and viscoelastic properties of Eco-Bridge-Crete. The first eight mixtures represent 16 mixture combinations, with the only difference being the duration of the initial moist curing (1 and 14 days); the rest of the mixtures were used for the central points and validation mixtures.

#### Fresh properties

**Table 3-1** shows the fresh properties of the eight tested Eco-Bridge-Crete mixtures that were used to establish the factorial design. The slump values varied between 4.75 and 5.6 in. for the non-fiber mixtures and 6.75 and 7.5 in. for the fiber-reinforced mixtures. The temperature, air content, and unit weight values ranged between 67 and 70 °F, 4.4% and 7.4%, and 134.4 and 145.6 lb./ft<sup>3</sup>, respectively. The other mixtures, including the central points, had similar fresh properties as those of the main mixtures reported below.

**Table 3-1 – Fresh properties of selected Eco-Bridge-Crete mixtures**

Mixture	Slump, in.	Temperature, °F	Air content, %	Unit weight, lb/ft <sup>3</sup>
REF	4.75	67.0	4.8	145.6
10EA	5.00	70.0	5.7	134.4
25LWS	5.60	68.5	4.4	143.9
0.5FR	7.50	67.5	7.0	142.4
10EA25LWS	5.50	69.5	6.8	135.0
10EA0.5FR	6.80	68.5	6.5	138.1
25LWS0.5FR	6.75	68.5	7.4	142.8
10EA25LWS0.5FR	7.50	68.0	7.0	140.2

## Compressive strength

**Table 3-2** summarizes the compressive strength results of the 25 Eco-Bridge-Crete mixtures tested after 28 and 56 days of age. The maximum compressive strength at 56 days was approximately 8200 psi and was achieved by the 0.5FR-14D and 7EA8L14D mixtures, the latter containing 6.67% of EA and 8.33% LWS after 14 days of moist curing. The minimum compressive strength at 56 days was approximately 4000 psi was recorded for the mixture made with 25% LWS and 0.5% fiber subjected to 1 day of moist curing (25LWS0.5FR-1D).

In general, the results indicate that the addition of EA or fiber, and their combination improved the compressive strength when the initial period of moist curing was increased from 1 to 14 days. A comparison between the compressive strength of the 10EA25LWS-1D and 10EA-14D mixtures shows that the initial moist curing of 14 days was more effective than limiting the curing time to 1 day and using 25% LWS for internal curing.

The same observation is valid for the 25LWS-1D mixture versus the REF-14D mixture. The use of 10% EA in addition to 0.5% fiber (10EA0.5FR-14D) improved the compressive strength slightly (4%) in comparison with the corresponding control mixture (REF-14D). The underlying reason is the self-stressing where fibers can restraint some of the expansion in the matrix and enhance the mechanical performance of the FRC (Sahamitmongkol and Kishi, 2011; He et al., 2011; Corinaldesi and Nardinocchi, 2016).

A more thorough analysis of the individual and coupled effects of the EA, LWS, and fiber contents and initial moist curing duration on compressive strength will be presented later in this report given the results of the factorial design models.

**Table 3-2 – Compressive strength results of the 25 Eco-Bridge-Crete mixtures**

Mixture	28-day compressive strength, psi	Avg., psi	COV*, %	56-day compressive strength, psi	Avg., psi	COV, %
REF-1D	6140	6730	8.7	6510	6800	3.8
	7300			6880		
	6750			7010		
REF-14D	7860	8080	2.8	7530	7590	1.0
	8310			7670		
	8050			7560		
10EA-1D	6470	6420	1.8	6250	5850	7.5
	6490			5910		
	6290			5380		
10EA-14D	7640	7490	1.9	7730	7650	1.3
	7500			7670		
	7350			7540		
25LWS-1D	5620	5470	2.8	5430	5465	-
	5480			5500		
	5310			(defective)		
25LWS-14D	7050	7110	5.0	7500	7620	1.6
	7480			7620		
	6790			7750		
0.5FR-1D	6770	6760	2.4	6740	6880	3.3
	6600			7140		
	6930			6750		
0.5FR-14D	8650	8630	1.4	8160	8220	1.9
	8490			8400		
	8740			8100		
10EA25LWS-1D	3870	3950	2.5	3800	3900	2.7
	3920			3900		
	4060			4010		
10EA25LWS-14D	6120	6190	4.2	6480	6810	4.2
	6480			6950		
	5970			7000		
10EA0.5FR-1D	5930	6000	2.2		N/A	
	5930					
	6160					
10EA0.5FR-14D	6470	6680	10.1	6960	7060	1.2
	7440			7100		
	6140			7110		
25LWS0.5FR-1D	4130	4080	1.5	3770	3950	4.8
	4100			3930		
	4020			4150		
25LWS0.5FR-14D	5220	5010	10.4	4670	5180	9.2
	5390			5610		
	4410			5250		
10EA25LWS0.5FR-1D	4510	5050	13.1	6510	6720	2.6
	5790			6790		
	4850			6850		
10EA25LWS0.5FR-14D	5160	5240	1.3	5710	5830	9.8
	5290			6450		
	5270			5320		

Mixture	28-day compressive strength, psi	Avg., psi	COV*, %	56-day compressive strength, psi	Avg., psi	COV, %
Mixture	28-day compressive strength, psi	Avg., psi	COV*, %	56-day compressive strength, psi	Avg., psi	COV, %
3EA8LWS0.5FR5D-1	5360	5840	7.1	6010	5950	0.9
	6020			5910		
	6130			5930		
3EA8LWS0.5FR5D-2	5730	5890	2.4	6350	5930	11.8
	5950			6320		
	6000			5120		
5EA0.25FR7D-1	4980	4760	8.3	4740	5320	9.4
	4990			5570		
	4300			5640		
5EA0.25FR7D-2	5010	5260	4.4	5570	5250	6.4
	5290			5280		
	5470			4900		
5EA0.25FR7D-3	5450	5600	3.3	6210	6110	2.4
	5810			5940		
	5540			6170		
5EA0.25FR7D-4	5920	5740	4	6160	6260	1.4
	5480			6340		
	5830			6270		
7EA8L14D-1	7250	7220	3.3	8420	8190	3.6
	6960			7860		
	7440			8290		
7EA8L14D-2	7360	7570	2.9	8160	8170	0.3
	7560			8200		
	7800			8150		
10EA0.17FR14D		N/A		5385	5420	5.3
				5150		
				5720		

**Note:** \* indicates coefficient of variation (COV).

### Flexural strength

The flexural strength results at 56 days are summarized in **Table 3-3**. The results are averages of two samples. Flexural strength results of the 25 mixtures are reported in **Appendix A**. The maximum flexural strength of the mixtures shown in **Figure 3-1** was 2015 psi and was achieved by the 10EA0.5FR-14D mixture made with 10% of EA and 0.5% fibers at moist cured for 14 days. The minimum flexural strength was 660 psi and was recorded for the REF-1D mixture. The maximum residual strength, which represents the ductility, was obtained by the 25LWS0.5FR-14D mixture. The residual strength was 270% greater than the non-fiber-



reinforced concrete subjected to 1 day of moist curing (REF-1D), and 140% more than the reference FRC with 14 days of moist curing (0.5FR-14D). This improvement highlights the importance of internal and external curing and their effect on extending the hydration process. This phenomenon results in the formation of dense and homogeneous interfacial transition zone leading to a superior bond between the fibers and concrete matrix (Lam and Hooton, 2005; Khayat et al., 2018).

**Table 3-3 – Flexural strength results of Eco-Bridge-Crete at 56 days**

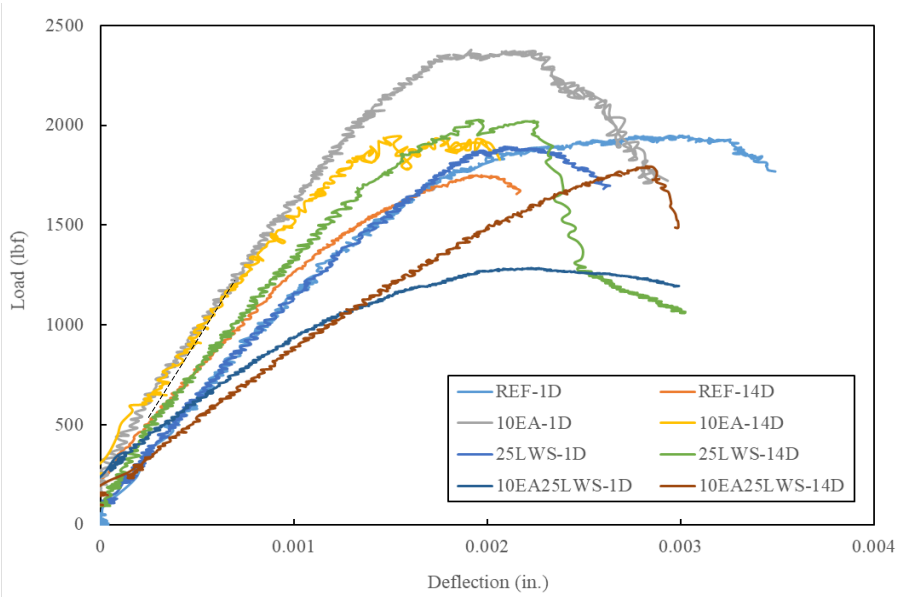
Mixture	Flexural strength, psi	Deflection at peak load, in.	Residual strength at net deflection of L/600, psi	Residual strength at net deflection of L/150, psi	Toughness (area from 0 to L/150), lbf-in.
REF-1D	660	0.041	410	460	40
REF-14D	785	0.0021	N/A	N/A	N/A
10EA-1D	860	0.004	N/A	N/A	N/A
10EA-14D	770	0.002	N/A	N/A	N/A
25LWS-1D	815	0.002	N/A	N/A	N/A
25LWS-14D	925	0.002	N/A	N/A	N/A
10EA25LWS-1D	1365	0.0025	N/A	N/A	N/A
10EA25LWS-14D	1730	0.0025	N/A	N/A	N/A
0.5FR-1D	765	0.0025	435	425	80
0.5FR-14D	780	0.002	625	565	110
10EA0.5FR-1D	1895	0.0026	1055	1166	92
10EA0.5FR-14D	2015	0.0027	1408	1024	100
25LWS0.5FR-1D	1465	0.0026	745	1015	73
25LWS0.5FR-14D	1595	0.0089	1515	1180	111
10EA25LWS0.5FR-1D	650	0.002	335	310	60
10EA25LWS0.5FR-14D	745	0.0025	535	370	90
3EA8LWS0.5FR5D-1	1780	0.0025	1005	965	45
3EA8LWS0.5FR5D-2	1650	0.002	595	515	30
5EA0.25FR7D-1	1655	0.002	465	410	50
5EA0.25FR7D-2	1650	0.0018	395	380	25
5EA0.25FR7D-3	1675	0.002	515	475	25
5EA0.25FR7D-4	1655	0.002	545	510	25
7EA8LWS14D-1	1875	0.002	1315	-	-
7EA8LWS14D-2	1685	0.002	1230	-	-

**Note:** N/A denotes samples with abrupt failure.

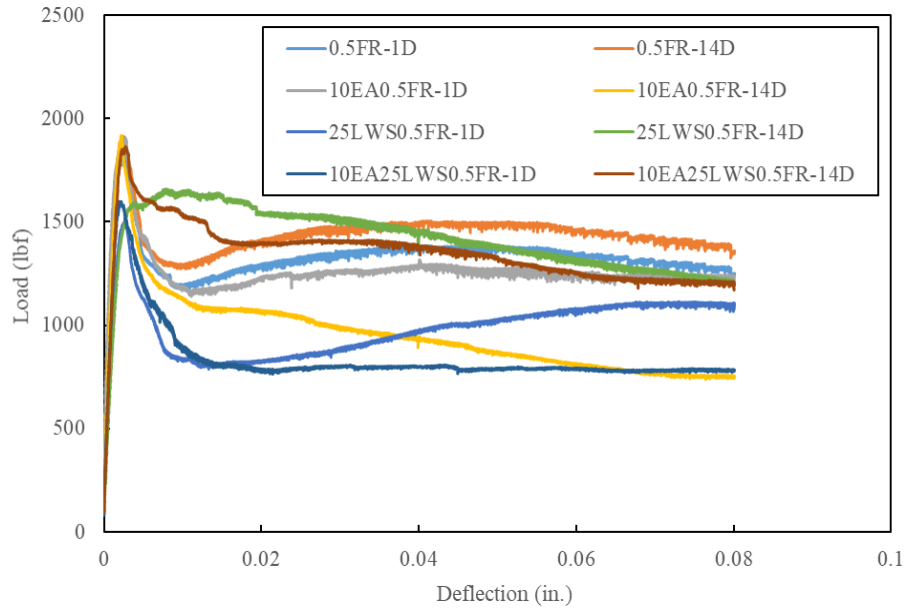
**Figure 3-1** shows the high ductility of the FRC compared to the mixture made without any fibers.

An increase in initial moist curing from 1 to 14 days for the 0.5FR mixture resulted in a

significant enhancement of residual strengths at deflection values of L/600 and L/150 where the residual strength increased from 335 psi to 1515 psi and 310 psi to 1180 psi, respectively. This gain suggests an improvement of bond strength with increased moist curing duration. For example, the residual strength of the 10EA25LWS0.5FR mixture at L/600 and L/150 increased from 335 to 535 psi and 310 to 370 psi, respectively, with the prolongation of moist curing from 1 to 14 days.



(a)



(b)

**Figure 3-1 – Load vs. deflection of a) non-fiber mixtures and b) fiber-reinforced mixtures**

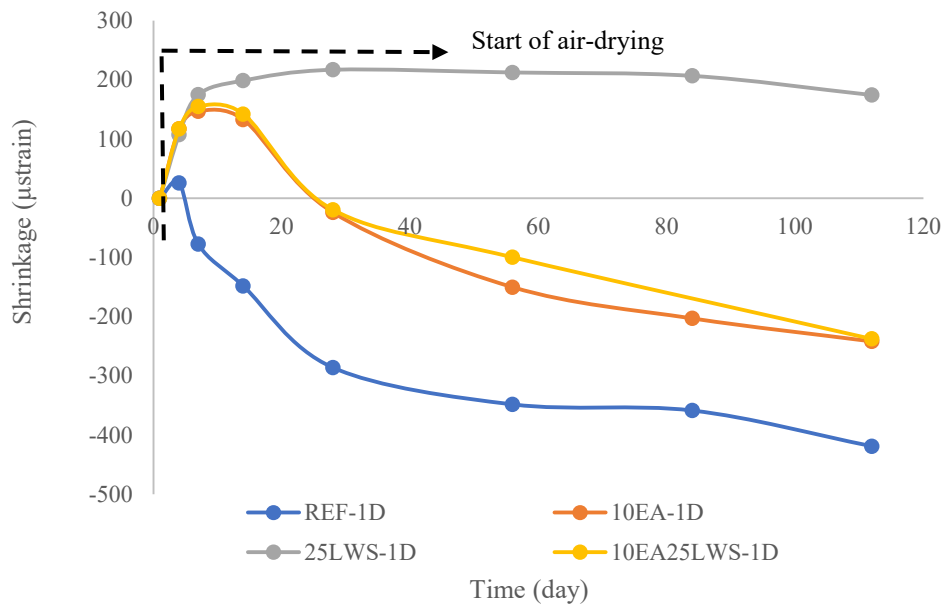
### **Drying shrinkage and restrained expansion**

The drying shrinkage and restrained expansion of the 25 mixtures are reported in **Appendix A**. **Figures 3-2 and 3-3** show the shrinkage results of selected mixtures made with and without fibers subjected to initial moist curing of 1 and 14 days, respectively. The addition of fibers is shown to reduce both the degrees of initial expansion when using an EA and drying shrinkage. For example, according to **Figure 3-2-b**, the addition of 0.5% of steel fiber limited both the initial expansion and final shrinkage by 26% and 23%, respectively.

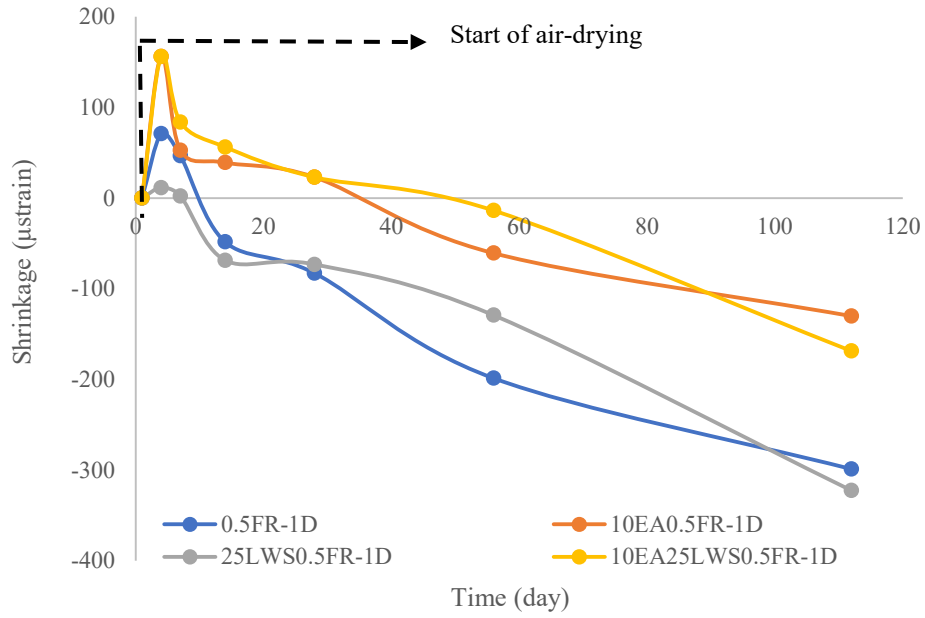
The incorporation of LWS had a significant influence on reducing drying shrinkage. The shrinkage reduced with the increase in moist curing duration from 1 to 14 days. Additionally, for a given curing time, the shrinkage results indicate a delay in the onset of shrinkage for the mixtures made with LWS and EA. Among the non-fiber-reinforced mixtures, those including 25% LWS showed the best shrinkage behavior at both 1 and 14 days of wet curing. In the case of FRC, the 10EA0.5FR mixture showed the lowest volume change in the different curing regimes.

Therefore, as expected, significant shrinkage mitigation was achieved when using 10% EA in addition to 0.5% fiber. This result is consistent with previous research studies (Sun et al., 2001; Corinaldesi et al., 2015).

It is important to note that the drying shrinkage of the investigated mixtures with the various combinations of EA, LWS, and fiber resulted in shrinkage compensation and reduction in shrinkage values that are significant compare to standard MoDOT reference concrete for bridges. As reported in MoDOT/RE-CAST TR2015-03, MoDOT reference concrete can develop a maximum drying shrinkage of 500  $\mu$ strain. Such air-entrained concrete is proportioned with 25% Class C fly ash and a w/cm of 0.40. The reference concrete was reported to develop 56-day compressive and flexural strengths of 7830 and 800 psi, respectively, and a 91-day modulus of elasticity of 5510 ksi (MoDOT/RE-CAST TR2015-03).

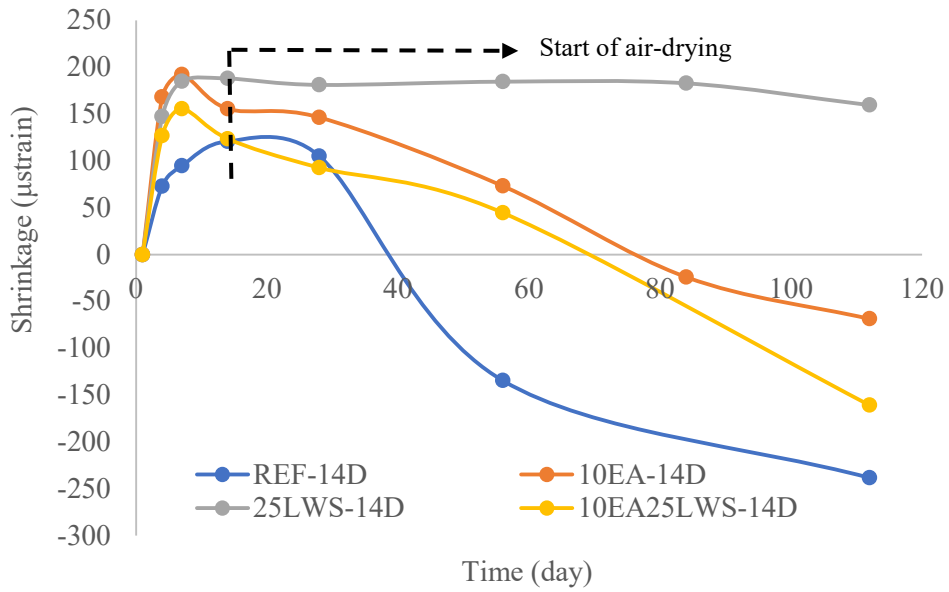


(a)

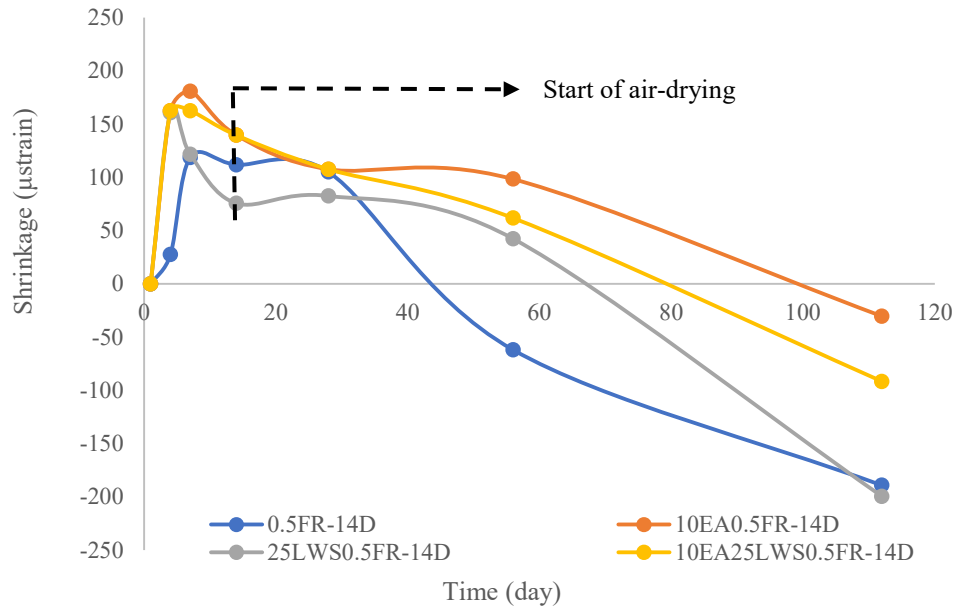


(b)

**Figure 3-2 – Shrinkage of a) non-fiber Eco-Bridge-Crete, b) fiber-reinforced Eco-Bridge-Crete mixtures subjected to 1-day moist curing**



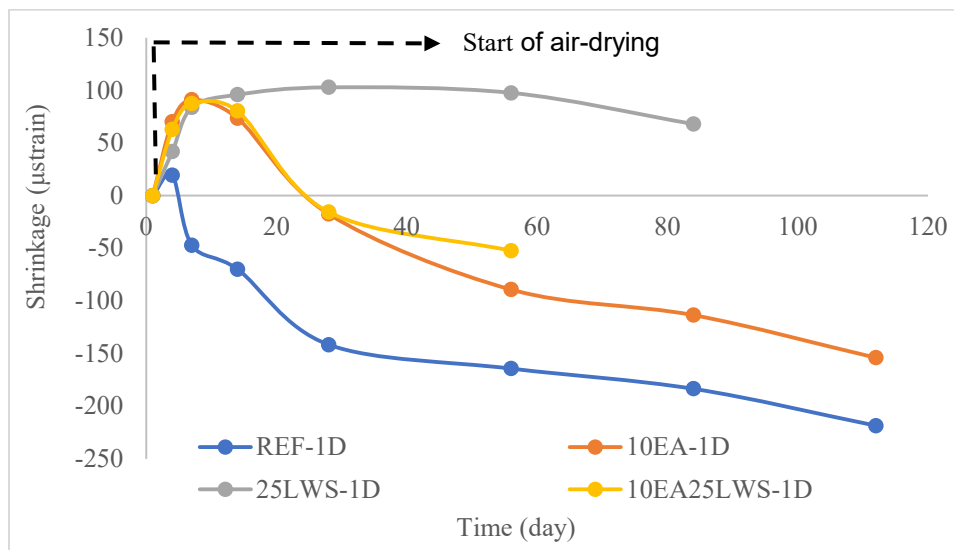
(a)



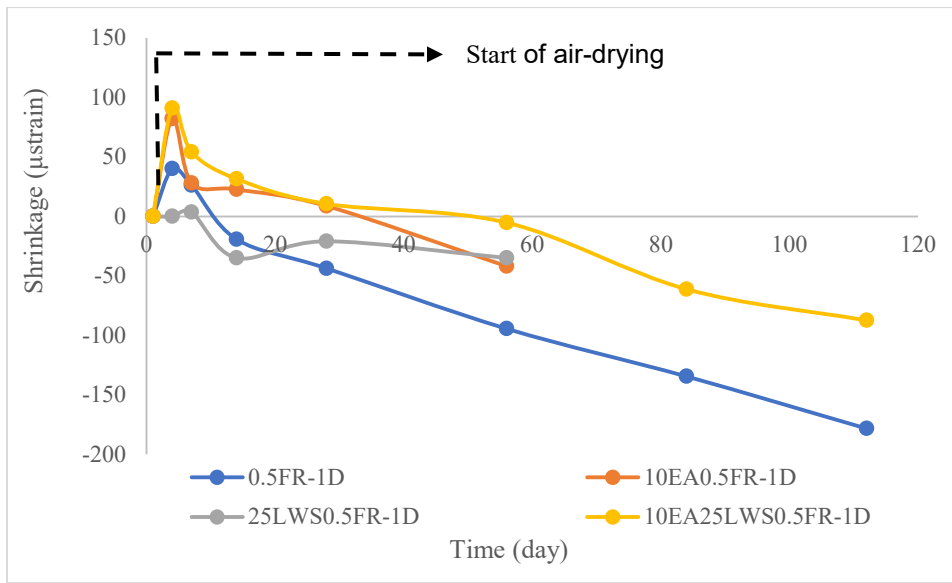
(b)

**Figure 3-3 – Shrinkage of a) non-fiber Eco-Bridge-Crete and b) fiber-reinforced mixtures subjected to 14 day-moist curing**

Figures 3-4 and 3-5 show the variations in restrained expansion with time for selected Eco-Bridge-Crete mixtures made with and without fiber and initial moist curing durations of 1 and 14 days, respectively.

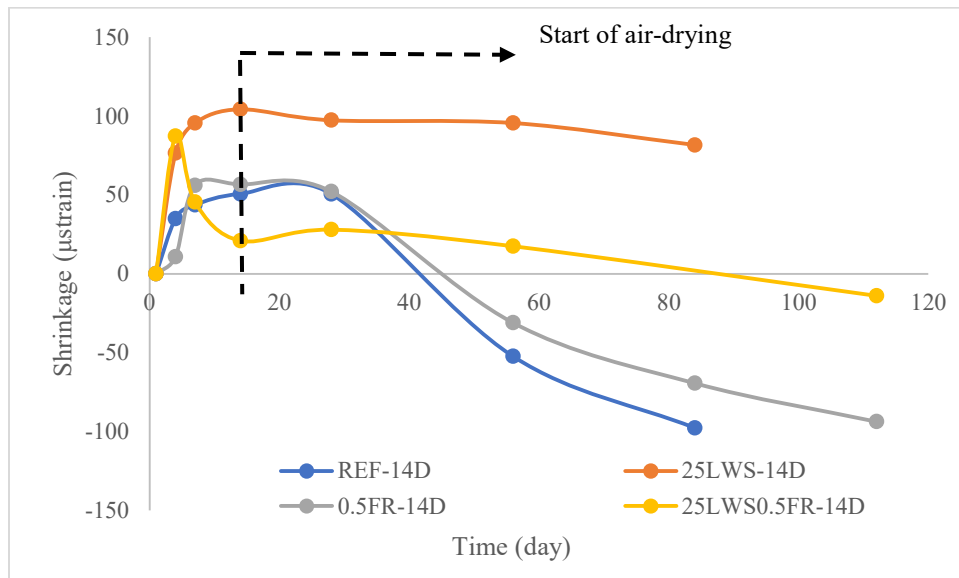


(a)

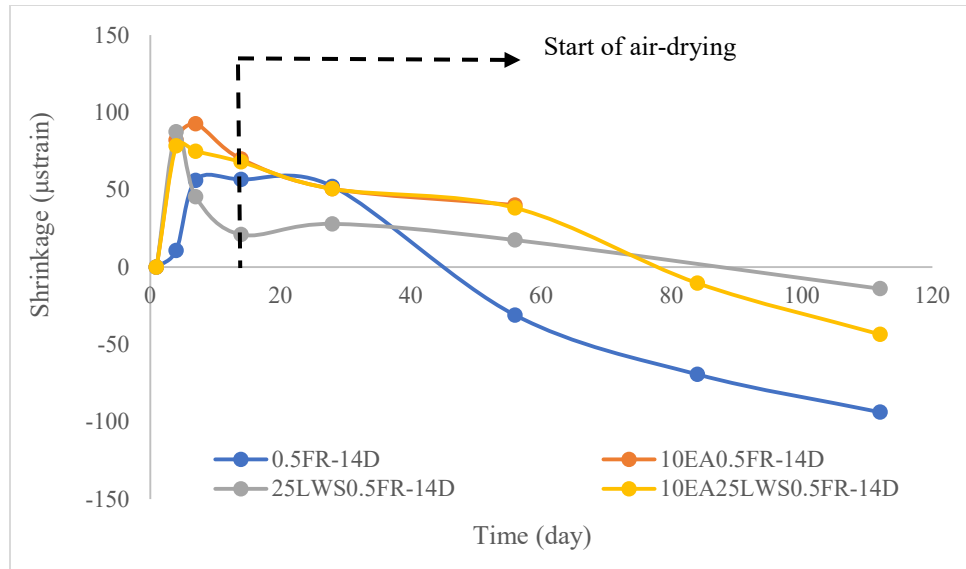


(b)

**Figure 3-4 – (a) Restrained expansion of non- fiber Eco-Bridge-Crete, and (b) fiber-reinforced mixtures subjected to 1-day moist curing**



(a)



(b)

**Figure 3-5 – (a) Restrained expansion of non-fiber Eco-Bridge-Crete, and (b) fiber-reinforced mixtures subjected to 14 days moist curing**

The results in **Figures 3-4 and 3-5** indicate that the presence of EA delayed the onset of shrinkage. The use of LWS reduced the shrinkage, considerably. Similar to drying shrinkage, the restrained expansion results showed a reduction in shrinkage with the addition of fibers and the extension of the moist curing duration from 1 to 14 days. For the tested duration, the non-fiber-reinforced mixture, including LWS (i.e., 25LWS-1D and 25LWS-14D mixtures), presented a promising behavior with low shrinkage. Among the investigated FRC, the 10EA0.5FR mixture was selected as an optimum mixture. Additional mixtures with intermediate contents of EA, LWS, FR, and different curing durations were also cast and tested for use as validation points of the factorial design models.

### **Factorial design optimization**

Statistical models were derived from the 25 concrete mixtures investigated in Task I-A to estimate the effect of three mixture design parameters (EA, LWS, and fiber contents) and the initial moist curing (MC) period on key parameters of Eco-Bridge Crete. The mixture parameters



having significant effects on the various mechanical and viscoelastic properties are summarized in **Table 3-4**.

**Table 3-4 – Derived statistical models**

Parameters and interactions	28-day compressive (MPa)	56-day compressive (MPa)	56-day flexural (MPa)	7-day shrinkage ( $\mu$ strain)	56-day shrinkage ( $\mu$ strain)	7-day expansion ( $\mu$ strain)	56-day expansion ( $\mu$ strain)
Intercept	44.15	42.88	7.96	112.2	-30.8	60.7	-12.4
EA	-2.98	-2.13	1.18	27.1	-	15.6	-
LWS	-8.91	-3.94	0.54	20.8	73.4	-	27.8
MC	7.95	3.89	-	38.9	66.5	21.0	40.9
Fiber	-6.93	-2.11	1.08	-	-	-	-
EA*LWS	-	-	-0.94	-	-62.8	-	-25.5
EA*MC	-	-	-	-	-	-9.6	-
LWS*MC	-	-	-	-	-	-	16.1
EA*Fiber	-	2.05	-	-	37.7	-11.0	-
LWS*Fiber	-3.19	-1.79	-0.9	-	-44.9	-13.9	-26.4
MC*Fiber	-	-	-	-	-	-	-
EA*LWS*MC	-	-	-	-	-	-	-
EA*LWS*Fiber	5.08	3.6	-2.0	29.5	-50.4	19.5	-26.4
EA*MC*Fiber	-	-	-	-	-	-	-
LWS*MC*Fiber	-	-2.03	-	-	-	-	-

**Note:** (-) denotes that the effect of parameter is less or not significant. 1MPa = 145 psi.

The derived models for predicting the key concrete properties are also presented in **Table 3-5**. For each model, the influence of the four input factors and their binary and ternary interactions that have significant effects on the modeled responses are indicated. A positive sign of a given coefficient denotes that the increase in that factor (e.g., EA) can increase the magnitude of the investigated property, and vice versa for a negative sign. The input factors are expressed in coded values (-1 to +1), and the magnitude of the various coefficients correspond to their relative influence on the modeled property. The  $R^2$  values for the derived models were greater than 0.90, and the probability value ( $P_{\text{value}}$ ) (under the null hypothesis) was less than 0.1, which reflects the reliability of the derived models.

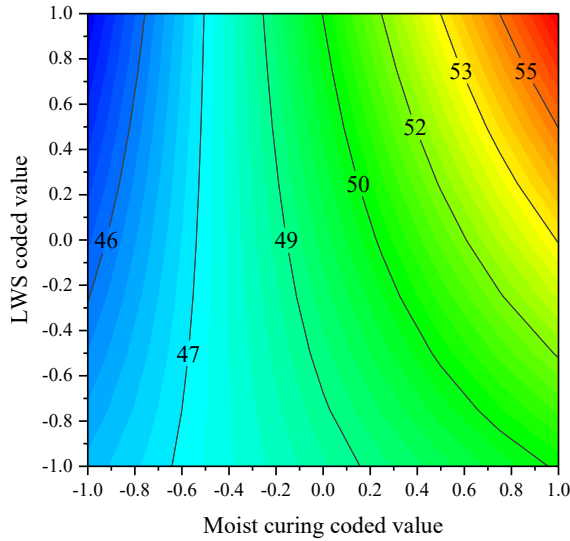
**Table 3-5 – Derived statistical models (based on coded values)**

Derived statistical models (based on coded value)
<b>Response 28-day compressive strength (MPa) <math>R^2 = 0.99</math>, <math>P_{\text{value}} = 0.0032</math></b>
44.15 - 8.91LWS + 7.95MC - 6.93Fiber + 5.08EA*LWS*Fiber - 3.19LWS*Fiber - 2.98EA
<b>Response 56-day compressive strength (MPa) <math>R^2 = 0.93</math>, <math>P_{\text{value}} = 0.0633</math></b>
42.88 - 3.94LWS + 3.89MC + 3.06EA*LWS*Fiber - 2.13EA+2.05EA - 2.11Fiber - 2.03LWS*MC*Fiber - 1.79LWS*Fiber
<b>Response 56-day flexural strength (MPa) <math>R^2 = 0.99</math>, <math>P_{\text{value}} = 0.0038</math></b>
7.96 - 2.0EA*LWS*Fiber + 1.18EA + 1.08Fiber - 0.94EA*LWS - 0.9LWS*Fiber + 0.54LWS
<b>Response 7-day drying shrinkage (<math>\mu</math>strain) <math>R^2 = 0.94</math>, <math>P_{\text{value}} = 0.0591</math></b>
112.2 + 38.9MC - 29.5EA*LWS* Fiber + 27.1EA + 20.8LWS
<b>Response 56-day drying shrinkage (<math>\mu</math>strain) <math>R^2 = 0.97</math>, <math>P_{\text{value}} = 0.0127</math></b>
-30.8 + 73.4*LWS + 66.5*MC-62.8EA*LWS - 50.4 EA*LWS*Fiber - 44.9LWS*Fiber + 37.7EA*Fiber
<b>Response 7-day restrained expansion (<math>\mu</math>strain) <math>R^2 = 0.94</math>, <math>P_{\text{value}} = 0.0786</math></b>
60.7 + 21MC + 19.5EA*LWS*Fiber + 15.6EA - 13.9LWS*Fiber - 11EA *Fiber - 9.6EA *MC
<b>Response 56-day restrained expansion (<math>\mu</math>strain) <math>R^2 = 0.95</math>, <math>P_{\text{value}} = 0.0758</math></b>
-12.4 + 40.9MC + 27.8LWS - 26.4LWS*Fiber - 26.4 EA*LWS*Fiber - 25.5EA*LWS + 16.1LWS*MC

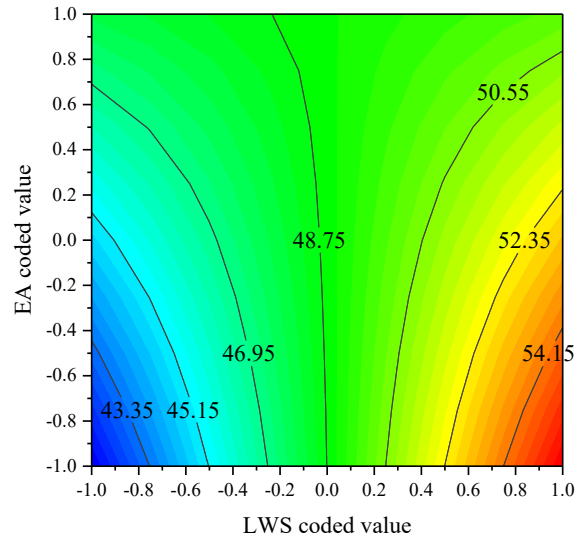
**Figure 3-6** presents contour diagrams showing the trade-off between the 56-day compressive and flexural strengths of Eco-Bridge-Crete with changes in two modeled factors (e.g., LWS and MC) with the other two factors (e.g., EA and Fiber). The derived statistical models indicate that the increase in LWS improves the 56-day compressive strength with the appropriate moist curing duration, while the increase in curing duration increases mechanical properties. With relatively low EA content, the increase in LWS improves the 56-day compressive strength, while with a higher EA content, the increase in LWS has a limited effect on compressive strength. **Figure 3-6-a** indicates that for a concrete made without any EA or fiber (coded values of -1), an increase in either LWS or MC can lead to gain in compressive strength when the minimum MC period is set to approximately -0.2 coded value (approximately 3.5 days). **Figure 3-6-b** shows that the

increase in LWS for a given EA content can increase the 56-day compressive strength for mixtures made without any fibers and subjected to only one day of moist curing (coded values of -1). For example, concrete made with an EA coded value of 0 (6% by mass of cement) can exhibit an increase in the 56-day compressive strength from approximately 45 to 53 MPa (6530 to 7690) psi if the LWS is increased from -1 to +1 (0 to 25%).

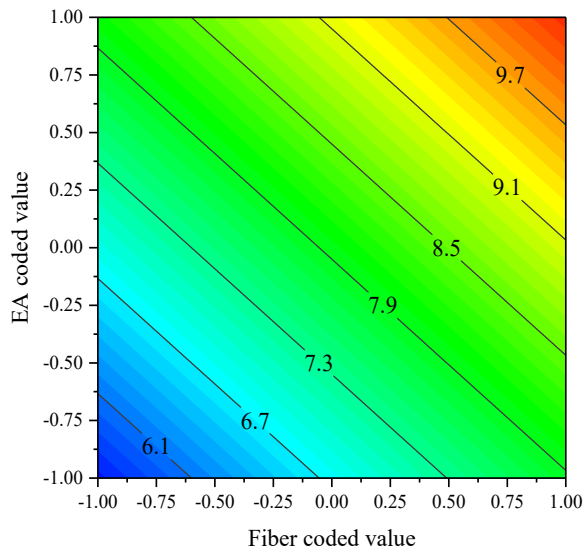
The contour diagrams indicate that the combined use of EA, LWS, and fiber can significantly increase the 56-day flexural strength by as much as 35%. The curing duration is the most significant factor for reducing shrinkage, while the LWS and EA contents can significantly reduce shrinkage. **Figure 3-6-c** illustrates that for a mixture made with 0.25% fibers, 12.5% LWS, and MC of 7 days (coded values of 0 for the three factors), the increase in EA content from 0 to 6% (coded values of -1 to +1) can increase the 56-day flexural strength from 6.8 to 9.1 MPa (985 to 1320 psi). The observed enhancement can be attributed to chemical pre-stressing of steel fibers induced by early age expansion. **Figure 3-6-d** also indicates the significant effect of using LWS and fiber contents on flexural strength. The increase in fiber content from -1 to +1 (0 to 0.5%) can increase the 56-day flexural strength from 6.5 to 8.4 MPa (940 to 1235 psi) for concrete made with LWS coded value of -0.5 (approximately 6%), and EA and MC coded values of 0 (6% and 7.5 days, respectively).



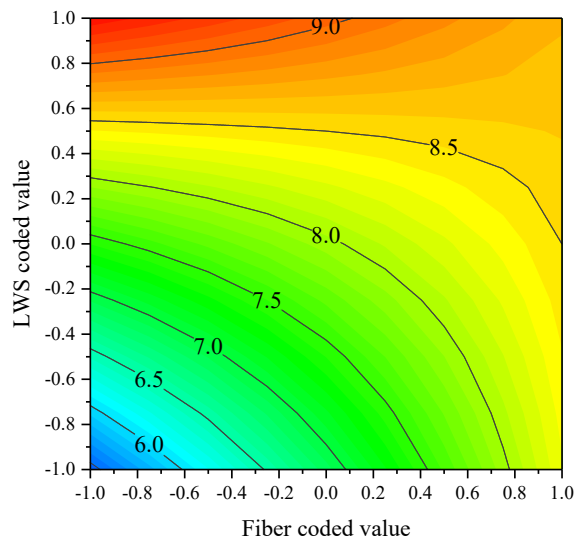
(a) EA and Fiber coded values as -1, -1



(b) Fiber and MC coded values as -1, 1



(c) LWS and MC coded values as 0, 0



(d) EA and MC coded values as 0, 0

**Figure 3-6 – Contour diagrams of effects of EA, LWS, Moist curing (MC) and Fiber content on 56-day compressive strength (a) and (b), 56-day flexural strength (c) and (d)**

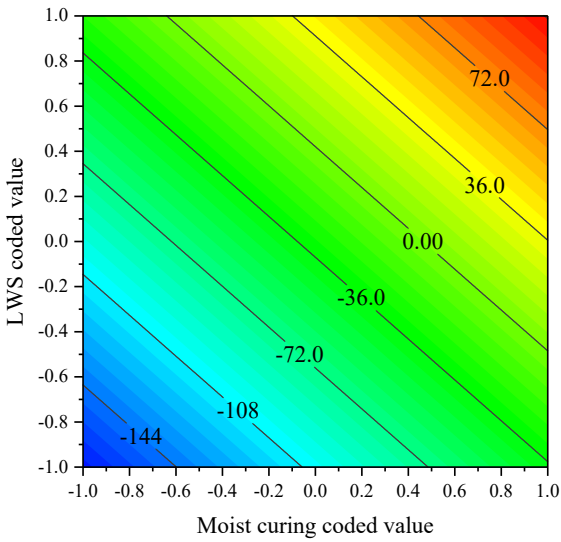
**Figure 3-7** presents contour diagrams showing the trade-off between the 56-day drying shrinkage and 56-day restrained expansion with changes in two modeled factors with the other two factors held constant. The analysis indicates a significant benefit/collective role of internal and external curing on the mitigation of drying shrinkage and restrained expansion. For example, **Figure 3-7-a** shows that the increase in LWS from -1 to +1 (0 to 25%) in concrete subjected to

moist curing period of -0.6 (approximately 3.5 days) can lead to shrinkage reduction of 145  $\mu$ strain after 56 days; the latter value corresponds to no net drying shrinkage after 56 days due to the initial expansion and shrinkage compensation effect of the EA.

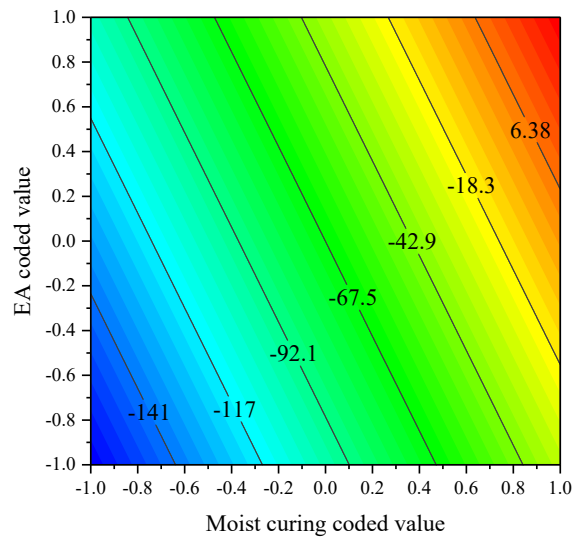
The increase LWS from -1 to +1 (0 to 25%) in concrete subjected to a moist curing period of 0.4 (10 days) can also lead to a change of restrained expansion from approximately -30 to + 40  $\mu$ strain after 56 days, as shown in **Figure 3-7-c**.

Other contour diagrams showing trade-offs between the various modeled factors of key properties of Eco-Bridge-Crete are included in **Appendix B**.

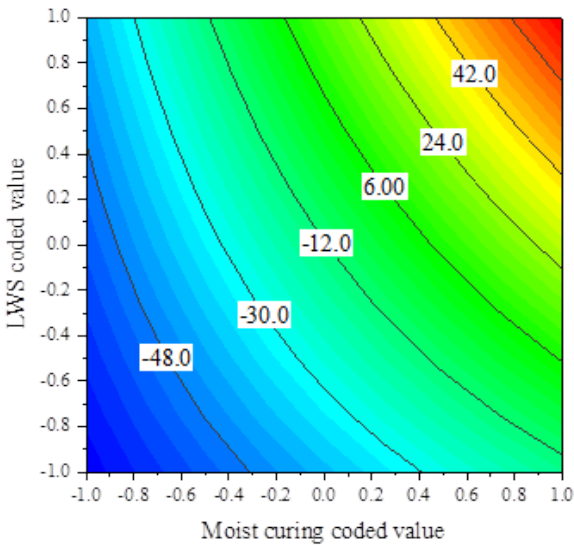
**Table 3-6** shows the relative effect of the four input factors on the different modeled mechanical and viscoelastic properties. The number of (+) or (-) signs shown in the table correspond to the degree of influence (increase or decrease, respectively) of a given input factor on the modeled response. Mixture optimization seeks to increase mechanical properties and decrease viscoelastic properties (i.e., reduce drying shrinkage). A (=) refers to the insignificant effect of the input factor on the associated property.



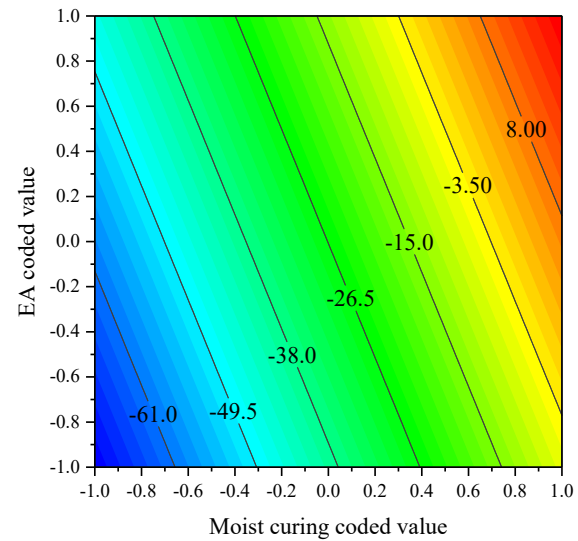
(a) EA, Fiber coded values as 0, 0



(b) LWS and Fiber coded values as -0.5, 0



(c) EA and Fiber coded values as 0, 0



(d) LWS and Fiber coded values as -0.5, 0

**Figure 3-7 – Contour diagrams of effects of EA, LWS, Moist curing (MC) and Fiber content on 56-day drying shrinkage (a) and (b), 56-day restrained expansion (c) and (d)**

The relative analysis of the results in **Table 3-6** indicates that an increase in fiber volume can have a very positive effect (++) on the 56-day flexural strength with the presence of intermediate contents of EA and LWS and MC period (-0.5 and 0 coded values). On the other hand, at coded values of -1 or +0.5 of these factors, the increase in fiber volume can lead to a degree of enhancement (+) of flexural strength. The increase in LWS up to the coded value of 0.5 is shown

to slightly increase the flexural strength; beyond that limit, a reduction in flexural strength can take place. The increase in the EA content with the presence of intermediate contents of LWS and fibers and MC duration (0 and -0.5 coded values) can lead to enhanced flexural properties and reduced shrinkage. However, the use of such values of EA had a negative effect (--) on compressive strength at 28 days, which can be attributed to microcracking of the cement paste at an early age under unrestrained expansion conditions

**Table 3-6 – Relative effect of four parameters on the different properties**

Recommended mixtures				28-day comp. strength	56-day flexural strength	7-day shrinkage	56-day shrinkage	7-day expansion	56-day expansion
Coded value									
EA	LWS	MC	Fiber						
↑	-1	-1	-1	-	+	---	--	+++	++
↑	-0.5	-0.5	-0.5	--	++	--	-	++	+
↑	0	0	0	--	++	--	-	++	+
↑	0.5	0.5	0.5	-	+	-	-	+	+
-1	↑	-1	-1	+	+	---	---	+++	+++
-0.5	↑	-0.5	-0.5	-	+	--	---	++	++
0	↑	0	0	---	+	-	-	+	++
0.5	↑	0.5	0.5	---	-	-	-	=	=
-1	-1	↑	-1	+++	=	--	---	++	++
-0.5	-0.5	↑	-0.5	+++	=	--	---	++	++
0	0	↑	0	+++	=	--	-	++	+
0.5	0.5	↑	0.5	++	=	--	-	+	+
-1	-1	-1	↑	+	+	--	--	++	++
-0.5	-0.5	-0.5	↑	-	++	=	=	+	++
0	0	0	↑	--	++	=	=	=	=
0.5	0.5	0.5	↑	--	+	=	=	=	=

**Note:** number of + or – signs indicates extent of increase or decrease in measured response, while = refers to insignificant effect of input factor on associated property.

The derived statistical models in **Table 3-5** were employed to optimize the Eco-Bridge-Crete mixtures using a numerical optimization technique that estimates desirability indices according to the responses of the materials properties (Montgomery, 2017). For a material property with the goal of securing a minimal response (i.e., minimum shrinkage), the desirability can change linearly from -1 at the lower limit to 0 at the upper limit. Similarly, for a material property with a

goal of maximizing the performance (i.e., enhanced flexural strength), the desirability can vary linearly from 1 at the upper limit to 0 at the lower limit. A higher desirability index (D) indicates a greater performance level (Lotfy et al., 2014; Montgomery, 2017).

With the desirability indices corresponding to the modeled properties shown in **Table 3-7**, an overall desirability index was defined to represent the overall performance of each concrete (Meng et al., 2018; Montgomery, 2017). The significance level of each factor was based on the relevance of the associated property to the desired performance of the concrete for used for bridge construction (i.e., maximize flexural strength and minimize drying shrinkage). The coded values of the EA, LWS, and fiber contents and moist curing period of the concrete with the highest desirability (D) were 1, -1, 1, 0, respectively. The moist curing value was then set to 0, and the overall desirability values of all mixtures were calculated and compared.

**Table 3-7 – Performance optimization and significant levels to estimate overall desirability**

Properties	Significant Level
28-day compressive strength	2
56-day flexural strength	5
7-day drying shrinkage	1
56-day drying shrinkage	2
7-day restrained expansion	1
56-day restrained expansion	2

Seven mixtures with the highest desirability were then identified and are listed in **Table 3-8**. Some of these mixtures were selected for further evaluation in Task I-B to investigate the effect of the modeled four response factors as well as fiber type on key characteristics of mixture Eco-Bridge-Crete and FR-SWC. As elaborated in **Table 3-8**, the investigated mixtures selected for further testing in Task I-B are prepared with EA contents of 5% and 10%, LWS contents of 0 to 25%, a fixed fiber volume of 0.5%, and subjected to 7 days of moist curing.



**Table 3-8 – Seven mixtures with high overall desirability values and four selected mixtures with different desirability values**

Recommended mixtures								Desirability	28-day compressive Strength, MPa	56-day flexural strength, MPa	7-day shrinkage, $\mu$ strain	56-day shrinkage, $\mu$ strain	7-day expansion, $\mu$ strain	56-day expansion, $\mu$ strain
Coded value				Absolute value										
EA	LWS	Curing	Fiber	EA (%)	LWS (%)	Curing (day)	Fiber (%)							
1	-1	0	1	10	0	7	0.5	0.7788	44	13.5	105	-8	61	-1
0.5	-1	0	1	10	0	7	0.5	0.7186	46	11.4	99	-39	62	-7
1	-0.5	0	1	10	6.3	7	0.5	0.7025	41	11.8	110	-1	61	-2
0	-1	0	1	5	0	7	0.5	0.6391	48	9.4	94	-69	64	-14
0.5	0	0	1	7.5	12.5	7	0.5	0.6175	40	9.6	105	-16	58	-7
0	0	0	1	5	12.5	7	0.5	0.6077	40	9.0	94	-41	54	-12
0	0.5	0	1	5	18.8	7	0.5	0.5846	36	8.9	95	-27	49	-11

Recommended mixtures								Desirability	28-day compressive Strength, MPa	56-day flexural strength, MPa	7-day shrinkage, $\mu$ strain	56-day shrinkage, $\mu$ strain	7-day expansion, $\mu$ strain	56-day expansion, $\mu$ strain
Coded value				Absolute value										
EA	LWS	Curing	Fiber	EA (%)	LWS (%)	Curing (day)	Fiber (%)							
1	-1	0	1	10	0	7	0.5	0.7788	44	13.5	105	-8	61	-1
0	0	0	1	5	12.5	7	0.5	0.6077	40	9.0	94	-41	54	-12
0	1	0	1	5	25	7	0.5	0.5541	33	8.7	95	-12	45	-11
1	1	0	1	10	25	7	0.5	0.4403	33	6.8	128	24	64	-4

**Note:** 1MPa = 145 psi.

### **3.1.2 Task I-B: Performance of selected FR-SWC and Eco-Bridge-Crete mixtures made with different fibers**

As mentioned earlier, four optimized EA-LWS-fiber systems associated with Eco-Bridge-Crete were selected from Task I-A to enhance the characteristics of reference Eco-Bridge-Crete (EBC) and FR-SWC mixtures recommended in the MoDOT/RE-CAST TR2015-03 and TR2015-05 investigations, respectively. The mixtures were proportioned using two different types of steel fibers (STST and 5D), and a synthetic fiber (PLP) incorporated at 0.5% by volume. In total, 16 concrete mixtures were investigated, and their mixture proportioning is provided in **Table 2-8**. The concrete was subjected to 7 days of moist curing followed by air curing. As presented in **Table 2-9**, each mixture was tested to determine the unit weight, air content, slump, slump flow, passing ability, surface settlement, drying shrinkage, and restrained expansion.

**Table 3-9** shows the fresh properties of the Eco-Bridge-Crete mixtures, herein denoted as (EBC), and the FR-SWC mixtures. The temperature, air content, and unit weight values of the mixtures ranged between 65 °F and 72 °F, 4.0% and 8.0%, and 134.4 lb/ft<sup>3</sup> and 145.6 lb/ft<sup>3</sup>, respectively. The slump values of the Eco-Bridge-Crete varied between 6 and 8 in., and the slump flow of the FR-SWC ranged between approximately 19 and 25 inches. The modified J-Ring values of the FR-SWC mixtures ranged between approximately 19 and 25 in. and the diameter over the height of the concrete at the conclusion of the test (D/a) was higher than 10.5, indicating high passing ability. The FR-SWC did not exhibit signs of blockage or segregation.

The rate of surface settlement of the FR-SWC determined between 25 and 30 min ranged between 0.06 and 0.19%/hour. These values reflect high stability (< 0.2%/hour for concrete made with ½ in. MSA, which reflects a high resistance to bleeding, segregation, and surface settlement. The rate of surface settlement of the Eco-Bridge-Crete mixtures ranged between 0.04

and 0.25%/hour. For such concrete with MSA of 1 in., high stability can be attained when the rate of settlements is limited to 0.12%/hour. Mixtures with a rate of settlement values greater than 0.25%/hour may exhibit stability issues. Only two of the 16 investigated fiber-reinforced Eco-Bridge-Crete mixtures attained such high settlement rates. Yet, the mixtures did not exhibit signs of bleeding or segregation. It is important to note that the Eco-Bridge-Crete was proportioned with a low binder content (475 pcy) and low paste volume to reduce cost, CO<sub>2</sub> emissions, and shrinkage. The reduction in binder content can reduce stability if proper aggregate gradation is not used, especially when at high slump values associate with FRC.

**Table 3-9 – Fresh properties of FR-SWC and Eco-Bridge-Crete mixtures**

Mixture	T, °F	Slump, in.	Slump flow, in.	Mod. J-Ring		Air vol., %	Unit weight, lb/ft <sup>3</sup>	Surface settlement rate, %/h
				D, in.	D/a			
10EA0.5FR (STST)-FR-SWC	69	-	22.6	22.4	14.2	6.9	139.2	0.14
10EA-0.5FR (5D)-FR-SWC	66	-	20.5	21.2	15.4	8.0	136.7	0.13
5EA12.5LWS0.5FR (STST)-FR-SWC	65	-	21.2	23.4	19.8	6.3	134.8	0.11
5EA12.5LWS0.5FR (5D)-FR-SWC	70	-	24.6	24.1	22.7	6.6	137.0	0.12
5EA25LWS0.5FR (STST)-FR-SWC	72	-	22.4	22.5	22.0	7.2	133.9	0.19
5EA25LWS0.5FR (5D)-FR-SWC	72	-	24.7	25.1	26.5	6.1	137.5	0.08
10EA25LWS0.5FR (STST)-FR-SWC	68	-	19.9	18.6	10.5	8.1	133.0	0.20
10EA25LWS0.5FR (5D)-FR-SWC	65	-	19.4	20.1	14.6	7.9	131.6	0.06
10EA0.5FR (ST)-EBC	71	8	-	-	-	4.9	141.7	0.25
10EA-0.5FR (PLP)-EBC	66	7	-	-	-	5.9	146.2	0.16
5EA12.5LWS0.5FR (ST)-EBC	67	8	-	-	-	5.6	146.0	0.14
5EA12.5LWS0.5FR (PLP)-EBC	69	8	-	-	-	7.2	146.5	0.18
5EA25LWS0.5FR (ST)-EBC	65	7	-	-	-	8.0	140.2	0.15
5EA25LWS0.5FR (PLP)-EBC	64	7	-	-	-	5.5	143.9	0.25
10EA25LWS0.5FR (ST)-EBC	66	8	-	-	-	6.9	142.8	0.15
10EA25LWS0.5FR (PLP)-EBC	69	6	-	-	-	4.0	145.8	0.04

**Figure 3-8** shows the drying shrinkage of the FR-SWC mixtures containing 0.5% STST and 5D fibers. All mixtures incorporated EA that led to an initial expansion. The maximum early expansion was exhibited by the mixtures containing 10% EA (10EA0.5FR (STST)-SWC and 10EA0.5FR (5D)-SWC). Test results showed that the fibers did not significantly restrain early

expansion when a high content of EA was applied. The minimum shrinkage was recorded for the 10EA0.5FR (STST)-SWC and 5EA25LWS0.5FR (5D)-SWC mixtures. In the former mixture, the restrained shrinkage can be attributed to the initial high expansion of 10% EA that reduced shrinkage at later ages. In the latter mixture, the internal curing by the use of 25% LWS reduced shrinkage by providing extra water in the matrix to maintain the internal humidity over time and extend the hydration of the binder and form a denser matrix. The maximum shrinkage was associated with the 5EA12.5LWS0.5FR (STST)-SWC mixture. The results indicate the effectiveness of the increased content of LWS for internal curing and better performance of the 5D fibers in inhibiting shrinkage of FR-SWC mixtures.

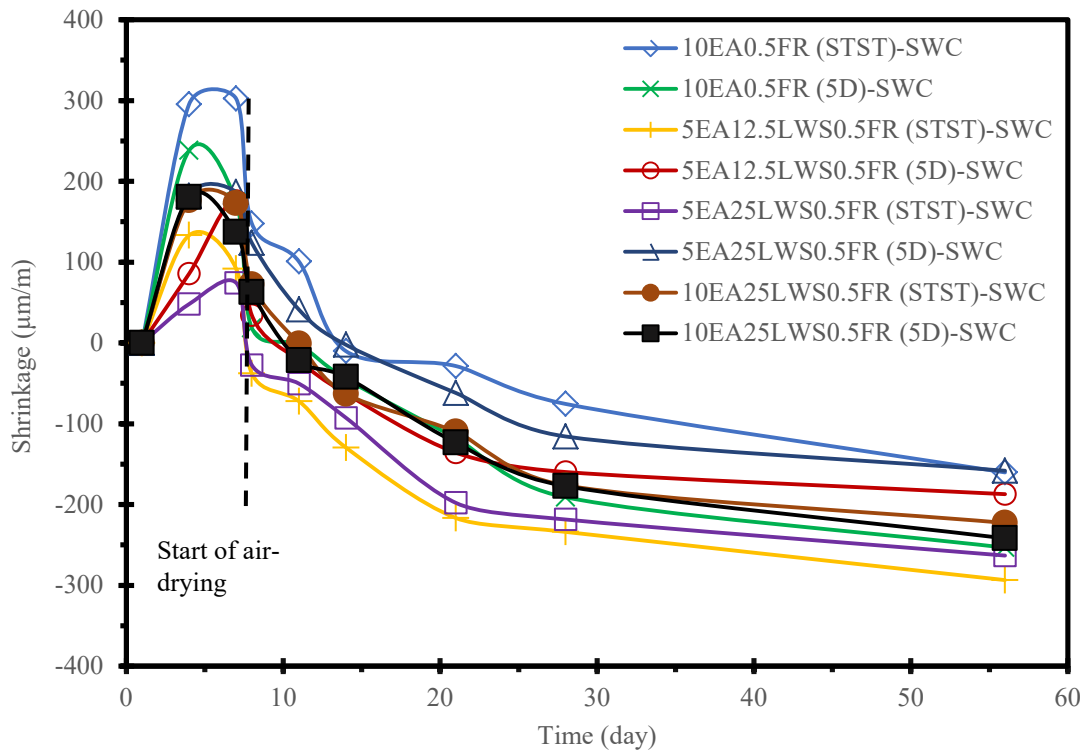


**Figure 3-8 – Drying shrinkage of FR-SWC mixtures containing 0.5% micro-macro steel fiber (STST) and 5D steel fiber (5D)**

**Figure 3-9** compares the shrinkage of EBC mixtures made with PLP and ST fibers. Similar to FR-SWC, the maximum early expansion was obtained during the first 7 days of moist curing for EBC mixtures containing 10% EA, which contributed to lower shrinkage. The comparison between the 10EA0.5FR (PLP)-EBC and 10EA25LWS0.5FR (PLP)-EBC mixtures shows the more significant constraining effect of LWS on shrinkage. Although the mixture with EA experienced higher expansion at early age, mixtures with LWS presented better shrinkage compensation during air-drying conditions. The 10EA25LWS0.5FR (ST) mixture had 43% lower shrinkage than the 10EA25LWS0.5FR (PLP) mixture.

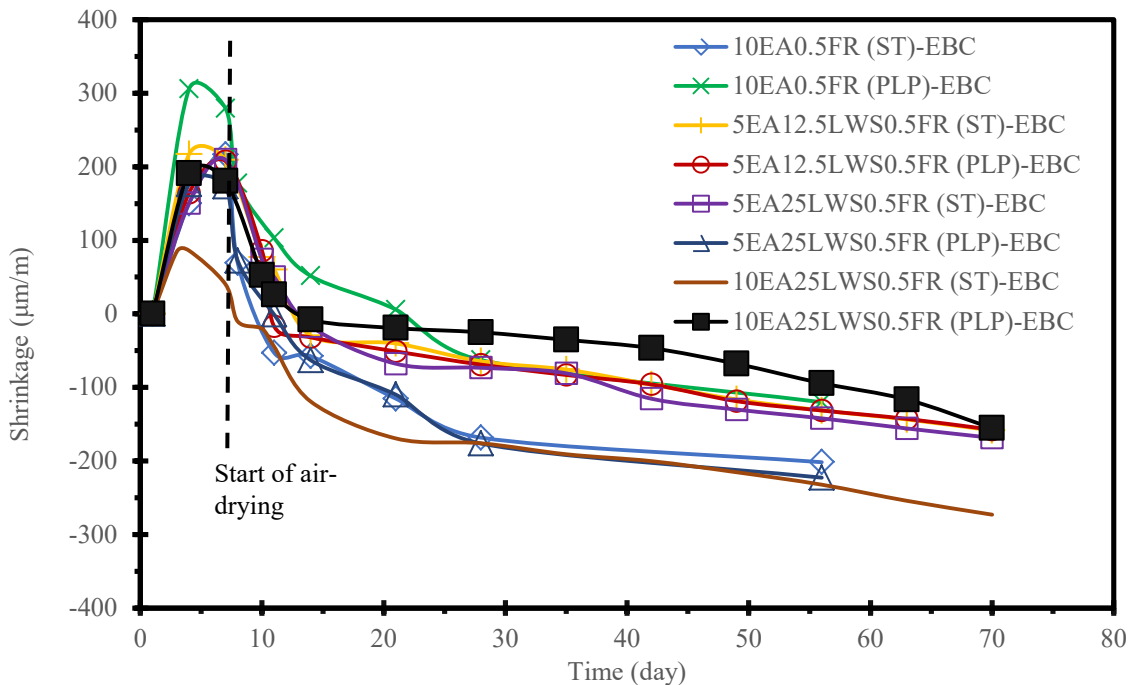


**Figure 3-9 – Drying shrinkage of Eco-Bridge-Crete mixtures made with 0.5% macro synthetic fiber (PLP) and macro steel fiber (ST)**

**Figure 3-10** shows the restrained expansion of FR-SWC mixtures containing 0.5% STST and 5D fiber. The use of these fiber types restricted expansion at all ages and delayed the onset of shrinkage considerably. The maximum expansion was recorded for the 10EA0.5FR (5D)-SWC mixture. The initial expansion associated with the use of 10% EA resulted in almost no shrinkage

at 56 days, total shrinkage compensation. However, such high content of EA can cause undesirable expansion leading to cracking of the cement paste and reduction of strength.

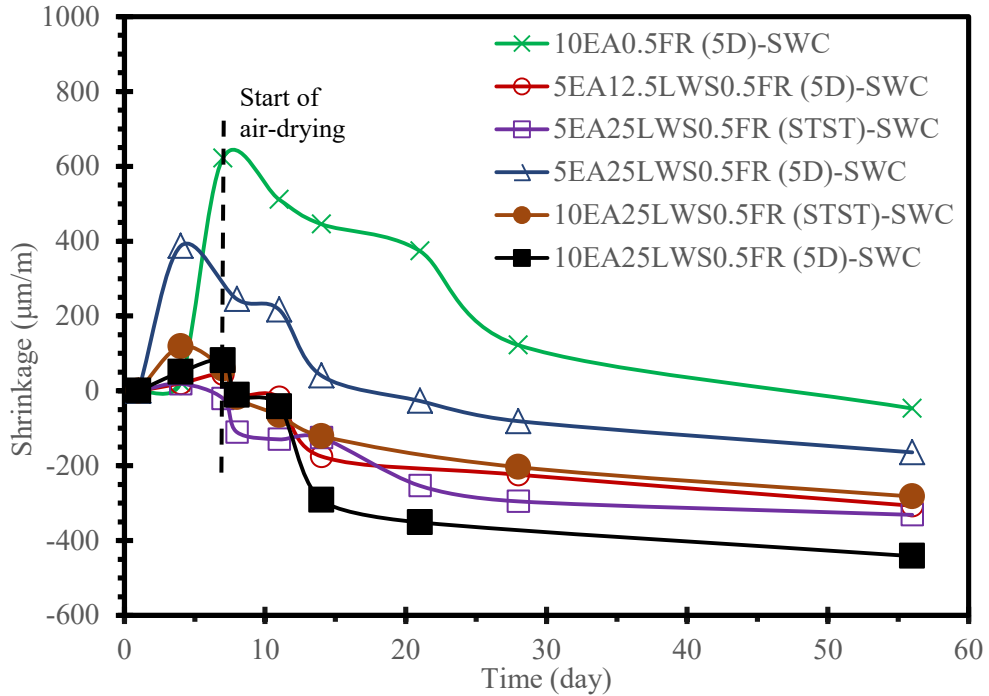


**Figure 3-10 – Restrained expansion test results on FR-SWC mixtures containing 0.5% micro-macro steel fiber (STST) and 5D steel fiber (5D)**

Figure 3-11 shows restrained expansion results on EBC mixtures with PLP and ST fibers. The ST fibers were more effective than the PLP fibers in limiting shrinkage. This is attributed to the higher modulus of elasticity of the steel fibers and their superior performance in confining the concrete matrix.

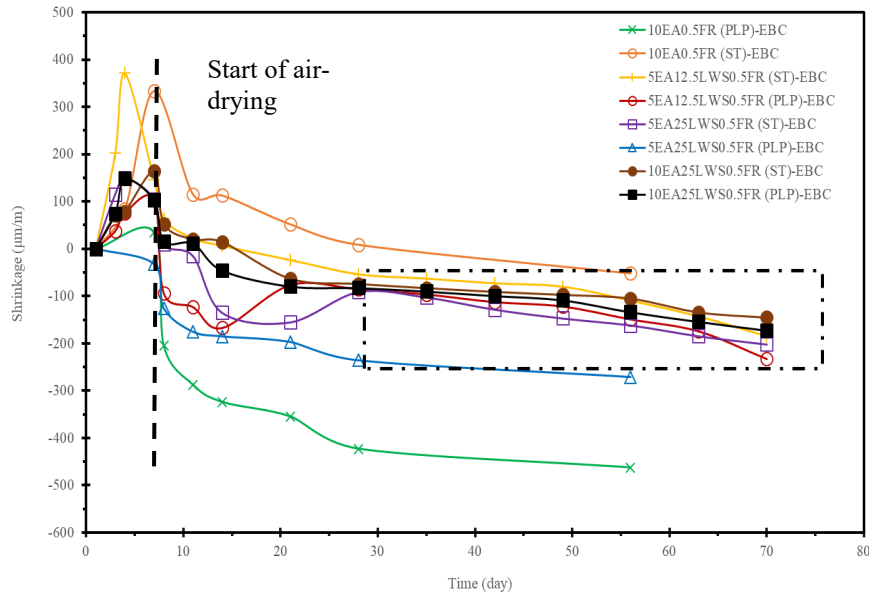


**Figure 3-11 – Restrained expansion test results of Eco-Bridge-Crete mixtures including 0.5% macro synthetic fiber (PLP) and macro steel fiber (ST)**

### 3.1.3 Task I-C: Corrosion resistance of reinforcing bars of optimized Eco-Bridge-Crete

This task focused on evaluating the corrosion resistance of selected Eco-Bridge-Crete mixtures made with different mixture parameters employed to reduce shrinkage and enhance flexural strength and resistance to cracking. Eight corrosion beam elements measuring  $25 \times 3.5 \times 8$  in. were cast. The samples had reinforcing steel bars embedded at cover depths of 1, 1.5, and 2 in. and received either 1 or 7 days of moist curing. The beams were prepared with steel and synthetic fibers at 0 and 0.5%, by volume, 0 and 25% LWS, by volume of sand, and EA at 0 and 5%, by mass of binder. The investigated parameters of the Eco-Bridge-Crete mixtures used to cast the beam elements are presented in **Table 3-10**.

The mixture proportioning of the concrete is reported in **Table 2-10**. As discussed in Section 2.3.2, four sets of beams were used to form a salt tank assembly for accelerated corrosion testing (**Figure 2-9**). The tanks were saturated with water for 5 days before the addition of NaCl (5% by

mass) for the corrosion testing. The tanks were cleaned every 30 to 40 days, and the salt water was replaced.

**Table 3-10 – Combinations of parameters selected for corrosion testing**

Mixture	5% EA	25% LWS	0.5% FR	Moist curing (day)
REF-7				7
0.5FR-7			x	7
5EA0.5FR-7	x		x	7
5EA0.5FR(PLP)-7	x		x*	7
5EA25LWS0.5FR-7	x	x	x	7
5EA0.5FR-1	x		x	1
25LWS0.5FR-1		x	x	1
5EA25LWS0.5FR-1	x	x	x	1

**Note:** \* indicates mixtures with synthetic fibers. Remaining fiber-reinforced mixtures had steel fibers.

For measuring corrosion of the reinforcing bars, the voltage drop across the shunt resistors was measured, and the current value was computed according to Ohm’s law. Therefore, the variations of electrical current across each reinforcing bar and the steel mesh were monitored to detect the onset of cracking due to corrosion. The eight concrete mixtures were also tested to determine the effect of fiber type, internal and external curing, and EA content and their combinations on water sorptivity and bulk resistivity of the concrete after approximately 100 days of age.

**Current variation across samples with chloride exposure time**

The current variations with time for reinforcing bars embedded at 1, 1.5, and 2 in. in the REF-7 and 25LWS0.5FR-1 mixtures are shown in **Figures 3-12-a** and **3.12-b**, respectively. Similar observations for the remaining mixtures are reported in **Appendix C**. The time corresponding to spike in the current gives an indication of concrete cracking due to corrosion. These time



durations are reported in **Table 3-11**. The water sorptivity and bulk resistivity of these investigated mixtures were also measured, and the results are presented in **Table 3-11**. The sorptivity refers to the transport of water into concrete through capillary action. A high value of sorptivity indicates high capillary porosity (Narayan 2006, Lockington and Parlange, 2003). Good correlations are reported in the literature between electrical resistivity of concrete and corrosion rate of reinforcing bars (Alonso et al., 1988; Hornbostel et al., 2013; Taillet et al., 2014).

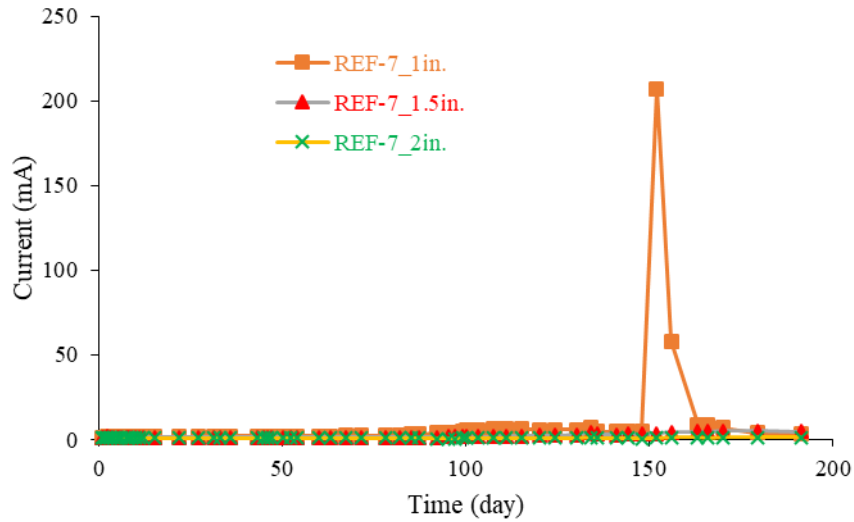
**Table 3-11 – Measured properties of investigated mixtures: Time of cracking due to corrosion (first peak in current), sorptivity and bulk resistivity**

Mixture	Time of first peak in current (day)			Sorptivity ( $10^{-4}$ mm/sec <sup>1/2</sup> )	Bulk Resistivity (ohm.m)
	1 in.	1.5 in.	2 in.		
REF-7	148-152			28.0	379.5
0.5FR-7	111-115			30.6	201.5
5EA0.5FR-7	100-103			38.4	171.0
5EA0.5FR(PLP)-7	148-152			28.4	374.5
5EA25LWS0.5FR-7	148-152			47.8	140.0
5EA0.5FR-1	46-50	78-82		99.8	114.5
25LWS0.5FR-1	50-52			102.4	101.5
5EA25LWS0.5FR-1	136-141			112.2	108.5

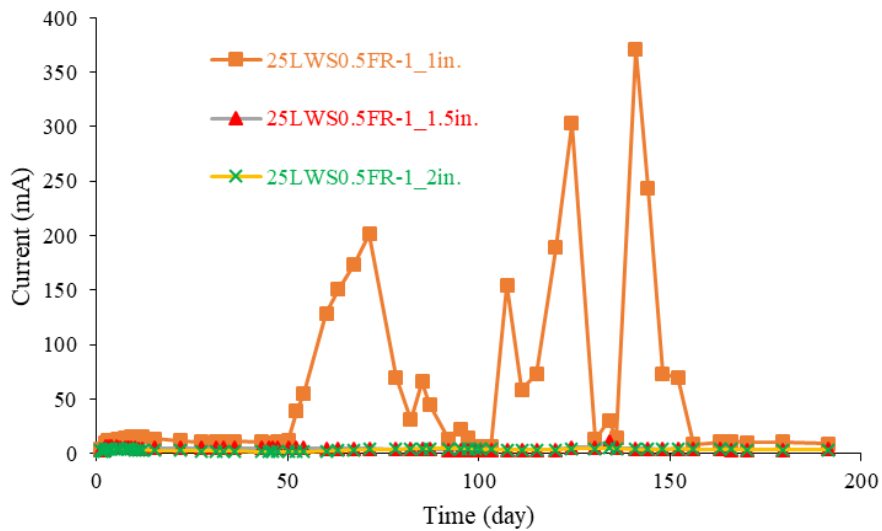
**Note:** Greyed out cells indicate absence of peak in current after 200 days.

All of the investigated mixtures did not exhibit signs of corrosion when the reinforcing bar cover was 2 inches. This was also the case for a cover of 1.5 in., in exception of the 5EA0.5FR-1 mixture. For beams with 1 in. cover, all mixtures exhibited sudden increase in current during the 200-day test period. The two mixtures that had the shortest times to the onset of corrosion were the 5EA0.5FR-1 and 25LWS0.5FR-1 mixtures, where the first peak in current occurred after approximately 50 days. Both of these mixtures received only 1 day of moist curing, with the latter one also prepared with 25% of LWS. While for the REF-7, 5EA25LWS0.5FR-7, and 5EA25LWS0.5FR-7 mixtures, the first peak in current occurred approximately at 150 days.

The results in **Figure 3-12-a** indicate a decrease in electrical current with increased cover depth. In **Figure 3-12-b**, for beams with 1 in. cover, a gradual increase in current from 2 to 200 mA was observed between 50 and 70 days.



(a)



(b)

**Figure 3-12 – Average current variations of reinforcing bars at 1, 1.5, and 2 in. of cover depths for a) REF-7 and b) 25LWS0.5FR-1 mixtures**

This increase is due to the decrease in the resistance as a result of concrete cracking under tensile stress exerted by the expansion of corrosion products. After the peak at 70 days, the drop in the

current can be attributed to the deposition of corrosion products in the concrete cracks (Al-Tayyib et al., 1990).

In order to investigate the influence of fiber type, moist curing type and duration, as well as the effect of EA and LWS contents on corrosion performance, the current plots for the investigated mixtures are compared.

*Influence of EA, LWS, fibers, and moist curing duration on corrosion resistance*

In order to investigate the effects of fiber type and content, moist curing duration, EA content, LWS content, and moist curing type (internal curing by 25% LWS vs. external curing of 7 days) on corrosion resistance, the electrical current, bulk resistivity, and sorptivity values of the selected mixtures are compared. These mixtures selected to investigate the effect each parameter are highlighted in **Table 3-12**.

**Table 3-12 – Mixtures compared to investigate influence of test parameters**

Mixture ID/ Parameter	REF-7	0.5FR-7	5EA0.5FR-7	5EA0.5FR(PLP)-7	5EA25LWS0.5FR-7	5EA0.5FR-1	25LWS0.5FR-1	5EA25LWS0.5FR-1
Fiber content								
Fiber type								
Curing time								
Curing type								
EA								
LWS								
EA & LWS								

**Note:** Colored cells in a given row correspond to concrete mixtures used to compare the various mixtures parameters and curing types.

### Effect of fiber content and type

To understand the effect of fiber addition and type on corrosion resistance, the current values for reinforcing bars with a cover depth of 1 in. used in the REF-7, 5EA0.5FR(PLP)-7, 0.5FR-7, and 5EA0.5FR-7 mixtures are plotted in **Figure 3-13**. Initially, the electrical current of the REF-7 and 0.5FR-7 mixtures was similar (1.4 mA) despite the presence of 0.5% conductive steel fibers in the 0.5FR-7 mixture. This indicates a lack of influence of steel fibers on current density between the anodic reinforcing bars and cathodic galvanized steel mesh. This could be due to the absence of conductive fiber path and electrochemical passivity of the steel fibers in the alkaline environment of concrete (Berrocal et al., 2016; Solgaard et al., 2014). The similar sorptivity values (**Table 3-11**) of the REF-7 and 0.5FR-7 mixtures also indicate no significant difference in transport properties with steel fiber addition. However, a lower bulk resistivity was observed for the 0.5FR-7 mixture.

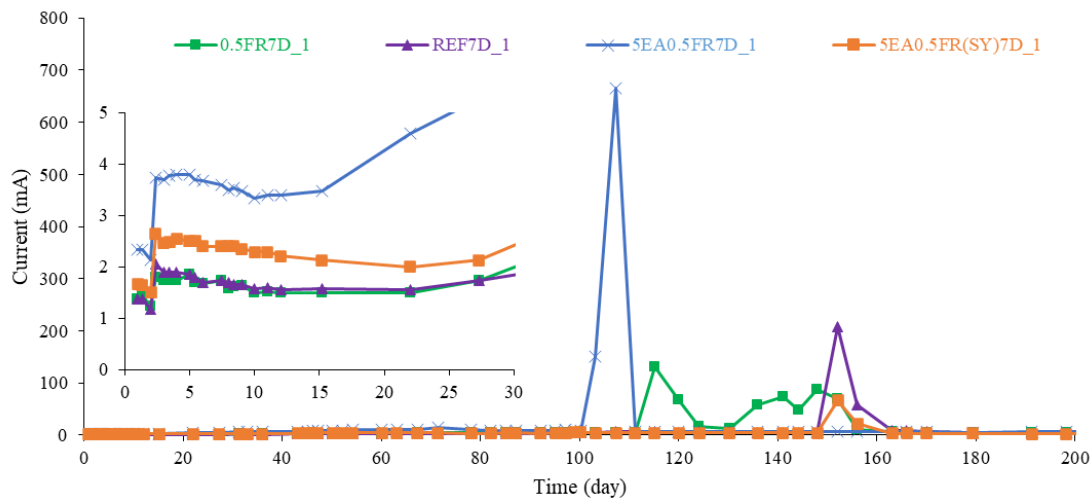


**Figure 3-13 – Influence of fiber content and type on current variation with time for reinforcing bars at 1 in. cover depth**

From **Table 3-11** and **Figure 3-13**, the peaks in the current happened at 111 and 152 days for 0.5FR-7 and REF-7, respectively. This peak in the current is result of cracking due to tensile

stresses exerted by the corrosion products. The early increase in the current for the 0.5FR-7 mixture indicates a decrease in the corrosion resistance with the incorporation of steel fibers.

The effect of fiber type (synthetic vs. steel) can be evaluated by comparing the time for the first peak in current (**Table 3-11**) for the 5EA0.5FR(PLP)-7 and 5EA0.5FR-7 mixtures. The early corrosion at approximately 100 days for the 5EA0.5FR-7 mixture indicates lower corrosion resistance with the steel fibers compared to approximately 150 days for the 5EA0.5FR(PLP)-7 mixture. This lower corrosion resistance for steel fiber reinforced mixtures can be attributed to the corrosion of steel fibers with exposure to  $\text{Cl}^-$  and, consequently, the loss of the steel fiber ability to bridge cracks (Berrocal et al., 2016).

#### Effect of moist curing duration

To understand the effect of moist curing duration on corrosion resistance, the current values for the 5EA0.5FR-7, 5EA0.5FR-1, 5EA25LWS0.5FR-7, and 5EA25LWS0.5FR-1 mixtures with 1 in. the cover depth are plotted in **Figure 3-14**. Based on the initial current values (1 day), the high current for the 5EA0.5FR-1 mixture (5.8 mA) compared to that of the 5EA0.5FR-7 mixture (2.3 mA) indicates a decrease in concrete resistivity with the reduction in moist curing time from 7 to 1 day. These results are in agreement with the bulk resistivity and water sorptivity values reported in **Table 3-11**. The relatively high sorptivity for the 5EA0.5FR-1 mixture ( $99.8 \times 10^{-4}$  mm/sec<sup>1/2</sup>) compared to the 5EA0.5FR-7 mixture ( $38.4 \times 10^{-4}$  mm/sec<sup>1/2</sup>) also indicate increased capillary porosity with the decrease in moist curing duration. Similar conclusions can be made by comparing the 5EA25LWS0.5FR-7 and 5EA25LWS0.5FR-1 mixtures.

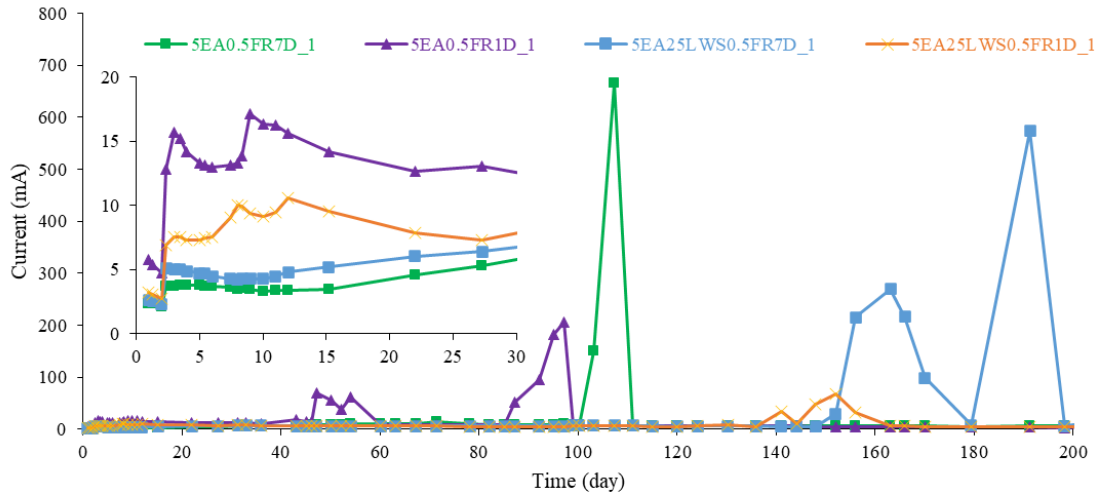


**Figure 3-14 – Influence of moist curing duration on current variation with time for reinforcing bars at 1 in. cover depth**

As shown in **Figure 3-14**, the 5EA25LWS0.5FR-7 mixture with 7 days of moist curing had an increase in current initially during the test period of 200 days. However, for the 5EA25LWS0.5FR-1 mixture that received only 1 day of moist curing, there was an opposite trend; i.e., a decrease in current with the increased exposure time. This could be due to hydration of cement and EA in the 5EA25LWS0.5FR-1 mixture upon water exposure (from NaCl solution), resulting in porosity reduction with time. Whereas for the 5EA25LWS0.5FR-7 mixture, significant hydration may have happened during the 7 days of moist curing with no significant impact on hydration degree when exposed to NaCl solution. From **Table 3-11**, the peak in the current was observed for both the 5EA25LWS0.5FR-1 and 5EA25LWS0.5FR-7 mixture at approximately 140 days. This indicates that the influence of curing time was not significant for mixtures with EA and LWS.

Comparing the 5EA0.5FR-7 and 5EA0.5FR-1 mixtures that had different initial curing times, the sudden increase in current in the first 50 days indicates low corrosion resistance for the latter mixture that had only 1 day of moist curing. From **Table 3-11**, the earlier appearance of the first

peak for the 5EA0.5FR-1 mixture compared to the 5EA0.5FR-7 mixture also indicates reduced corrosion resistance with the decrease in moist curing duration for mixtures with EA.

### Effect of curing type

To understand the effect of moist curing duration on corrosion resistance, the current values for reinforcing bars with 1 in. of cover depth embedded in the 0.5FR-7, 5EA0.5FR-7, 25LWS0.5FR-1, and 5EA25LWS0.5FR-1 mixtures are plotted in **Figure 3-15**. Initially, the current values were higher for the 25LWS0.5FR-1 mixture (4.3 mA) compared to the 0.5FR-7 mixture (1.4 mA) and for the 5EA25LWS0.5FR-1 mixture (3.2 mA) compared to the 5EA0.5FR-7 mixture (2.3 mA). These results indicate that providing 7 days of moist curing is more effective compared to the use of internal moist curing provided by the LWS. These results are in agreement with the bulk resistivity and sorptivity values reported in **Table 3-11**.

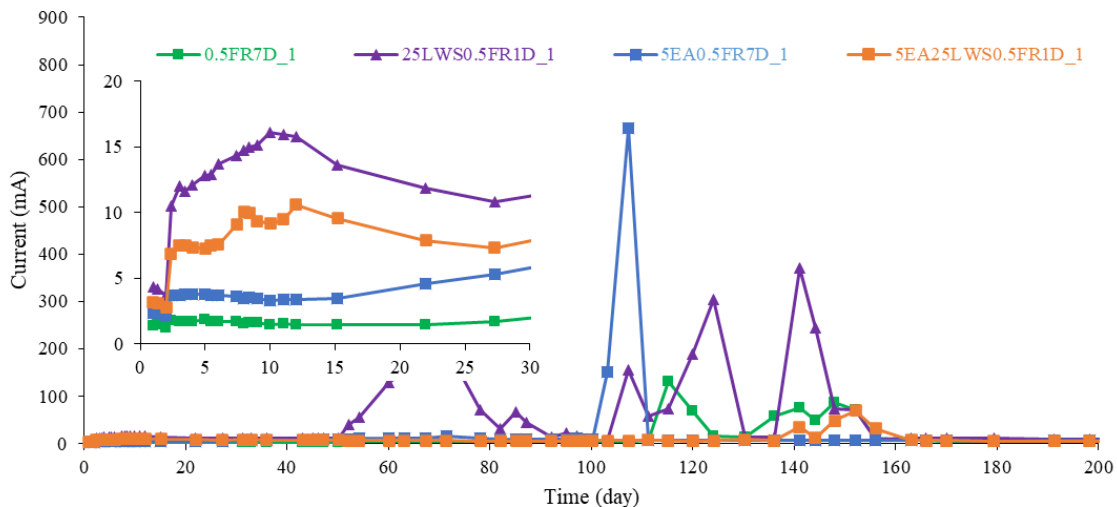


**Figure 3-15 – Influence of moist curing type on current variation with time for reinforcing bars at 1 in. cover depth**

In **Figure 3-15**, the current values at early ages are higher for the 25LWS0.5FR-1 mixture compared with the 0.5FR-7 mixture, and the early peak current for 25LWS0.5FR-1 mixture at 52

days (as per **Table 3-11**) indicates low corrosion resistance. However, the opposite effect; i.e., lower currents over test time can be observed for the 5EA25LWS0.5FR-1 mixture compared to the 5EA0.5FR-7 mixture. Also, the later occurrence of current peak value for the 5EA25LWS0.5FR-1 mixture (at 140 days) indicates the beneficial effect of internal curing by LWS over prolonged external moist curing in the presence of the EA.

#### Effect of EA and/or LWS

To understand the individual and combined effects of the EA and LWS on corrosion resistance, the current values for bars embedded at 1 in. of cover depth in the 0.5FR-7, 5EA0.5FR-7, 5EA25LWS0.5FR-7, 5EA25LWS0.5FR-1, 25LWS0.5FR-1, and 5EA0.5FR-1 mixtures are plotted in **Figure 3-16**. At 1 day, comparing the 0.5FR-7 and 5EA0.5FR-7 mixtures, the current was slightly higher for the 5EA0.5FR-7 mixture (2.3 mA) compared to the 0.5FR-7 mixture (1.4 mA). A similar trend can be seen for the sorptivity and bulk resistivity results in **Table 3-11**. However, such an increase in current with the EA was not observed for the 25LWS0.5FR-1 and 5EA25LWS0.5FR-1 mixtures.

Comparing the 5EA0.5FR-7 and 5EA25LWS0.5FR-7 mixtures, the current increased slightly with the use of 25% LWS. This can be due to the increased porosity of the concrete given the porous LWS (Meng and Khayat, 2017). A similar trend can be seen for sorptivity and bulk resistivity results in **Table 3-11**. However, such increase in current with LWS was not observed for the 5EA0.5FR-1 and 5EA25LWS0.5FR-1 mixtures. This can be due to the capability of water in LWS to promote hydration of cement and EA and mitigate shrinkage, which can reduce porosity (Bentz, 2009).



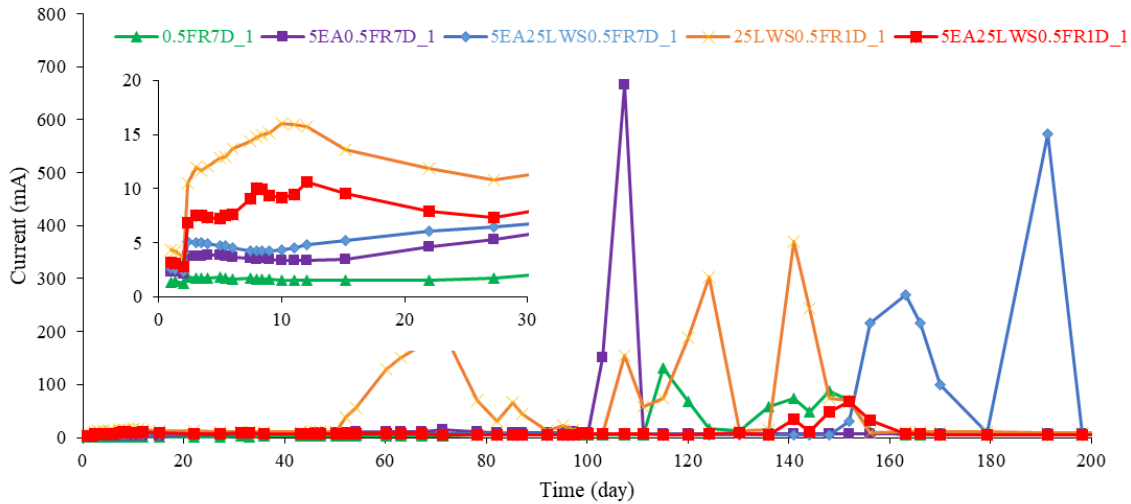


**Figure 3-16 – Influence of the EA and/or LWS on current variation with time for reinforcing bars at 1 in. cover depth**

Comparing the current peak results in **Table 3-11**, the early cracking of the 5EA0.5FR-7 mixture compared to the 0.5FR-7 mixture shows that the addition of EA reduces the corrosion resistance of the concrete. On the other hand, the comparison between the 5EA25LWS0.5FR-1 and 25LWS0.5FR-1 mixtures shows that the time of cracking was delayed with the addition of EA.

**Table 3-13** summarizes the overall effect of the investigated parameters on the corrosion resistance of the Eco-Bridge-Crete mixtures. Based on the time to the initial peak in current for the investigated mixtures, all mixtures exhibited reasonable corrosion resistance (>100 days) except for those subjected to only 1 day of moist curing and made with either EA or LWS. However, the combined use EA and LWS led to significantly improvement in corrosion resistance despite the limited duration of moist curing for 1 day. The use of synthetic fibers was more effective at delaying the initial peak current associated with cracking compared to steel fibers. Regardless of the mixture, the increase in cover depth from 1 to 1.5 and 2 in. increased significantly the corrosion resistance.

**Table 3-13 – Influence of investigated parameter on corrosion resistance**

Increase in parameter	Corrosion resistance	Comment
Cover depth	Increase	Increase in concrete electrical resistance
Moist curing duration	Increase	Decrease in capillary porosity
Use of fibers	Decrease with steel fibers No effect with synthetic fibers	Decrease as a result of fiber corrosion Synthetic fibers do not contribute to corrosion
LWS content	Increase	Decrease in capillary porosity Especially effective when used in combination with EA and fibers 7 days of moist curing without LWS led to higher corrosion resistance than 1 d of moist curing and 25% LWS
EA content	Increase/decrease	Increase when used in combination with LWS and fibers Decrease otherwise

### 3.2 Task II: Structural performance of FR-SWC made with different fiber types and reinforcing steel densities

The work presented in this task involved the testing of 10 reinforced concrete beam elements cast with FR-SWC mixtures made with STST and 5D fibers that are elaborated in **Table 1-1**. The beams were cast with different densities of steel reinforcement to determine the potential savings of reinforcing steel due to fiber use, as elaborated in **Figure 2-3**.

**Table 3-14** summarizes the properties of the FR-SWC mixtures used to cast the beam elements. The concrete had a slump flow of 20 to 23 in., the air content of 8% to 9%, and high passing ability with a modified J-Ring D/a value of 13.5 for the FR-SWC. The visual stability index (VSI) was 0, which indicates no signs of bleeding or segregation at the conclusion of slump flow test. Compressive strength and splitting tensile strengths are reported for specimens subjected to continuous curing in lime-saturated water until the time of testing at 28 and 56 days.

**Table 3-14 – Fresh and hardened properties of FR-SWC mixture**

Mixture abbreviation	Unit weight lb/ft <sup>3</sup>	Air vol., %	Slump flow, in.	D/a	VSI	Comp. strength 28 days, psi	Comp. strength 56 days, psi	Splitting tensile strength 28 days, psi	Splitting tensile strength 56 days, psi
SWC-0EA (SWC)	133	7.8	22.5	20	0	5500	6425	405	430
0.5-5D-SWC-5EA (FR-SWC 1)	140	8.7	20.1	13.5	0	6060	7250	740	770
0.5ST1-SWC-5EA (FR-SWC 2)	141	8.8	20.0	13.5	0	5350	6950	525	650

### 3.2.1 Load-deflection and toughness analysis

Figures 3-17 and 3-18 show the testing of the 10 reinforced concrete beams as well as the failure mode of each beam. Beams made with FR-SWC mixtures (all except Beam #5) experienced higher ductility and peak load compared to the SWC mixture (Beam #5). Higher ductility resulted in a concrete crushing and yielding of steel. Figure 3-19 shows the mid-span strain in the three reinforcing bars against mid-span strain for Beam #4 made with FR-SWC. The bars yielded, and the concrete had almost 3000  $\mu$ strain at the same time, which increased ductility.

### 3.2.2 Load-deflection curve analysis

Figure 3-20 shows the load-deflection curves for the 10 tested beams that were loaded until reaching a deflection of 3 in., except for Beam #6 that failed at a deflection of 1.6 in. The ultimate flexural load ranged from 21 to 40 kips for the non-fibrous SWC beams and 25 to 50 kips for the FR-SWC beams. The use of the STST fibers increased the ultimate load in a more significant way in the case of beams made with the lower steel reinforcement than those with the higher level of reinforcing bars compared to beams made with the SWC of the same level of reinforcement.



**Figure 3-17 – Testing Beams #1 to #5**



**Figure 3-18 – Testing Beams #6 to #10**

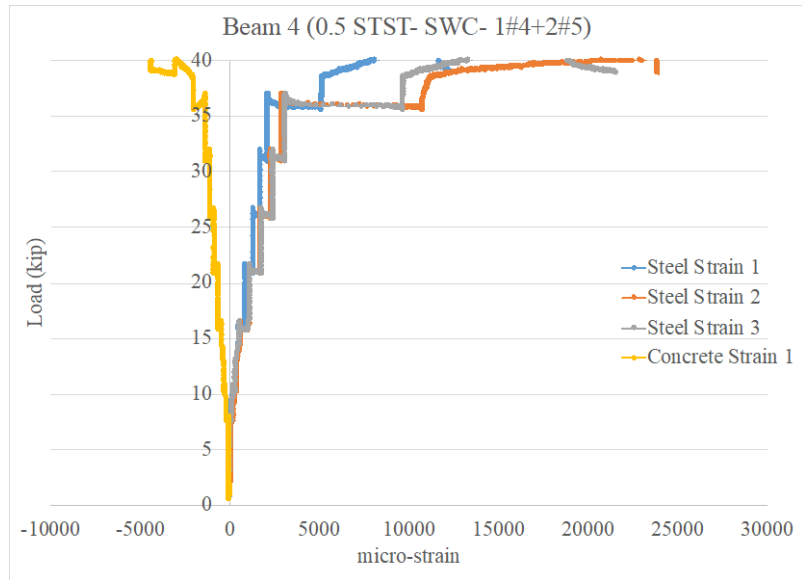
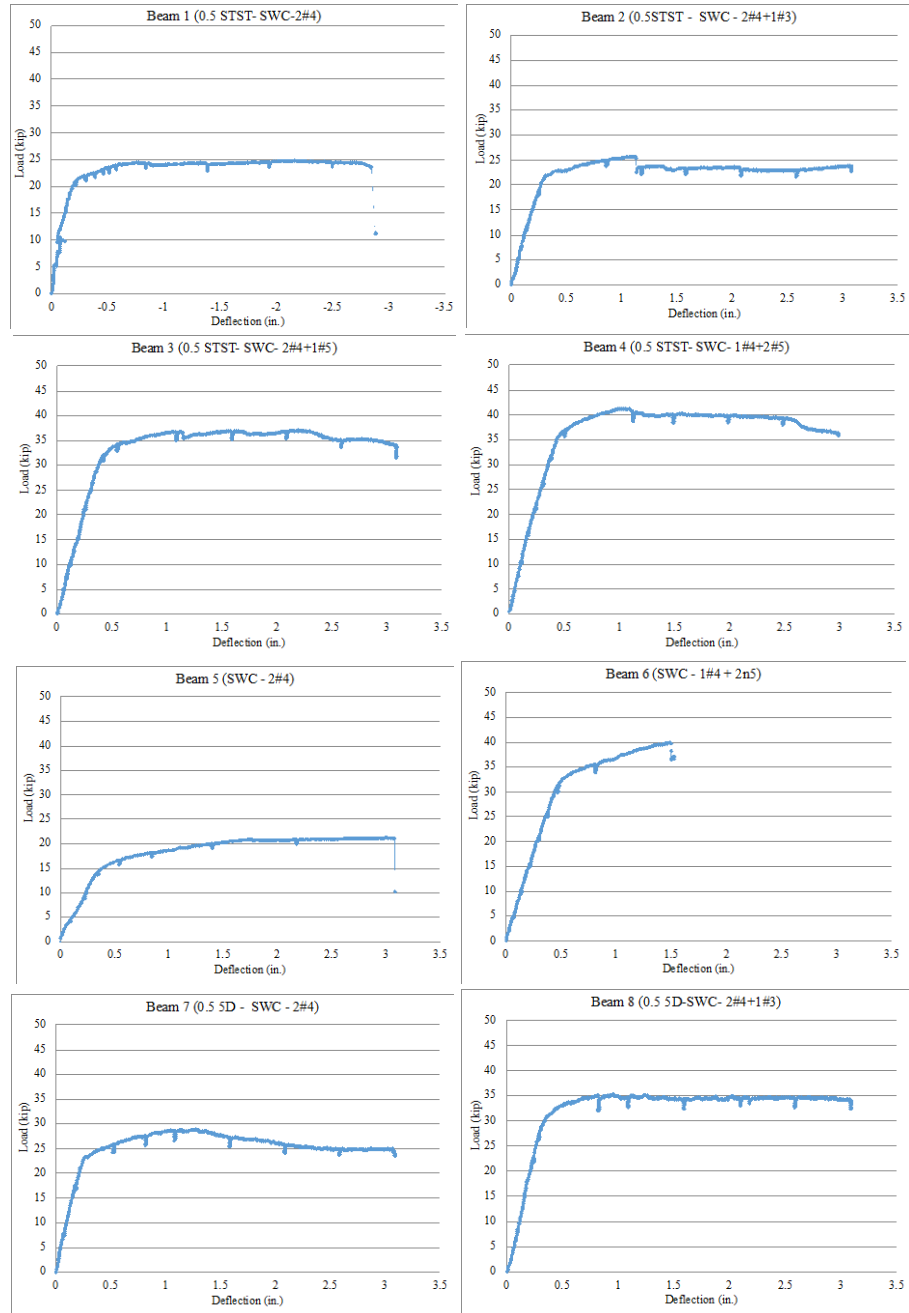


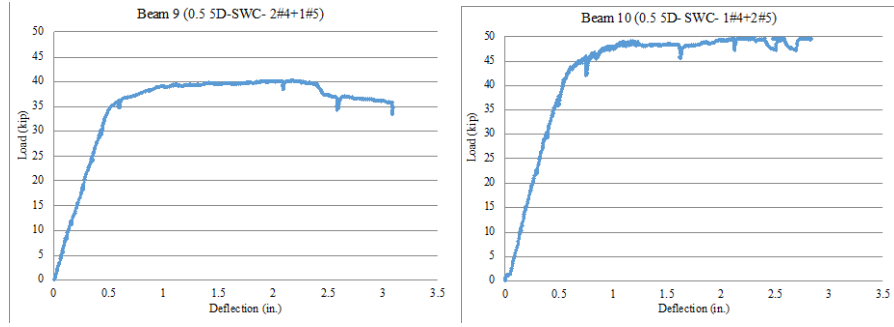
**Figure 3-19 – Load vs. strain values in concrete and steel reinforcing bars for FR-SWC made with STST fibers (Beam #4)**

### 3.2.3 Crack width analysis

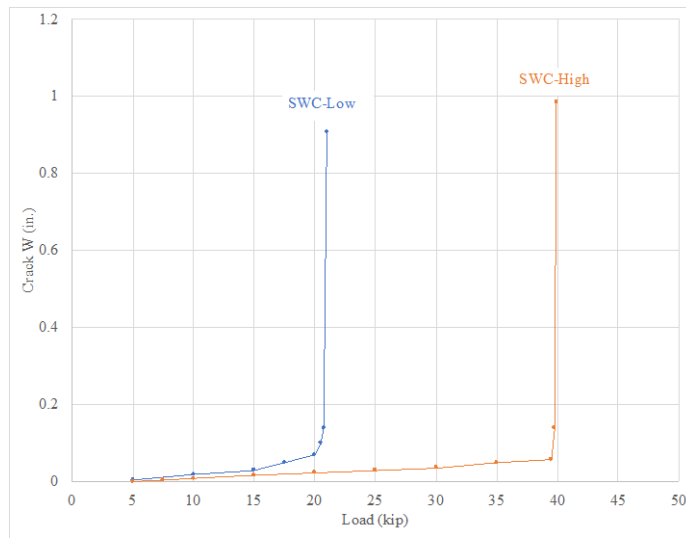
**Figure 3-21** shows the load-crack width relationship for the 10 investigated beams. The use of fibers had a significant effect on reducing crack width. The fibers helped increase the residual loads at small crack openings (<0.02 in.) and prevented a sudden increase in crack width and crack propagation beyond that limit compared to the non-fibrous SWC beams. For beams with low steel reinforcement, the crack width increased from 0.15 to 0.8 in. with an increase in loading from 23 to 25 kips for the FR-SWC beams made with STST fibers. Such increase was 26 to 28 kips for the beams made with 5D fibers. For the non-fibrous SWC beams, these values were 20.9 to 21 kips for the same range of crack widths. For beams made with high steel reinforcement, the crack width increased from 0.15 to 0.8 in. with an increase in loading from 37 to 41 kips for the FR-SWC beams made with STST fibers and 40 to 48 kips for the FR-SWC beams made with 5D fibers compared to 39.9 to 40 in case of the non-fibrous SWC beams. For both fibrous and non-fibrous SWC beams, the maximum crack width at failure was directly

proportional to the reinforcing bar density, which indicates that replacing some bars with steel fibers can reduce crack width.





**Figure 3-20 – Load-deflection curves for 10 investigated beams**





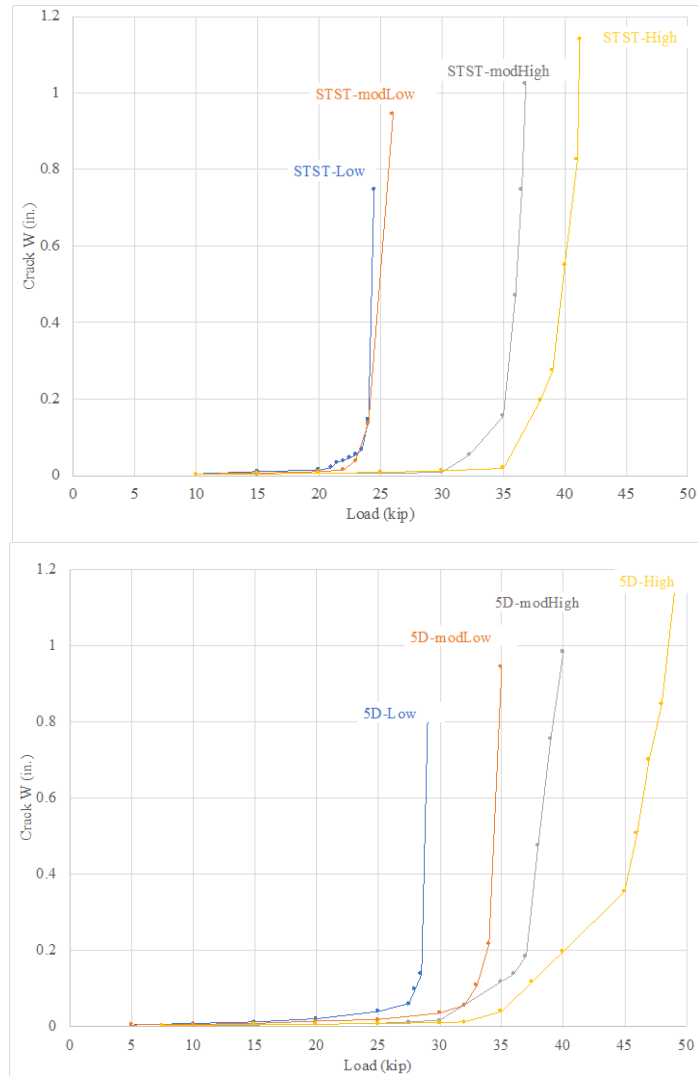


**Figure 3-21 – Load-crack width relationship for 10 tested beams (Low, modLow, modHigh, and High denote beams with 2 #4, 2 #4 + 1 #3, 2 #4 + 1 #5, and 1 #4 + 2 #5, respectively)**

The ultimate loads for the low and high reinforced FR-SWC beams made with STST fibers were 25 and 41 kips, respectively, compared to 21 and 40 kips, respectively, for the non-fibrous SWC beams. The use of the 5D fibers increased the ultimate load significantly for both low and high steel reinforcement compared to beams made with the non-fibrous SWC. The ultimate loads for the low and high reinforced FR-SWC beams made with 5D fibers were 29 and 50 kips, respectively, compared to 21 and 40 kips, respectively, for the non-fibrous SWC beams. This can be due to the double-hooked end effect and the longer development length for the 5D fibers

compared to the STST fibers. The ultimate load was directly proportional to the reinforcement density for both fibrous and non-fibrous SWC beam types, which reflects excellent consolidation of the FR-SWC that encapsulated all of the reinforced reinforcing bars.

#### **3.2.4 Load and strength analysis**

**Figure 3-22** shows the variations of the load results obtained at a crack width of 0.016 in. (0.4 mm) with the increase of the area of the reinforcing bars in the tension zone. The results include the 10 investigated concrete beams and with six other beams cast in MoDOT/RE-CAST TR2015-05. The results are shown for the beams cast with SWC and two different FR-SWC mixtures made with STST and 5D fibers. For the same reinforcing bar density, the load was greater by up to 25 kips (167% higher) and 20 kips (133% higher) in the case of the FR-SWC beams made with the 5D and STST fibers, respectively, compared to the non-fibrous SWC beams. At the lowest reinforcing bar density, the FR-SWC beams made with the STST fibers can sustain a higher load of 20 kips at 0.016 in. crack width compared to 17.5 kips in the case of the concrete with 5D fibers. A saving greater than 50% of steel reinforcing bars can, therefore, be achieved when using FRC, where the structural design is governed by crack width criteria.

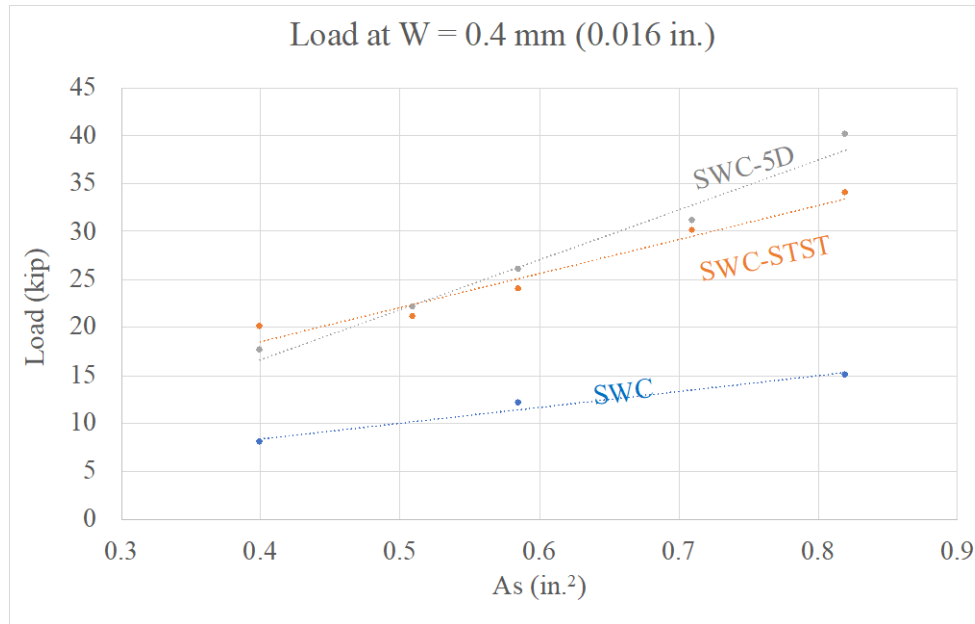


**Figure 3-22 – Load at crack width 0.016 in. (0.4 mm) vs. area of steel reinforcing bars**

**Figure 3-23** shows the variations of load at a deflection of 0.5 in. with the increase of flexural reinforcing bar density. For the same reinforcing bar density, the load was greater by up to 20 kips (60% higher), and 8 kips (50% higher) in the case of FR-SWC made with 5D and STST fibers, respectively, compared to the SWC beams. Savings greater than 40% and 16% of steel reinforcing bars can be achieved with FR-SWC flexural beams made with 5D and STST fibers, respectively.

**Figure 3-24** shows the variations of the ultimate load results with increasing the flexural reinforcing bar density. For the same reinforcing bar density, the load was greater by up 23% and 5% in the case of the FR-SWC beams made with 5D and STST fibers, respectively, compared to the SWC beams.

### 3.2.5 Toughness analysis

**Figure 3-25** shows the variations of the toughness computed at a crack width of 0.016 in. with increasing the flexural reinforcing bar density at the tension side for the beams. The results are

shown for beams cast made with SWC and FR-SWC. For the same reinforcing bar density, the toughness was higher by up to 5 and 3.5 times in the case of the FR-SWC beams made with 5D and STST fibers, respectively, compared to the SWC beams.

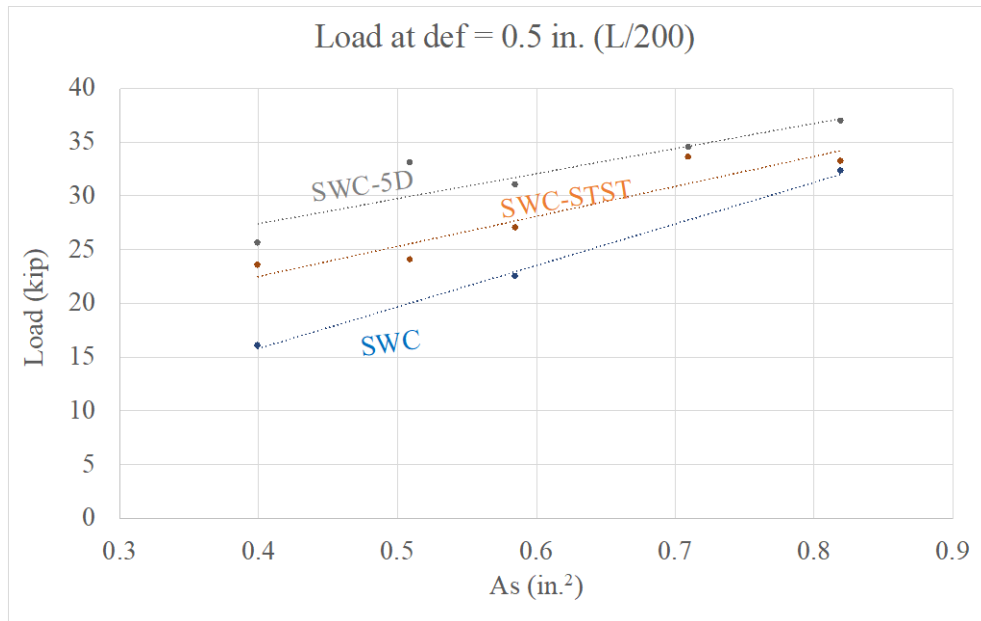


**Figure 3-23 – Load at def = 0.5 in. (L/200) vs. area of steel reinforcing bars**

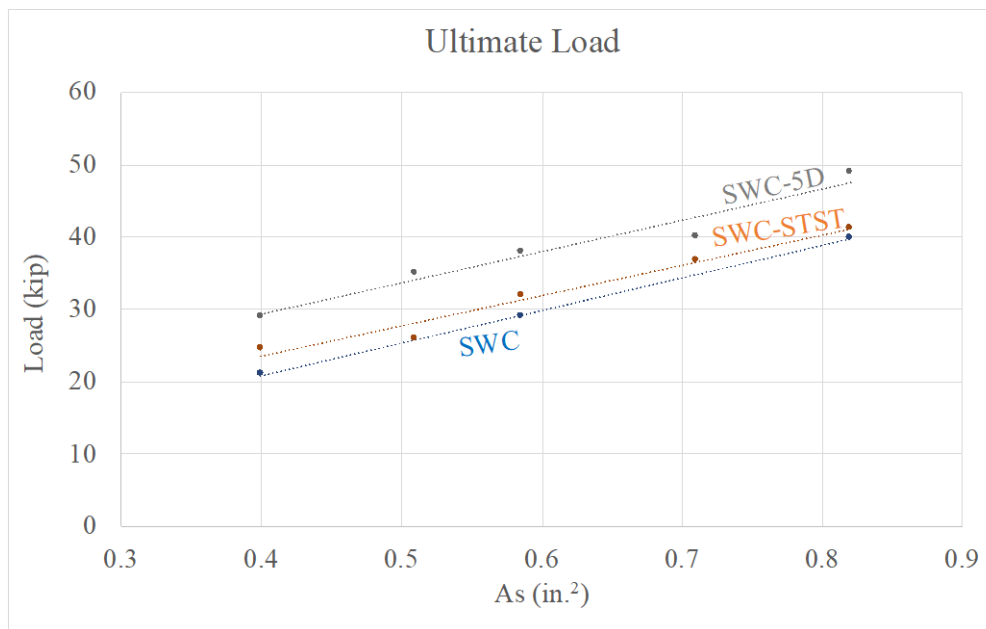


**Figure 3-24 – Ultimate load vs. area of steel reinforcing bars**

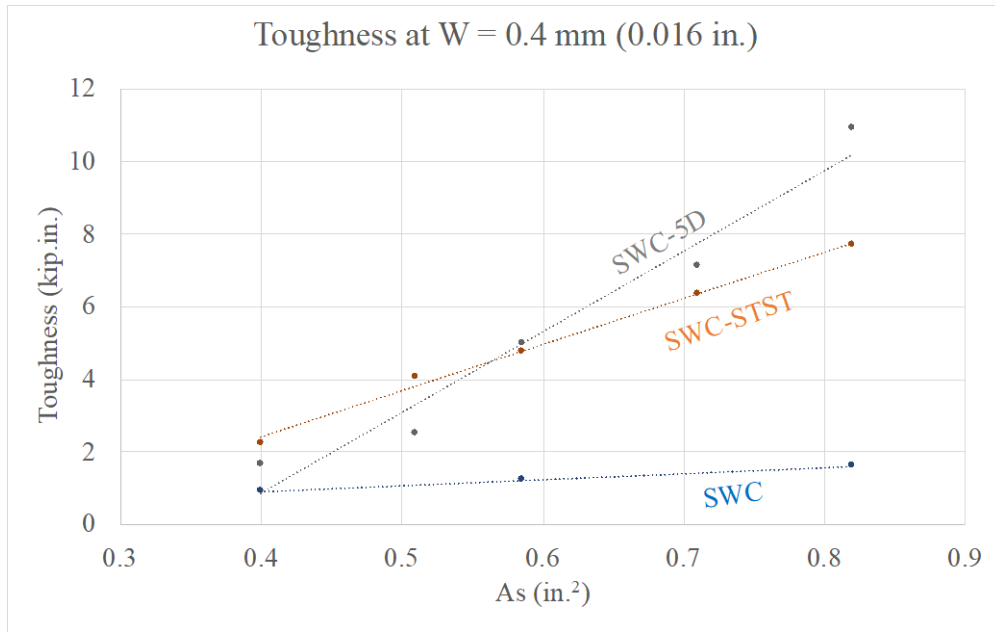


**Figure 3-25 – Toughness at crack width 0.016 in. (0.4 mm) vs. area of steel reinforcing bars**

**Figure 3-26** shows the variations of the toughness computed at 0.5-in. deflection with increasing of the flexural reinforcing bar density. For the same reinforcing bar density, the toughness was higher by up to 90% and 60% in the case of FR-SWC beams made with 5D and STST fibers, respectively, compared to the SWC beams.

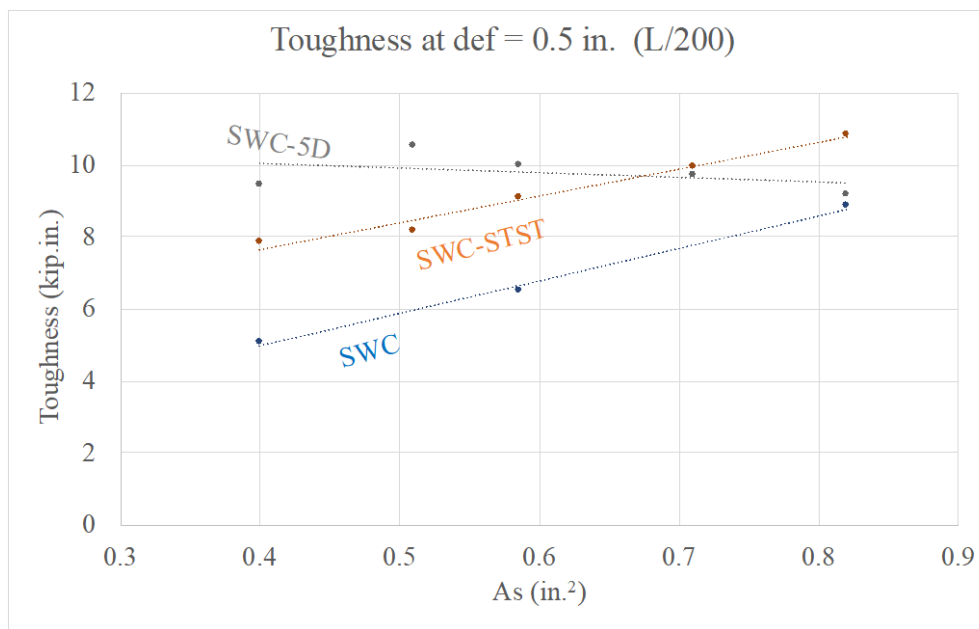


**Figure 3-26 – Toughness at def = 0.5 in. (L/200) vs. area of steel reinforcing bars**

**Figure 3-27** shows the variations of the toughness computed at 1.5-in. deflection with increasing area of flexural reinforcing bar density. For the same reinforcing bar density, the toughness was higher by up to 65% and 45% in the case of FR-SWC beams made with 5D and STST fibers, respectively, compared to the SWC beams.

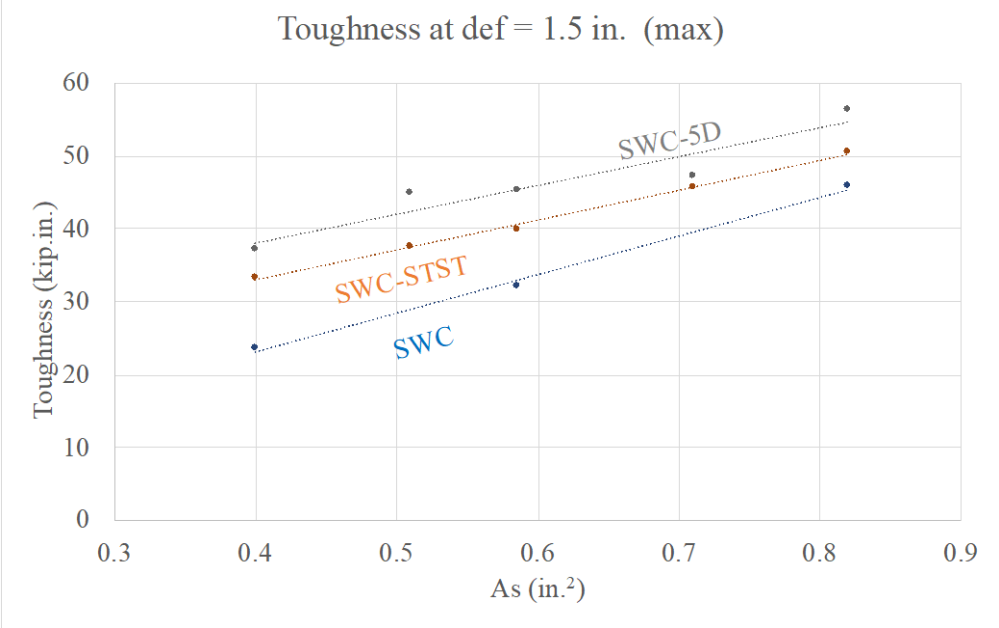


**Figure 3-27 – Toughness at def = 1.5 in. (max) vs. area of steel reinforcing bars**

**Figure 3-28** summarizes the savings that can be achieved when using FR-SWC compared to the SWC in flexural elements given different design criteria. FR-SWC beams made with the STST fibers showed significant savings up to 70% of steel reinforcement when a maximum crack width design criteria is used. Such criteria is critical to enhance durability and reduce the risk of corrosion of reinforcement. The same concrete showed moderate savings of up to 16% when considering the allowable deflection design criteria, which is critical for survivability design of bridges. Savings were limited to 6% if the ultimate load design criteria is considered.

The FR-SWC beams made with the 5D fibers showed significant savings in the three design criteria. The savings were up to 60%, 40%, and 25% for design criteria of maximum crack width, allowable deflection, and ultimate load, respectively.

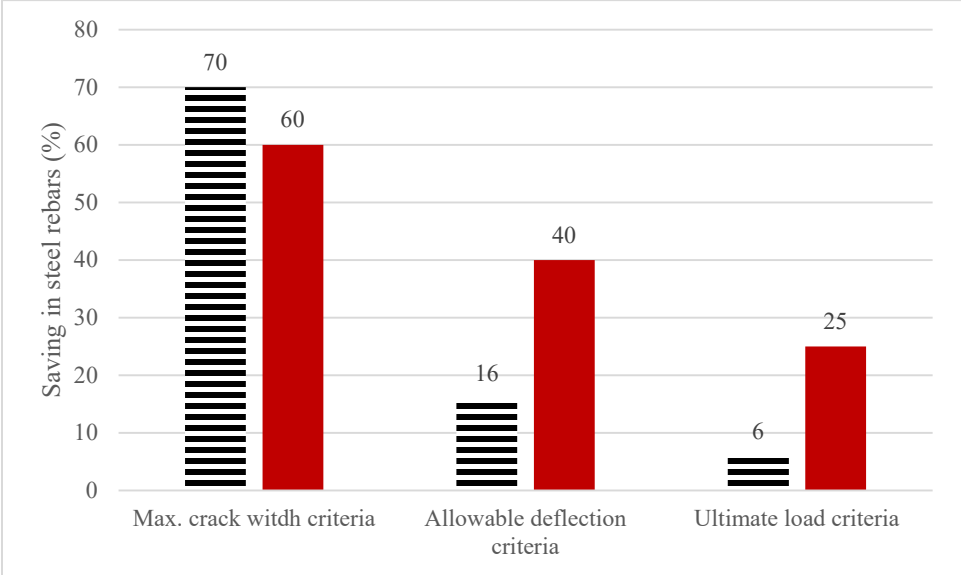


**Figure 3-28 – Savings in steel reinforcement bars with FR-SWC**

## 4. SUMMARY AND CONCLUSIONS

This project was undertaken to enhance the performance of Economical and Crack-Free High-Performance Concrete (Eco-Bridge-Crete) for bridge deck construction and replacement as well as Fiber-Reinforced Super-Workable Concrete (FR-SWC) that can be used for the infrastructure construction. The investigation involved the evaluation of the benefits of using saturated lightweight sand (LWS) for internal curing, expansive agent (EA) for shrinkage compensation, and fibers to reduce shrinkage and enhance strength and corrosion resistance of reinforcing bars of structural concrete that can be used in bridge construction and rehabilitation. The project also aimed to evaluate the feasibility to partially replace steel reinforcement in structural beams with steel fibers.

### **Synergistic effect of LWS, EA, fiber, and moist curing on performance of Eco-Crete-Bridge**

A total of 25 mixtures were prepared to establish and validate statistical models to predict the performance of Eco-Bridge-Crete made with different contents of EA, LWS, and steel fibers and to different durations of moist curing. The modeled responses included compressive and flexural strengths, drying shrinkage, and restrained expansion. The derived models can be interpreted by illustrating trade-offs among the four input factors on the modeled responses.

The relative analysis of the effect of the various shrinkage mitigation strategies on concrete performance is provided in **Table 4-1**. The analysis shows the effect of various combinations of the contents of EA, LWS, and steel fibers and moist curing duration on mechanical and viscoelastic properties. Based on the test results presented in this investigation, the following conclusions can be drawn:



- The duration of external/moist curing represents the most significant influence on reducing drying shrinkage and restricted expansion.
- The hybrid system of LWS and EA can also significantly reduce shrinkage drying shrinkage and restricted expansion.
- The internal curing provided by the LWS can reduce drying shrinkage and restrained expansion, especially for mixtures subjected to air-drying without additional external/moist curing after demolding.
- The combined incorporation of fibers (synthetic fibers or steel fibers) and EA in FR-SWC and Eco-Bridge-Crete mixtures can increase flexural strength by as much as 35%.

**Table 4-1 – Relative effect of four parameters on the different properties**

Recommended mixtures				28-day comp. strength	56-day flexural strength	7-day shrinkage	56-day shrinkage	7-day expansion	56-day expansion
Coded value									
EA	LWS	MC	Fiber						
↑	-1	-1	-1	-	+	---	--	+++	++
↑	-0.5	-0.5	-0.5	--	++	--	-	++	+
↑	0	0	0	--	++	--	-	++	+
↑	0.5	0.5	0.5	-	+	-	-	+	+
-1	↑	-1	-1	+	+	---	---	+++	+++
-0.5	↑	-0.5	-0.5	-	+	--	---	++	++
0	↑	0	0	---	+	-	-	+	++
0.5	↑	0.5	0.5	---	-	-	-	=	=
-1	-1	↑	-1	+++	=	--	---	++	++
-0.5	-0.5	↑	-0.5	+++	=	--	---	++	++
0	0	↑	0	+++	=	--	-	++	+
0.5	0.5	↑	0.5	++	=	--	-	+	+
-1	-1	-1	↑	+	+	--	--	++	++
-0.5	-0.5	-0.5	↑	-	++	=	=	+	++
0	0	0	↑	--	++	=	=	=	=
0.5	0.5	0.5	↑	--	+	=	=	=	=

**Note:** number of + or – signs indicates extent of increase or decrease in measured response, while = refers to insignificant effect of input factor on associated property.

## Viscoelastic properties of FR-SWC and Eco-Bridge-Crete mixtures made with different fibers and shrinkage mitigating strategies

The synergistic effect of combining shrinkage reducing materials, LWS and EA coupled with fibers (synthetic fibers or steel fibers) was investigated for Eco-Bridge-Crete made with ST and PLP fibers and FR-SWC made with STST and 5D fibers. The results illustrate that the developed EA-LWS-fiber system was useful in reducing shrinkage. **Figure 4-1** compares the results of the drying shrinkage of FR-SWC mixtures made with 0.5% micro-macro steel fibers (STST) and 5D steel fibers (double hooked-end macro fiber). The mixtures made with EA exhibited a net initial expansion. The maximum early expansion was recorded by FR-SWC containing 10% EA (10EA0.5FR (STST)-SWC and 10EA0.5FR (5D)-SWC mixtures). The lowest shrinkage was recorded by the 5EA25LWS0.5FR (5D)-SWC mixture. The results reflect the effectiveness of the higher content of LWS in extending cement hydration and possibly the better performance of 5D fibers in inhibiting shrinkage of the FR-SWC.

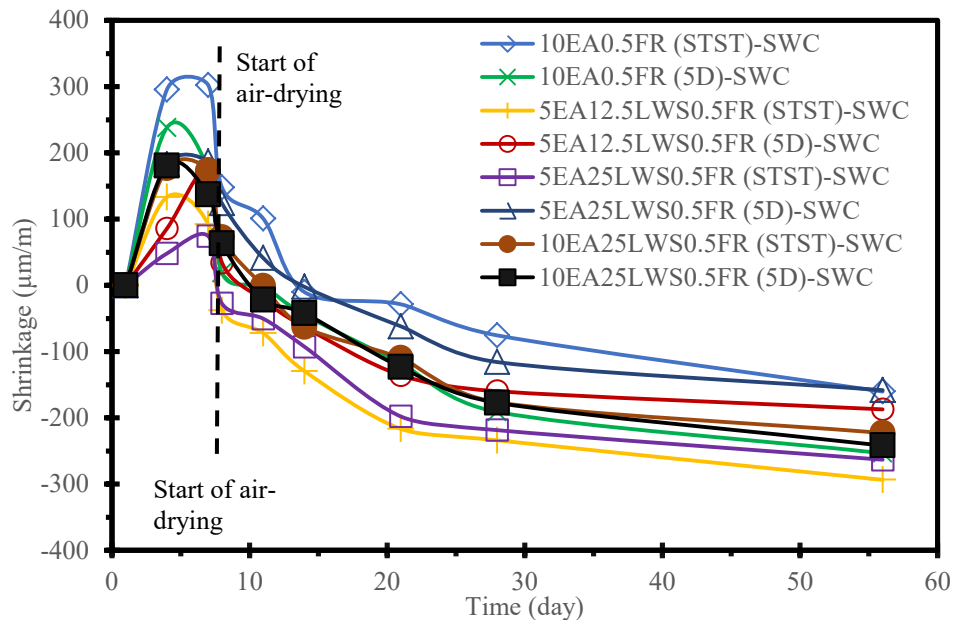


**Figure 4-1 – Drying shrinkage of FR-SWC mixtures containing 0.5% micro-macro steel fiber (STST) and 5D steel fiber (5D)**

## **Evaluation of corrosion resistance**

Eight beam elements were prepared using Eco-Bridge-Crete with either synthetic or steel fibers to evaluate the corrosion resistance of reinforcing bars embedded at cover depths of 1, 1.5, and 2 inches. The investigated mixtures were selected to emphasize the influence of fiber type, moist curing type and duration, as well as the effect of EA and LWS on corrosion resistance. The time of cracking due to corrosion was identified as the time at which there was a considerable increment in electrical current. The time of cracking initiation was used as an indicator of the corrosion resistance of the concrete. Based on the test results, the following conclusions can be warranted:

- The increase in the cover depth from 1 to 1.5 and 2 in. reduced concrete conductivity and improved corrosion resistance of the concrete.
- None of the investigated mixtures exhibited signs of corrosion during the 200-day testing period when a sufficient cover of 2 in. was provided. This was also the case for a cover of 1.5 in., in exception of the 5EA0.5FR-1 mixture. For beams with a cover of 1 in., all eight tested mixtures exhibited proper corrosion resistance (>100 days) except for mixtures subjected to only 1 day of moist curing made with either EA or LWS (5EA0.5FR-1 and 25LWS0.5FR-1 mixtures).
- The decrease in the moist curing duration from 7 days to 1 day drastically increased the conductivity of the investigated mixtures. However, a corresponding drop in corrosion resistance was not observed for mixtures made with both LWS and EA.
- Compared to internal moist curing provided by 25% LWS, the 7-day moist curing was more efficient at reducing concrete conductivity and improving corrosion resistance. However, the use of 25% LWS was more effective in the presence of EA.

- The use of synthetic fibers instead of steel fibers, EA along with LWS, and the increase in moist curing duration were all effective strategies for improving the corrosion resistance of Eco-Bridge-Crete.

**Table 4-2** summarizes the overall effect of the investigated parameters on the corrosion resistance of the Eco-Bridge-Crete mixtures.

**Table 4-2 – Influence of investigated parameter on corrosion resistance**

Increase in parameter	Corrosion resistance	Comment
Cover depth	Increase	Increase in concrete electrical resistance
Moist curing duration	Increase	Decrease in capillary porosity
Use of fibers	Decrease with steel fibers No effect with synthetic fibers	Decrease as a result of fiber corrosion Synthetic fibers do not contribute to corrosion
LWS content	Increase	Decrease in capillary porosity Especially effective when used in combination with EA and fibers 7 days of moist curing without LWS led to higher corrosion resistance than 1 d of moist curing and 25% LWS
EA content	Increase/decrease	Increase when used in combination with LWS and fibers Decrease otherwise

### Structural performance of Eco-Bridge-Crete

A comprehensive study involving the testing of 16 reinforced concrete beams (10 beams tested in this study and three others representing average values of six beams tested earlier in the MoDOT/RE-CAST TR2015-05 project) was undertaken to investigate the effect of fiber type on flexural strength and cracking resistance of FR-SWC and compare the performance to that of SWC beams. The testing involved the casting of beam elements made with different steel reinforcement densities in the tension zone with FR-SWC with 0.5% of the 5D or STST fibers. As indicated in **Figure 4-2**, the following conclusions can be warranted:

- Savings greater than 50% of steel reinforcing bars can be achieved in the case of FR-SWC flexural beams where the design is governed by the crack width criteria, which is important in the marine environment.
- Savings greater than 40% and 16% of steel reinforcing bars can be achieved in the case of FR-SWC flexural beams made with 5D and STST fibers, respectively, where the design is governed by allowable deflection of L/200 criteria, such as shallow beams.
- Savings greater than 25% and 6% of steel reinforcing bars can be achieved in the case FR-SWC flexural beams made with 5D and STST fibers, respectively, where the design is governed by ultimate load criteria.
- The FR-SWC beams made with the 5D fibers showed significant savings in the three design criteria. The savings were up to 60%, 40%, and 25% for design criteria of maximum crack width, allowable deflection, and ultimate load, respectively.

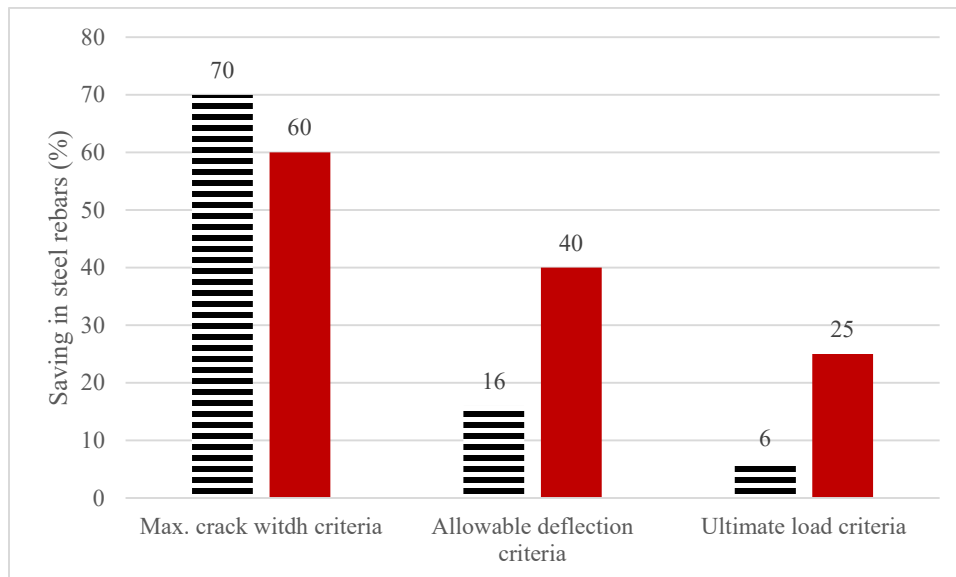


**Figure 4-2 – Savings in steel reinforcement bars with FR-SWC**

## REFERENCES

- Ahmad, S., 2003. Reinforcement Corrosion in Concrete Structures, Its Monitoring and Service Life Prediction—A Review. *Cement and Concrete Composites*, 25(4-5), pp.459-471.
- Al-Tayyib, A.J., Khan, M.S., Allam, I.M. and Al-Mana, A.I., 1990. Corrosion Behavior of Pre-Rusted Rebars after Placement in Concrete. *Cement and Concrete Research*, 20(6), pp.955-960.
- Alonso, C., Andrade, C. and Gonzalez, J.A., 1988. Relation Between Resistivity and Corrosion Rate of Reinforcements in Carbonated Mortar Made with Several Cement Types. *Cement and Concrete Research*, 18(5), pp.687-698.
- ASTM C39/C39M, 2003. Standard Test Method for Compressive Strength of Cylindrical Concrete Specimens. *Annual Book of ASTM Standards*.
- ASTM, C., 2005. 1609/C 1609M-05. Standard Test Method for Flexural Performance of Fiber-Reinforced Concrete (Using Beam with Third-Point Loading), ASTM International, PA, United States.
- ASTM C138, 2017. Standard Test Method for Density (Unit Weight), Yield, and Air Content (Gravimetric) of Concrete.
- ASTM, C231, 2004. Standard Test Method for Air Content of Freshly Mixed Concrete by the Pressure Method.
- ASTM, C143, 2015. Standard Test Method for Slump of Hydraulic-Cement Concrete. *ASTM Annual Book of ASTM Standards*.
- ASTM, C., 157/C 157 M-06, 2006. Standard Test Method for Length Change of Hardened Hydraulic-Cement Mortar and Concrete. *ASTM International*, West Conshohocken, PA.
- ASTM, C., 2012. Standard Test Method for Electrical Indication of Concrete's Ability to Resist Chloride Ion Penetration. C1202-18.
- ASTM, 2002. Standard Test Method for Determining the Penetration of Chloride Ion into Concrete by Pondering.
- ASTM, C1170, 2014. Standard Test Method for Determining Consistency and Density Of Roller Compacted Concrete Using a Vibrating Table.
- ASTM, A., C1611/C1611M-09b, 2009. Standard Test Method for Slump Flow of Self-Consolidating Concrete. *ASTM International* West Conshohocken, PA.

ASTM, C1435, 2014. Standard Practice for Molding Roller-Compacted Concrete in Cylinder Molds Using a Vibrating Hammer. ASTM International West Conshohocken, PA.

Bazant, Z.P., 1979. Physical Model for Steel Corrosion in Concrete Sea Structures-Theory. ASCE J STRUCT DIV, 105(6), pp.1137-1153.

Bentz, D.P., 2009. Influence of Internal Curing Using Lightweight Aggregates on Interfacial Transition Zone Percolation and Chloride Ingress in Mortars. Cement and Concrete Composites, 31(5), pp.285-289.

Berrocal, C.G., Lundgren, K. and Löfgren, I., 2016. Corrosion of Steel Bars Embedded in Fiber Reinforced Concrete under Chloride Attack: State of the Art. Cement and Concrete Research, 80, pp.69-85.

Corinaldesi, V., Nardinocchi, A. and Donnini, J., 2015. The Influence of Expansive Agent on the Performance of Fiber Reinforced Cement-Based Composites. Construction and Building Materials, 91, pp.171-179.

Corinaldesi, V. and Nardinocchi, A., 2016. Mechanical Characterization of Engineered Cement-Based Composites Prepared with Hybrid Fibers and Expansive Agent. Composites Part B: Engineering, 98, pp.389-396.

El Maaddawy, T. and Soudki, K., 2007. A Model for Prediction of Time from Corrosion Initiation to Corrosion Cracking. Cement and Concrete Composites, 29(3), pp.168-175.

Hornbostel, K., Larsen, C.K. and Geiker, M.R., 2013. Relationship between Concrete Resistivity and Corrosion Rate—A Literature Review. Cement and Concrete Composites, 39, pp.60-72.

He, H.A., Dong, W. and Wu, Z.M., 2011. Study on Long-Term Expansive Deformation of Self-Stressing Concrete with Combined Restrictions of Steel Fibers and Steel Bar. In Key Engineering Materials (Vol. 452, pp. 533-536). Trans Tech Publications Ltd.

Khayat, K.H., Meng, W., Valipour, M. and Hopkins, M., 2018. Use of Lightweight Sand for Internal Curing to Improve Performance of Concrete Infrastructure (No. cmr 18-005). Missouri. Dept. of Transportation. Construction and Materials Division.

Lam, H., 2005. Effects of Internal Curing Methods on Restrained Shrinkage and Permeability.

Lockington, D.A. and JY Parlange, 2003. Water Absorption in Porous Materials. Journal of Physics D: Applied Physics, 36(6): p.760.

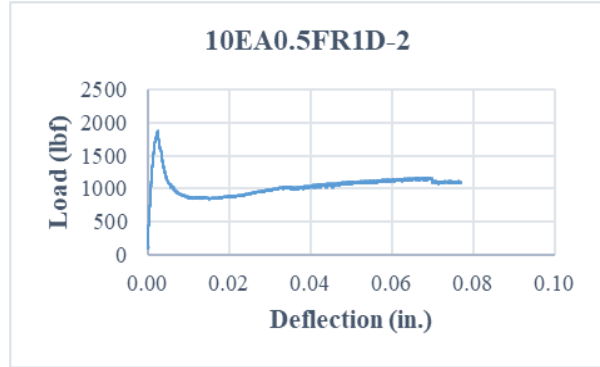
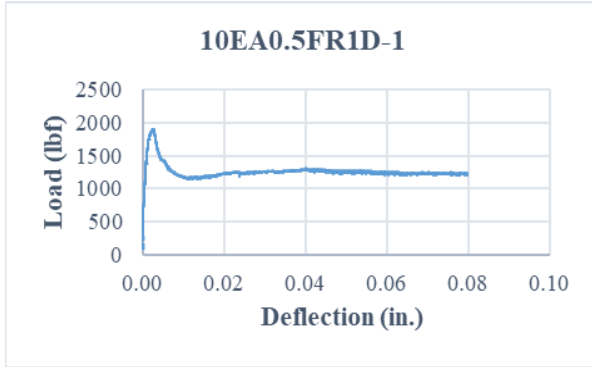
Lotfy, A., Hossain, K.M. and Lachemi, M., 2014. Application of Statistical Models in Proportioning Lightweight Self-Consolidating Concrete with Expanded Clay Aggregates. Construction and Building Materials, 65, pp.450-469.

- Mehdipour, I. and Khayat, K.H., 2016. Shrinkage Mitigating Strategies for Low Shrinkage Self-Consolidating Concrete. Washington DC, USA 15-18 May 2016 Edited by Kamal H. Khayat, p.783.
- Meng, W. and Khayat, K., 2017. Effects of Saturated Lightweight Sand Content on Key Characteristics of Ultra-High-Performance Concrete. *Cement and Concrete Research*, 101, pp.46-54.
- Meng, W., Samaranayake, V.A. and Khayat, K.H., 2018. Factorial Design and Optimization of Ultra-High-Performance Concrete with Lightweight Sand. *ACI Materials Journal*, 115(1).
- Montgomery, D.C., 2001. *Design and Analysis of Experiments*. John Wiley & Sons. Inc., New York, 1997, pp.200-1.
- Narayanan, N., 2006. Analysis of Moisture Transport in Mortars and Concrete Using Sorption-Diffusion Approach. *ACI Materials Journal*, 103(3).
- Raupach, M., 1996. Chloride-Induced Macrocell Corrosion of Steel in Concrete—Theoretical Background and Practical Consequences. *Construction and Building Materials*, 10(5), pp.329-338.
- Sun, W., Chen, H., Luo, X. and Qian, H., 2001. The Effect of Hybrid Fibers and Expansive Agent on the Shrinkage and Permeability of High-Performance Concrete. *Cement and Concrete Research*, 31(4), pp.595-601.
- Sahamitmongkol, R. and Kishi, T., 2011. Tension Stiffening Effect and Bonding Characteristics of Chemically Prestressed Concrete under Tension. *Materials and Structures*, 44(2), pp.455-474.
- Solgaard, A.O.S., Geiker, M., Edvardsen, C. and Küter, A., 2014. Observations on the Electrical Resistivity of Steel Fiber Reinforced Concrete. *Materials and Structures*, 47(1-2), pp.335-350.
- Taillet, E., Lataste, J.F., Rivard, P. and Denis, A., 2014. Non-Destructive Evaluation of Cracks in Massive Concrete Using Normal DC Resistivity Logging. *NDT & E International*, 63, pp.11-20.
- Khayat, K.H. and Mehdipour, I., 2017. Economical and Crack-free High-Performance Concrete for Pavement and Transportation Infrastructure Construction (No. cmr 17-007). Missouri. Dept. of Transportation.
- Khayat, K.H. and Abdelrazik, A., 2017. Performance of Fiber-Reinforced Self-Consolidating Concrete for Repair of Bridge Sub-Structures and Fiber-Reinforced Super-Workable Concrete for Infrastructure Construction (No. cmr 17-012).

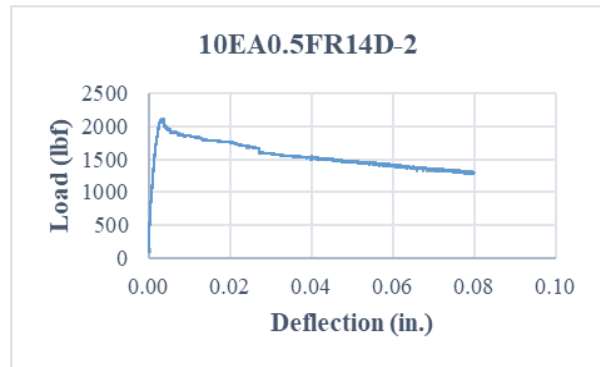
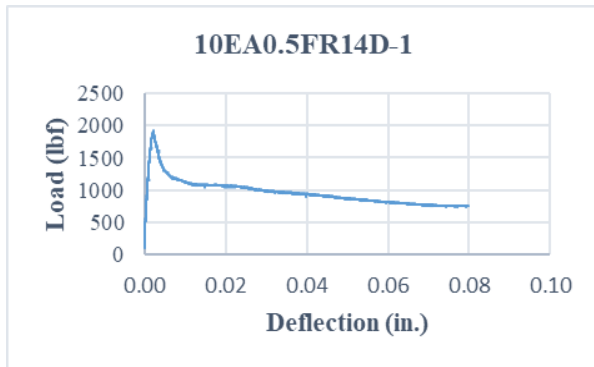


## Appendix-A

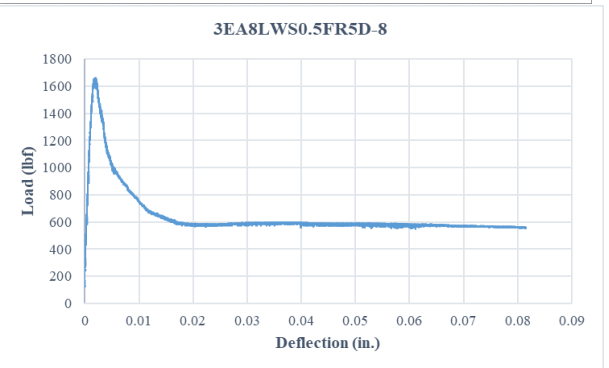
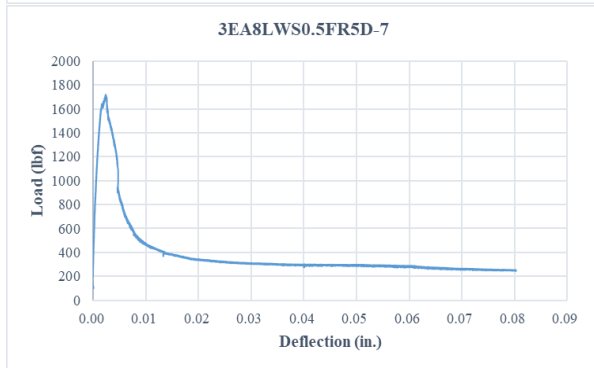
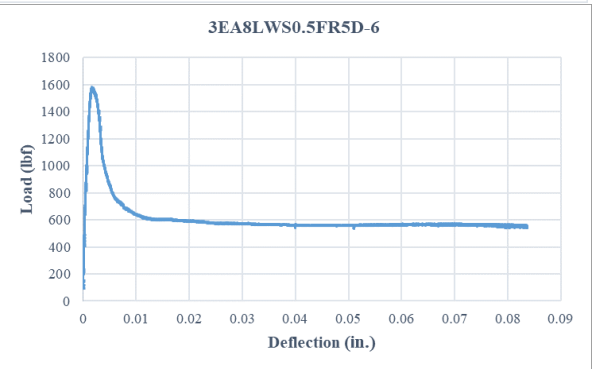
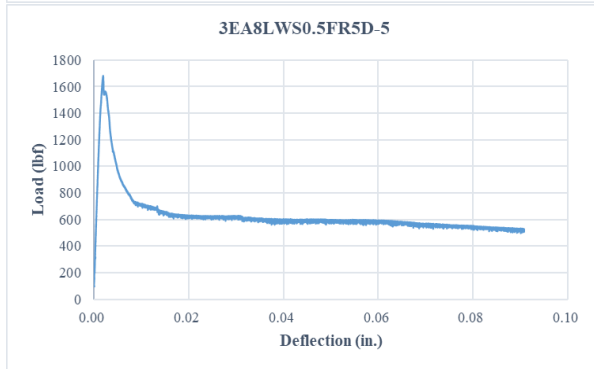
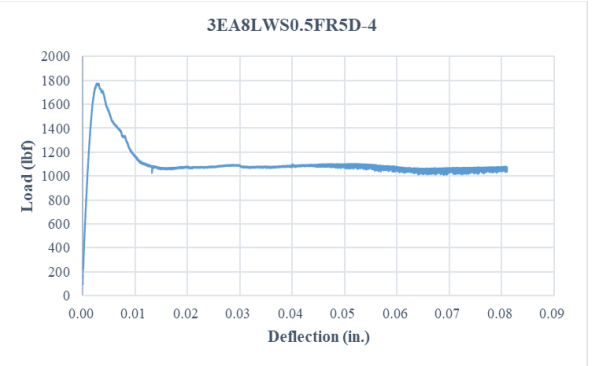
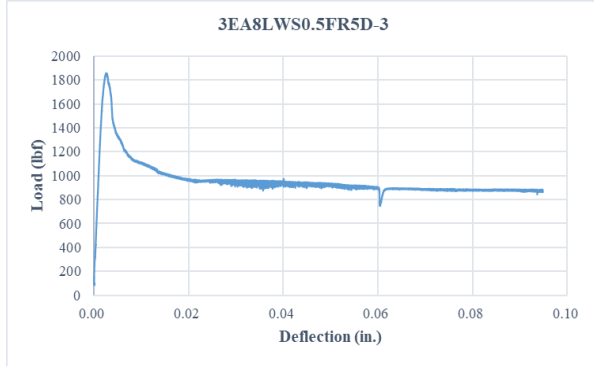
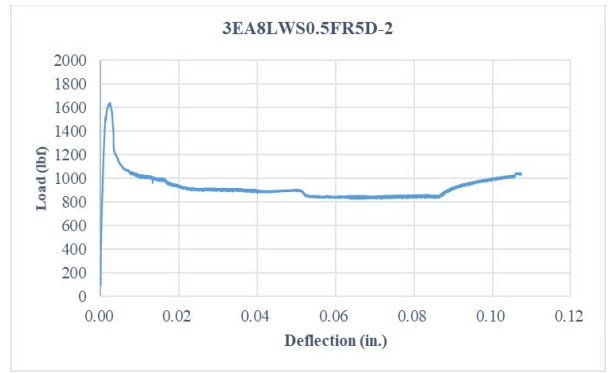
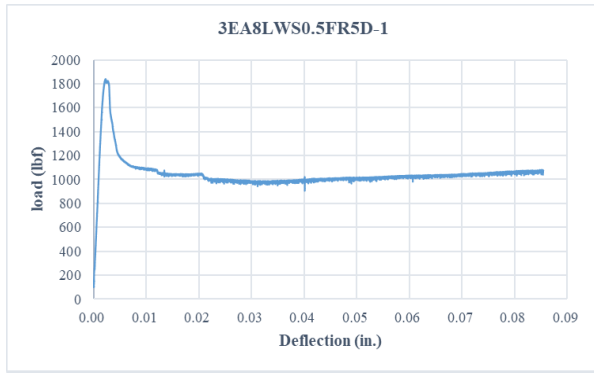
### Task I-A Optimization for Eco-Bridge-Crete and FR-SWC – results of 25 Eco-Bridge-Crete mixtures



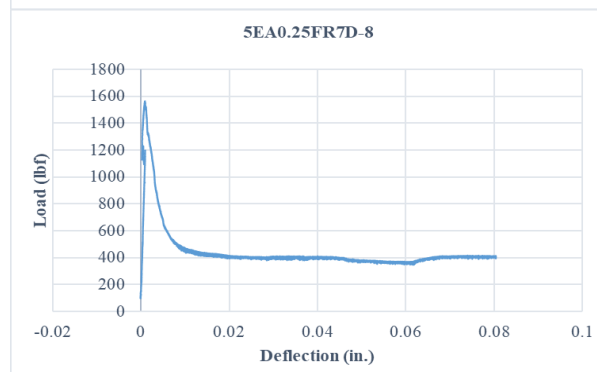
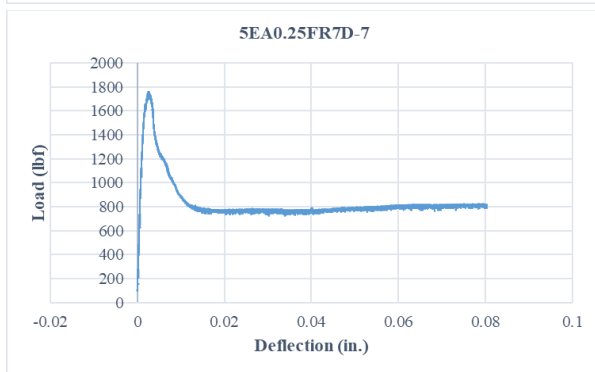
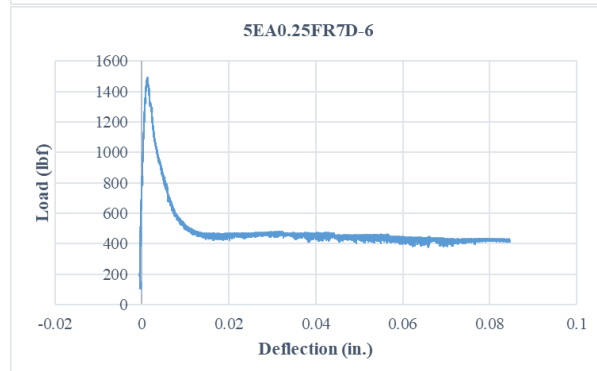
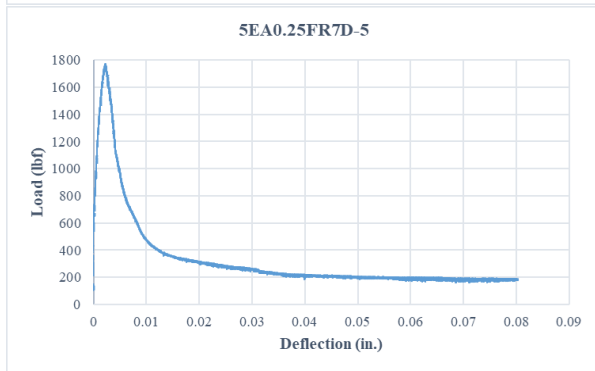
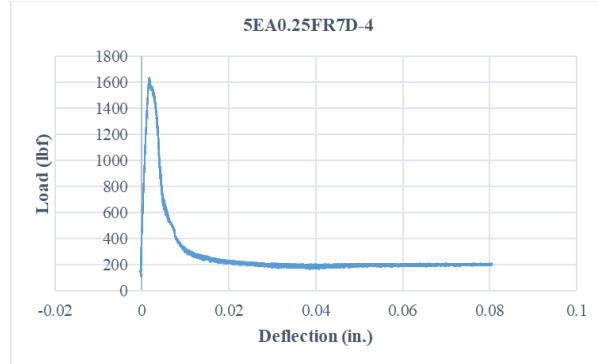
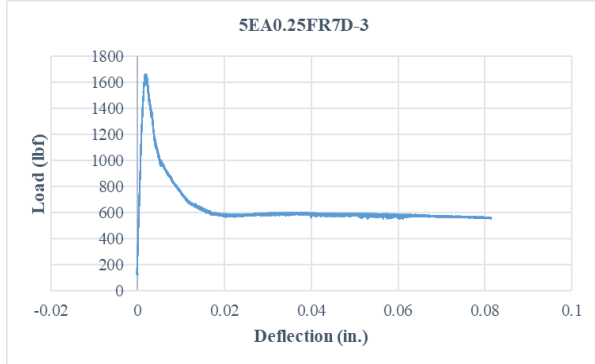
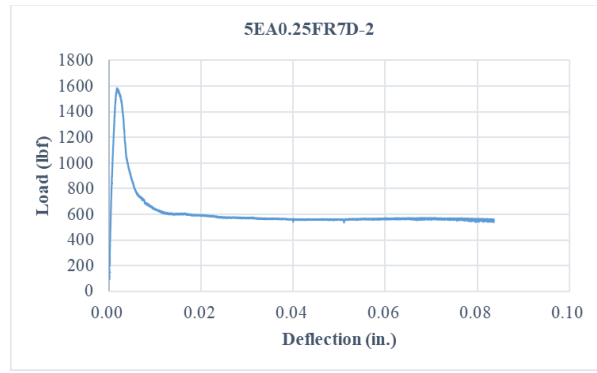
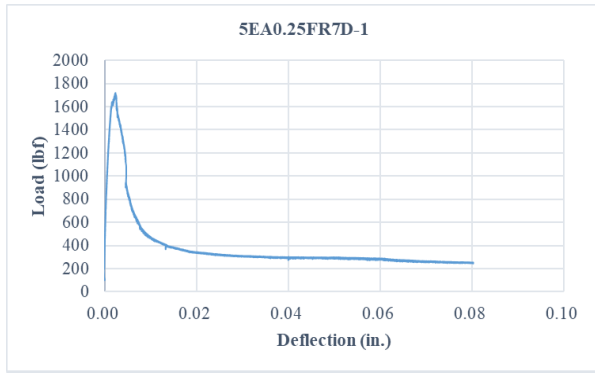
10EA0.5FR1D-(2 samples)

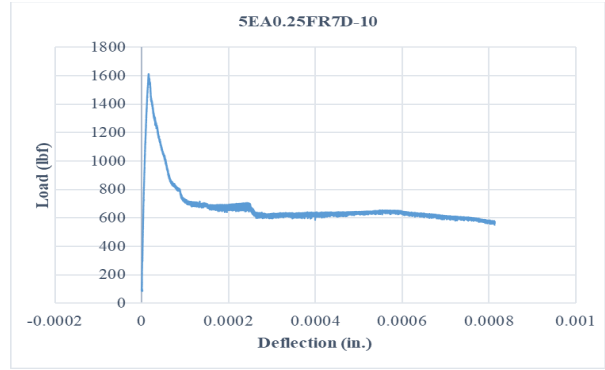
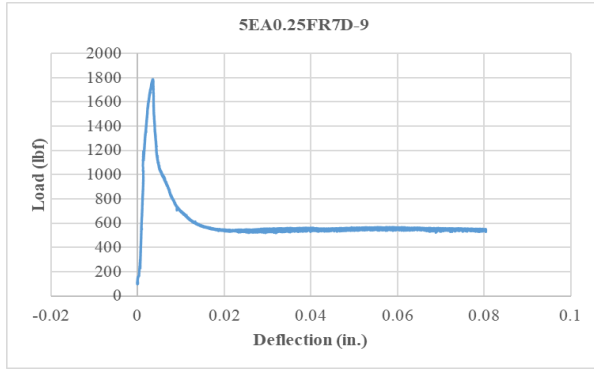


10EA0.5FR14D-(2 samples)

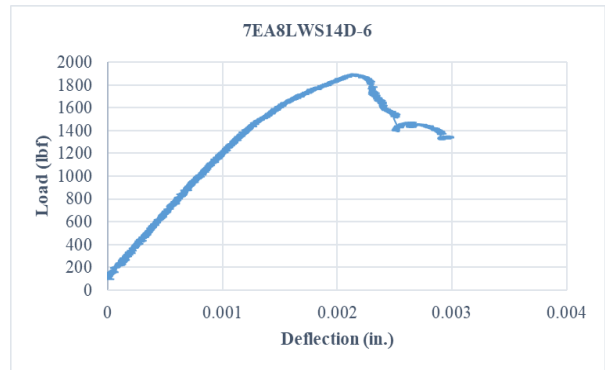
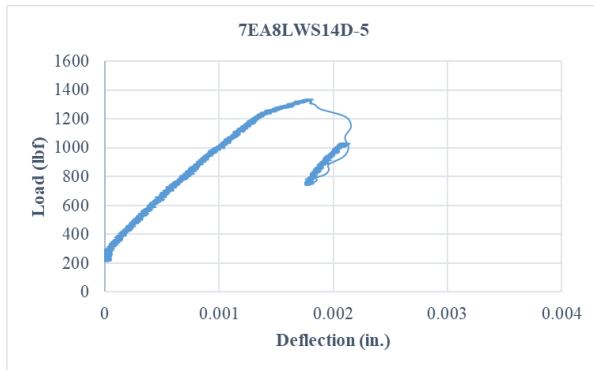
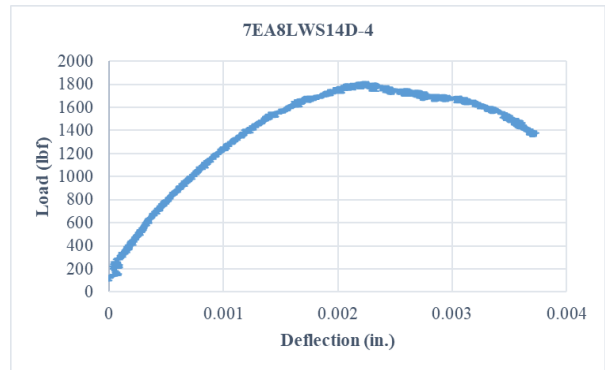
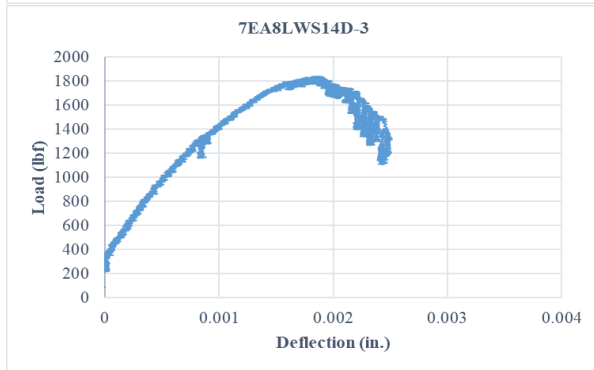
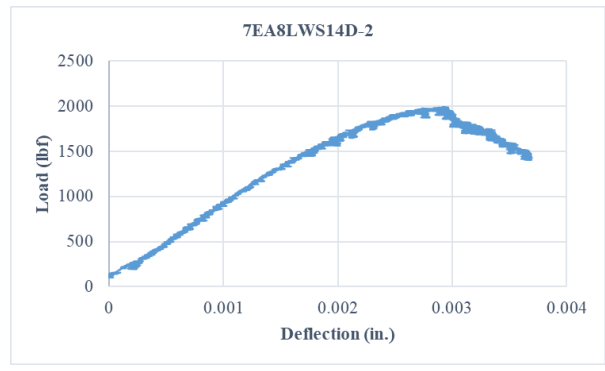
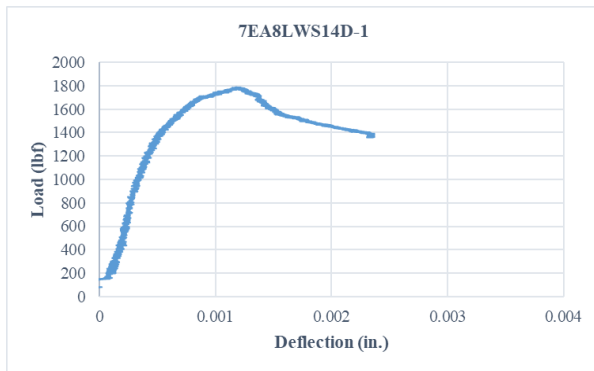


3EA8LWS0.5FR5D-(8 samples)





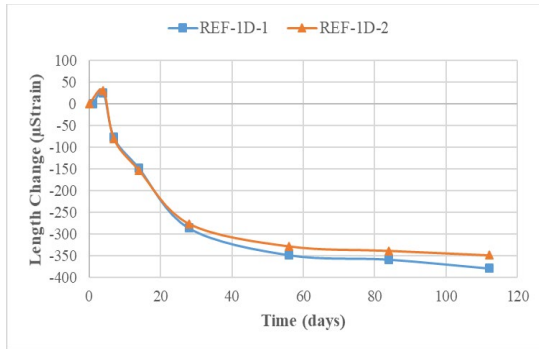
5EA0.25FR7D-(10 samples)



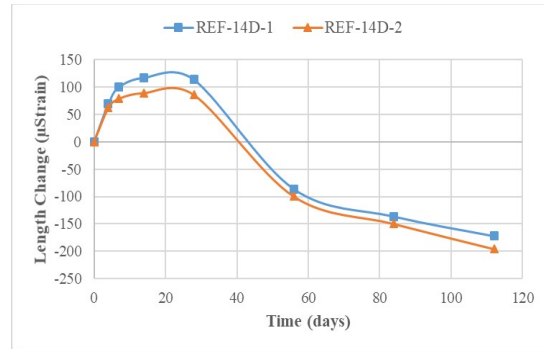
7EA8LWS14D-(6 samples)

Figure A-1 – Flexural strength results of mixtures used for experimental design

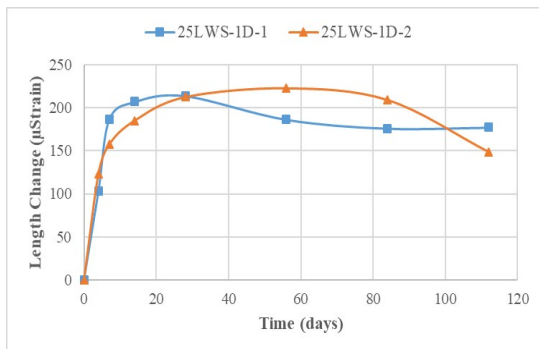
**Note:** 10EA-10% expansion agent; 0.5FR-0.5% fiber; 8LWS-8% lightweight sand; 1D-1-day moist curing.



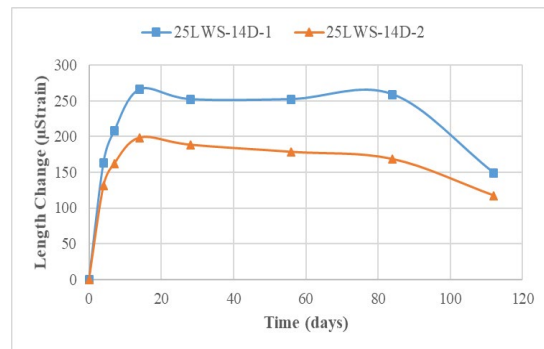
REF-1D



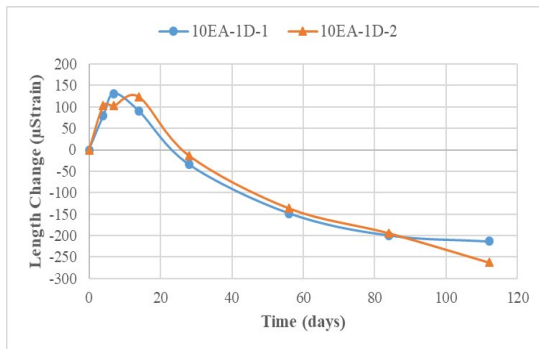
REF-14D



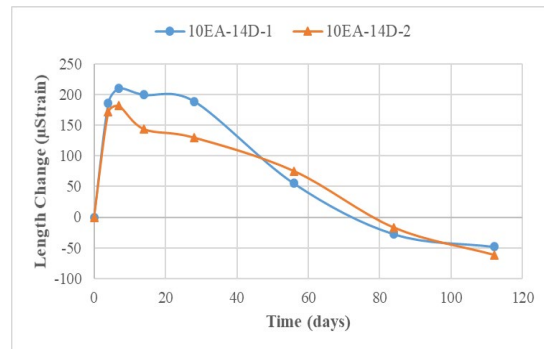
25LWS-1D



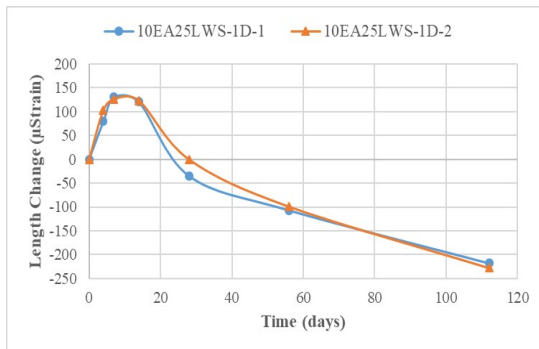
25LWS-14D



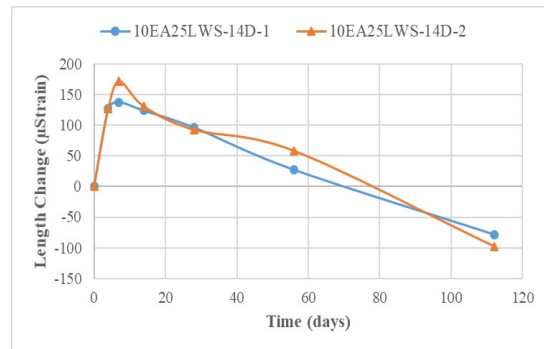
10EA-1D



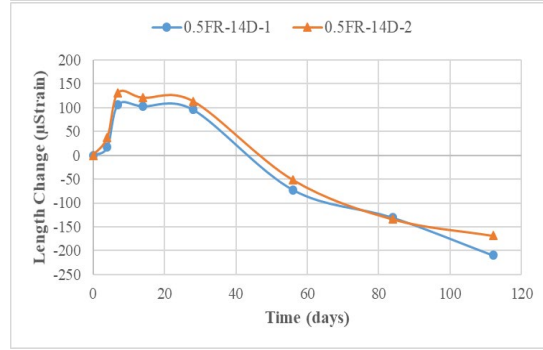
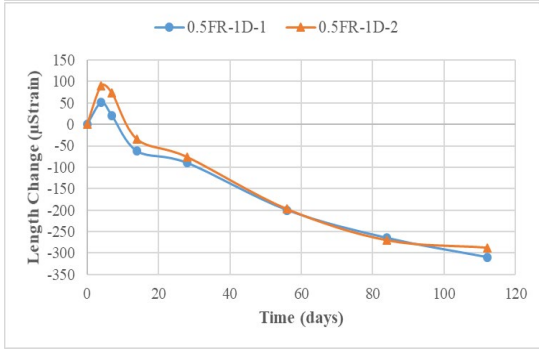
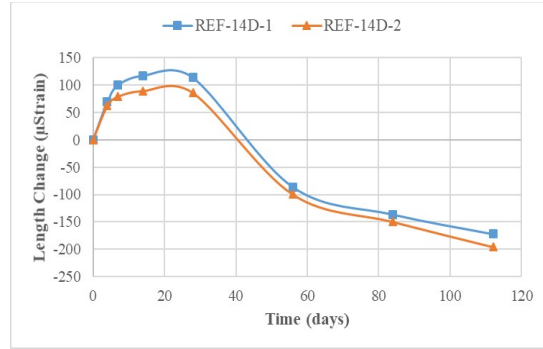
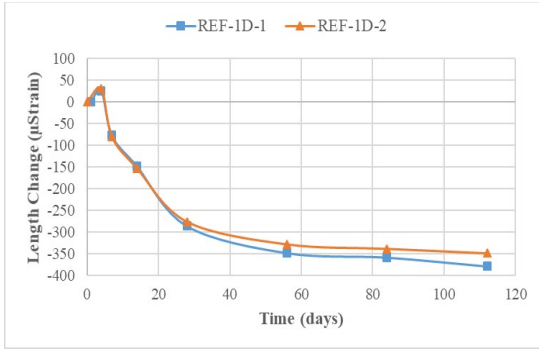
10EA-14D



10EA25LWS-1D

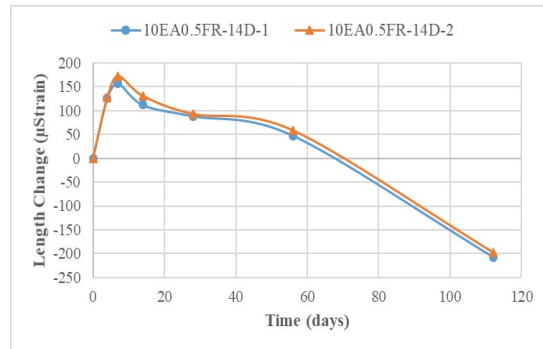
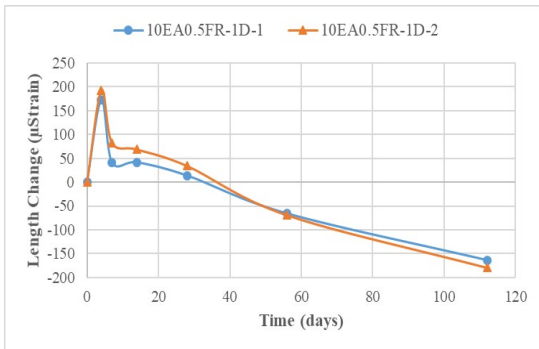


10EA25LWS-14D



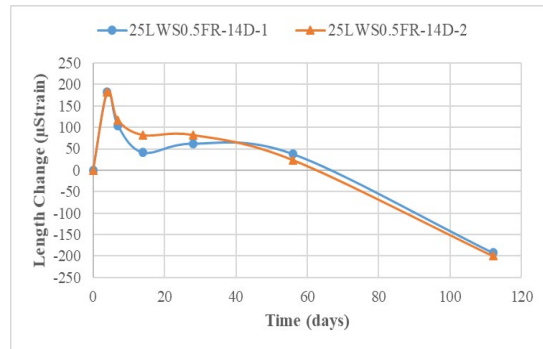
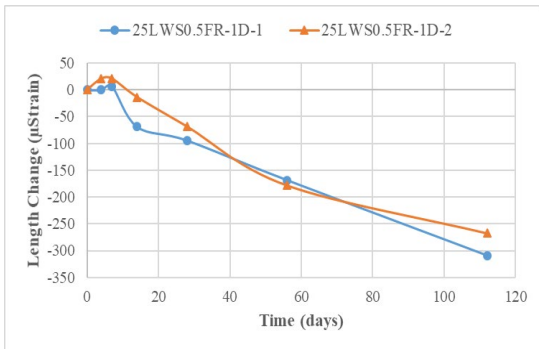
0.5FR-1D

0.5FR-14D



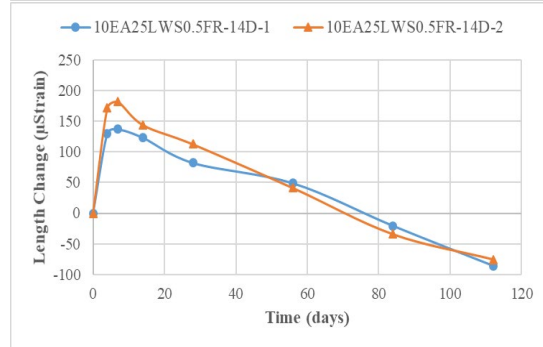
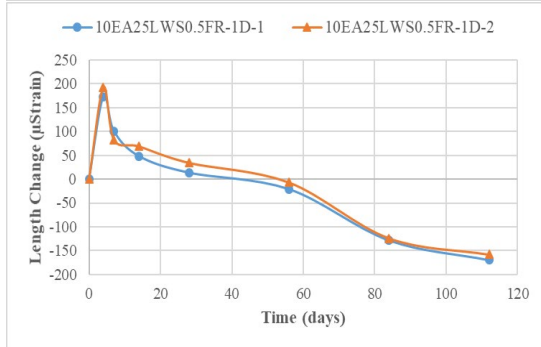
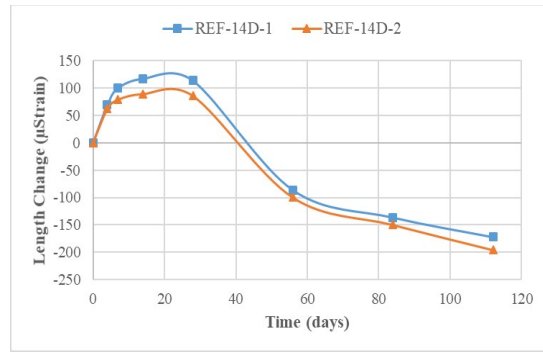
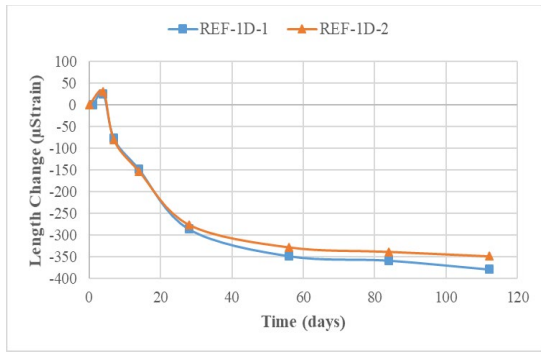
10EA0.5FR-1D

10EA0.5FR-14D



25LWS0.5FR-1D

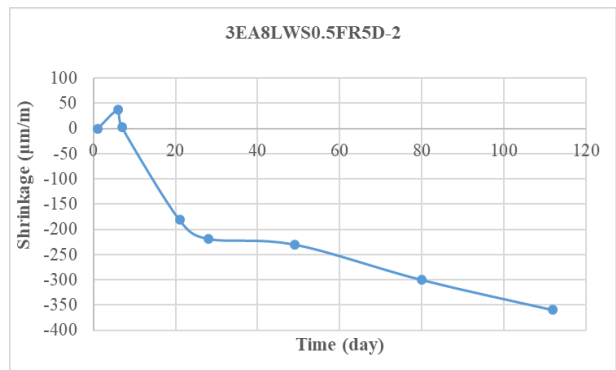
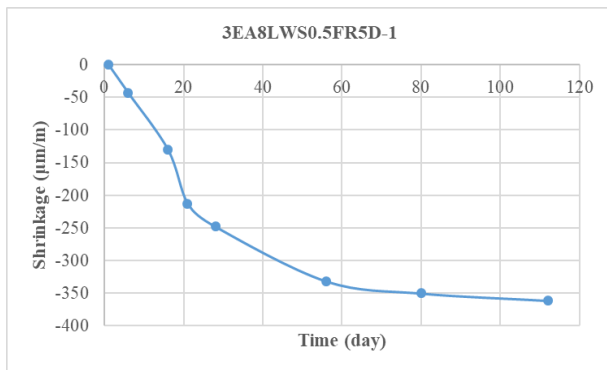
25LWS0.5FR-14D



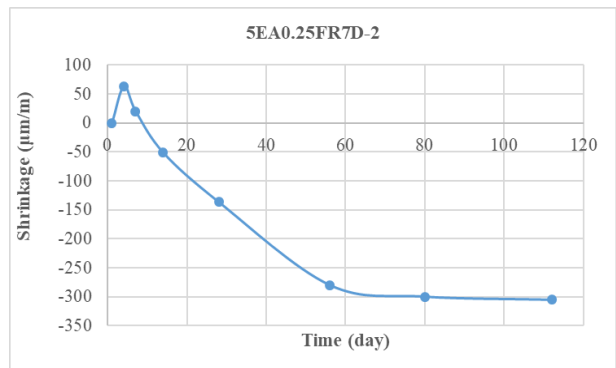
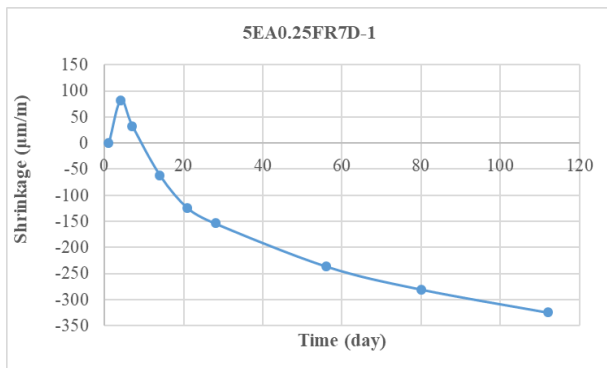
10EA25LWS0.5FR-1D

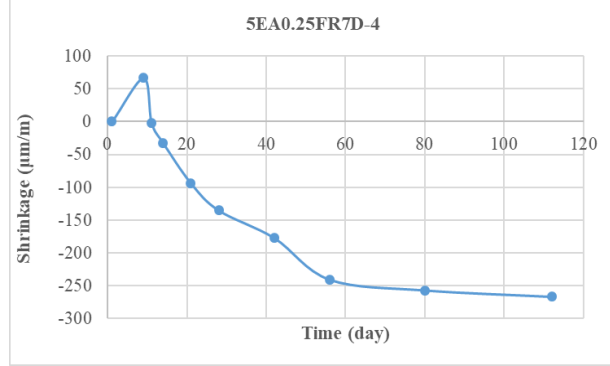
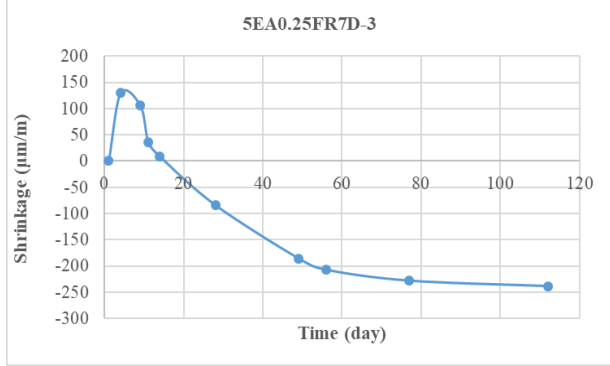
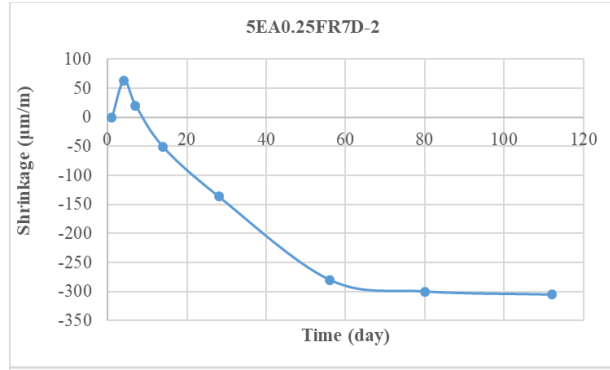
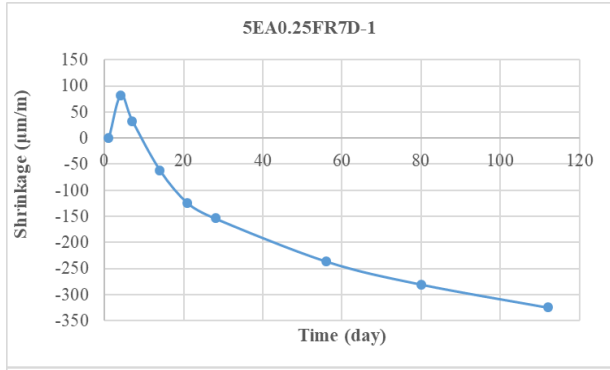
10EA25LWS0.5FR-14D

Figure A-2 – Drying shrinkage used for statistic design for mixtures

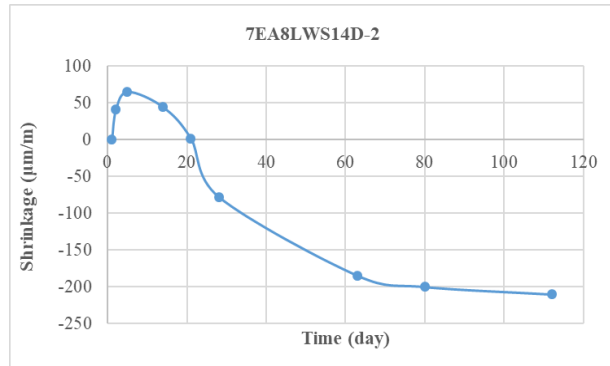
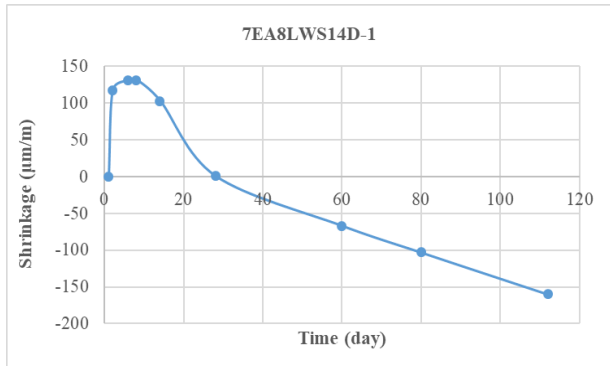


3EA8LWS0.5FR5D-(2 samples)

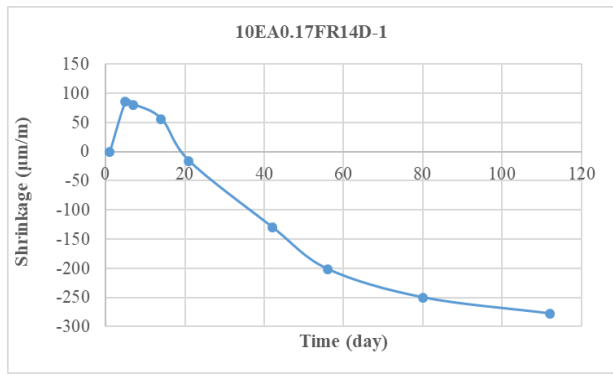




5EA0.25FR7D-(4 samples)



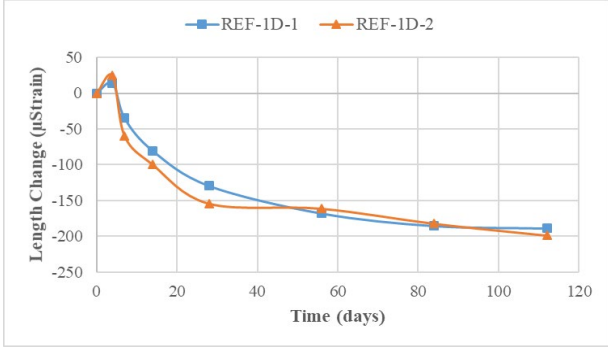
5EA0.25FR7D-(2 samples)



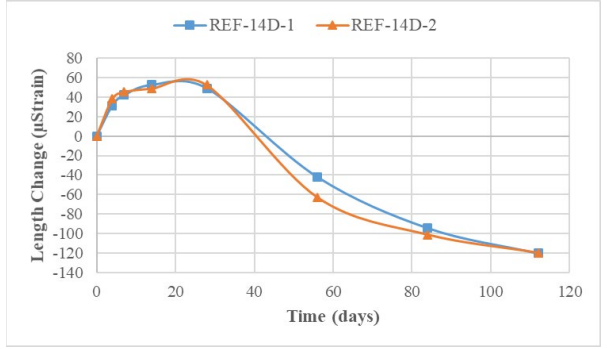
10EA0.17FR14D-(1 sample)

Figure A-3 – Drying shrinkage used for statistic design for mixtures (validation points)

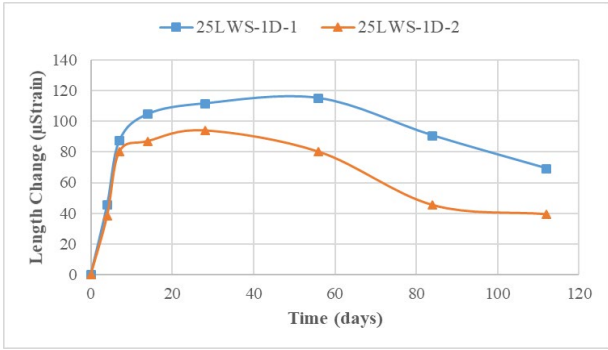




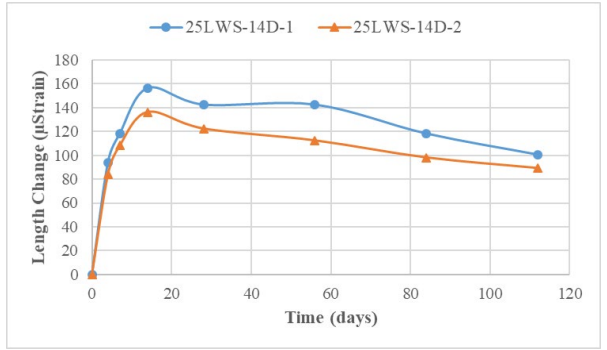
REF-1D



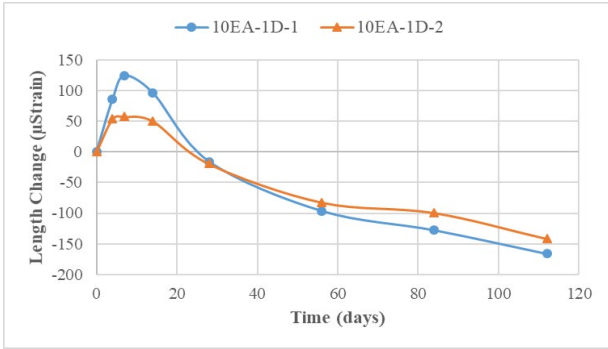
REF-14D



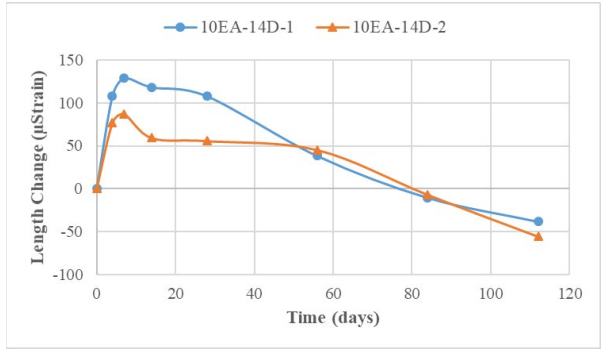
25LWS-1D



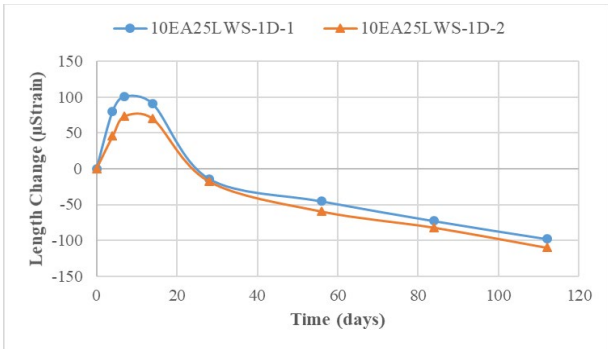
25LWS-14D



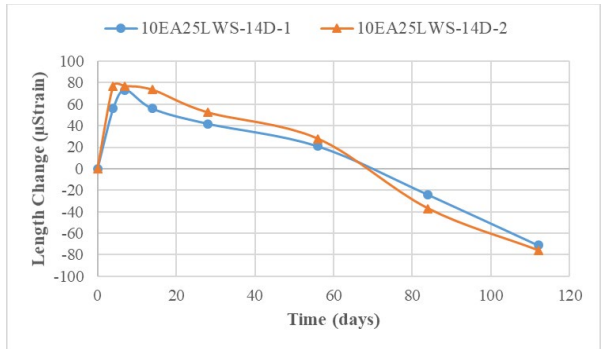
10EA-1D



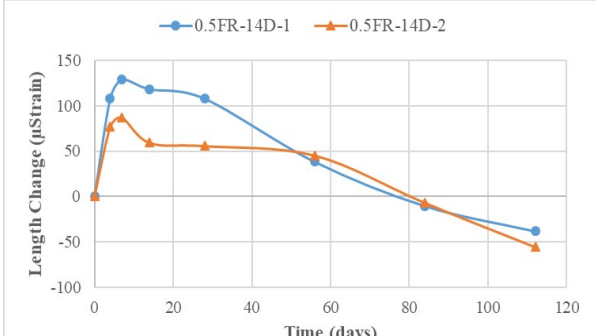
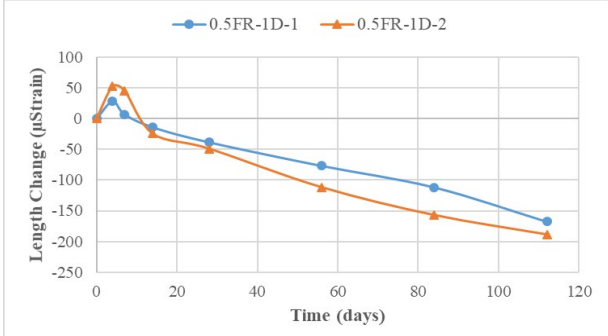
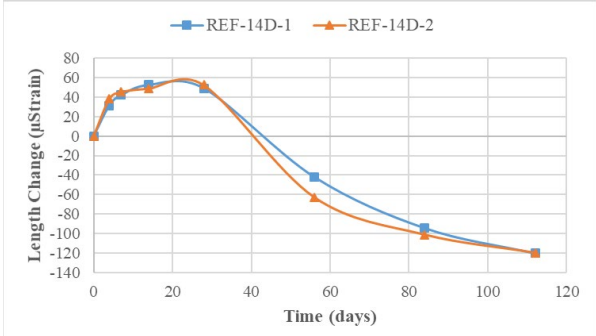
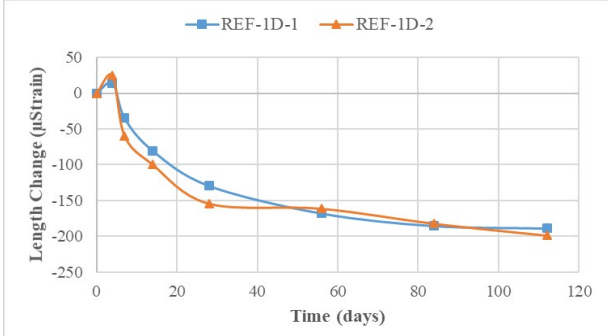
10EA-14D



10EA25LWS-1D

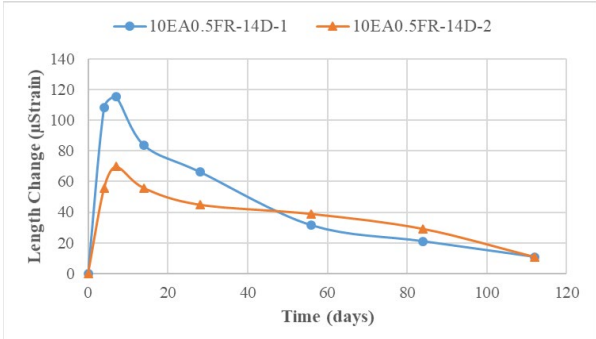
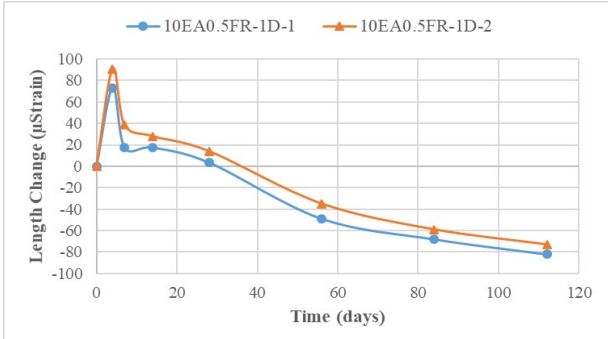


10EA25LWS-14D



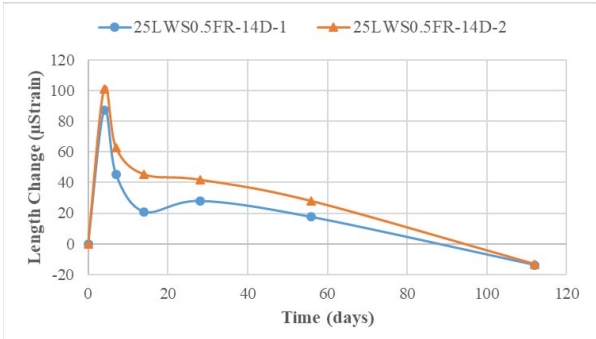
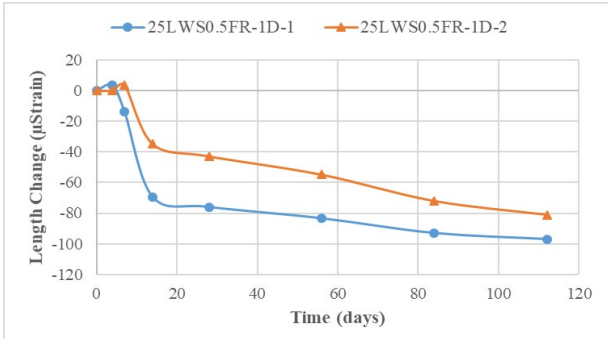
0.5FR-1D

0.5FR-14D



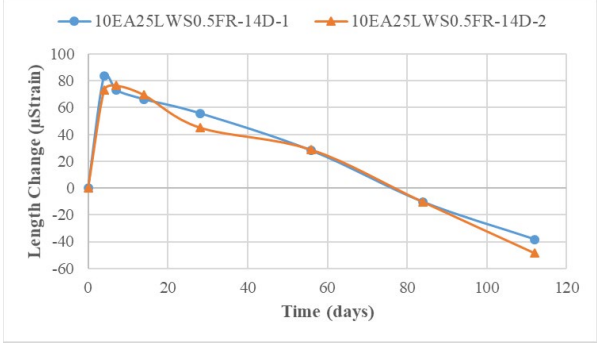
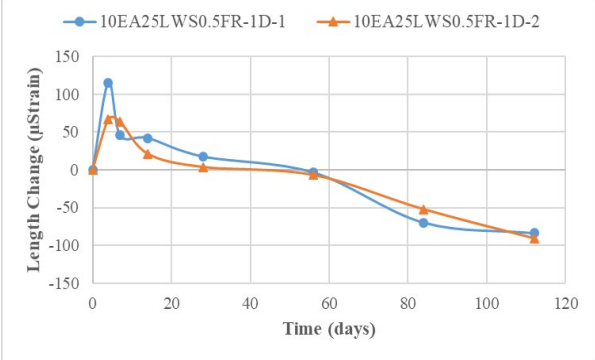
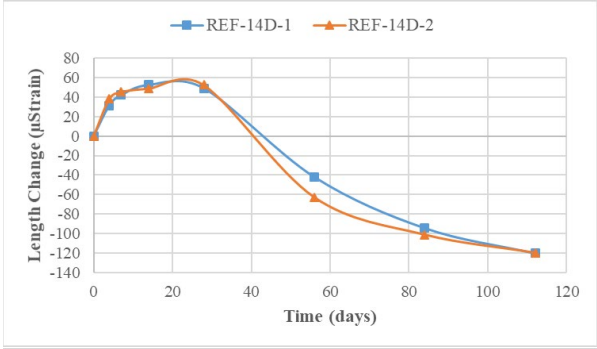
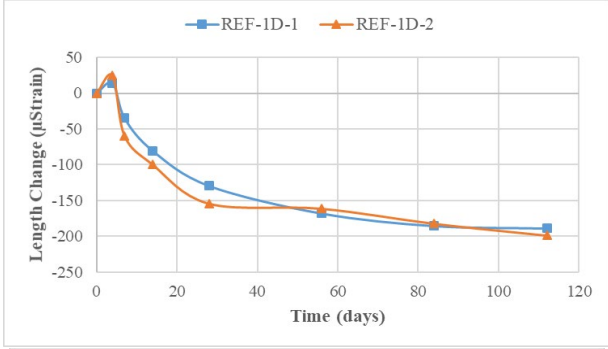
10EA0.5FR-1D

10EA0.5FR-14D



25LWS0.5FR-1D

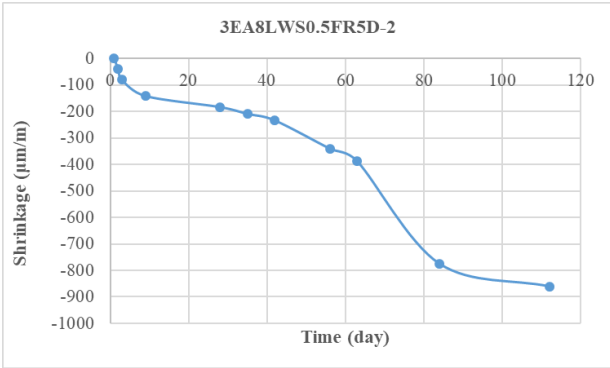
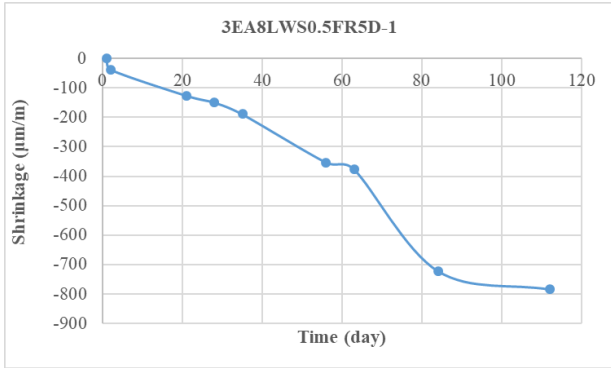
25LWS0.5FR-14D



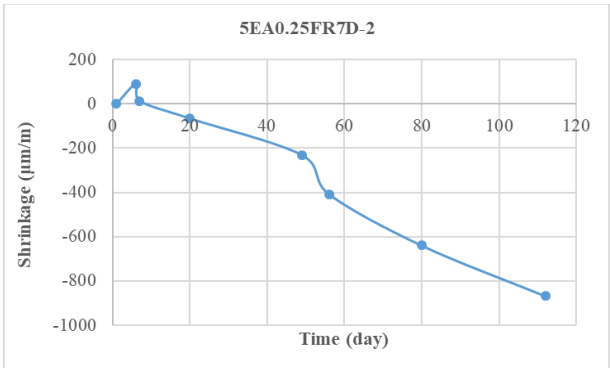
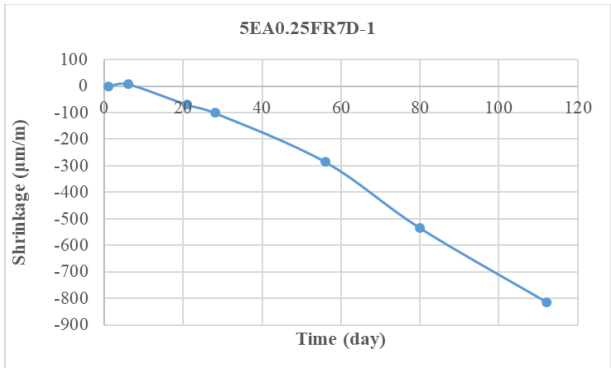
10EA25LWS0.5FR-1D

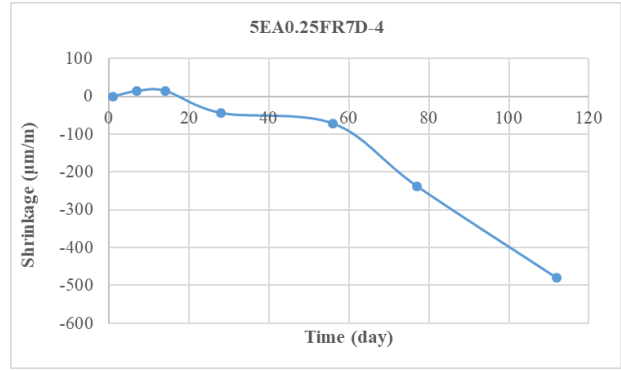
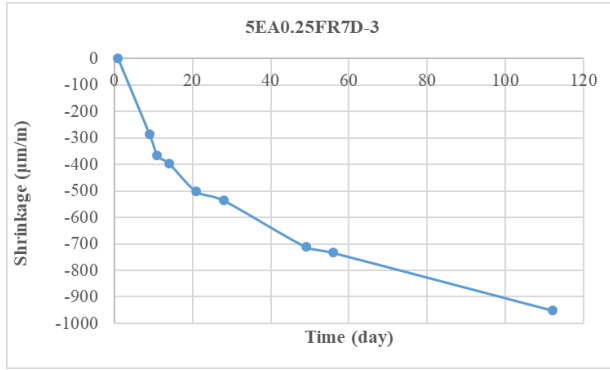
10EA25LWS0.5FR-14D

Figure A-4 – Restrained expansion used for statistic design for mixtures

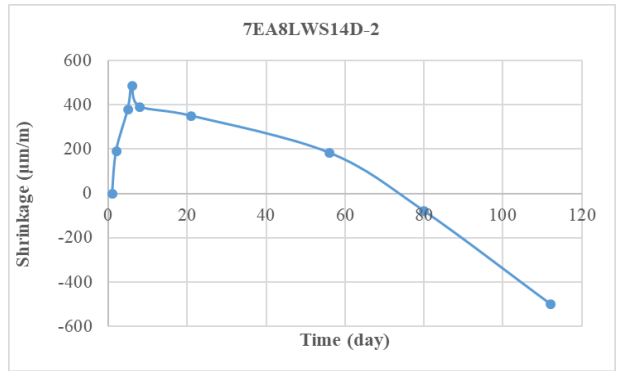
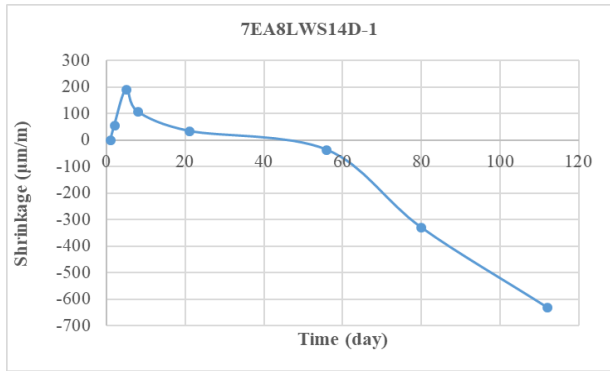


3EA8LWS0.5FR5D-(2 samples)

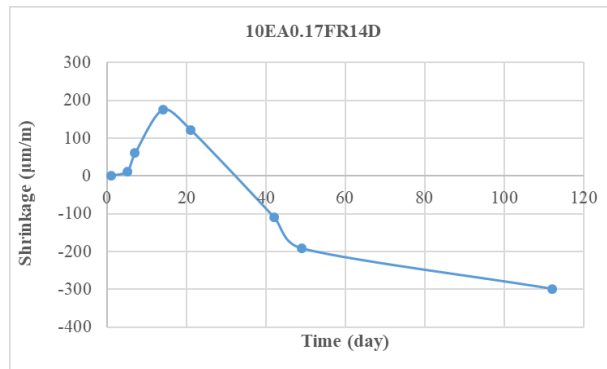




75EA0.25FR7D-(4 samples)



7EA8LWS14D-(2 samples)

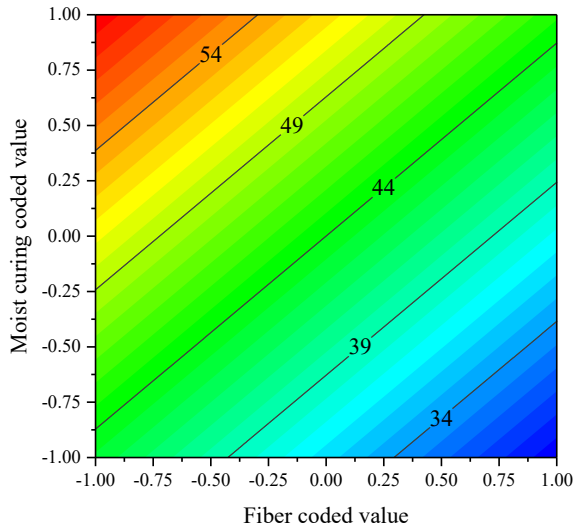


10EA0.17FR14D-(1 sample)

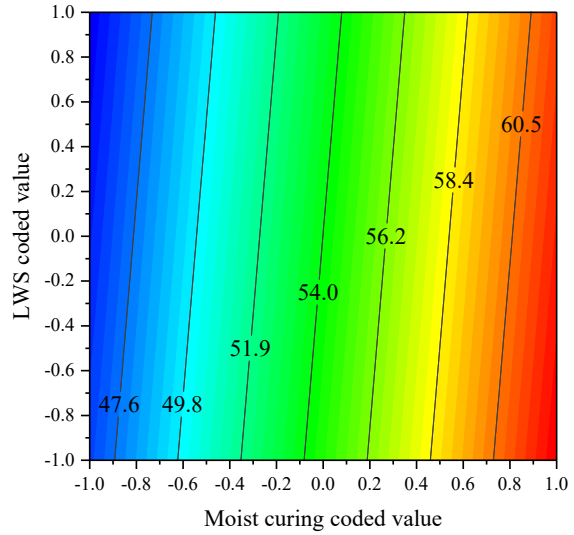
Figure A-5 – Restrained expansion used for statistic design for mixtures (validation points)

## Appendix-B

### Task I-A Optimization for Eco-Bridge-Crete and FR-SWC – contour diagrams from derived statistical models

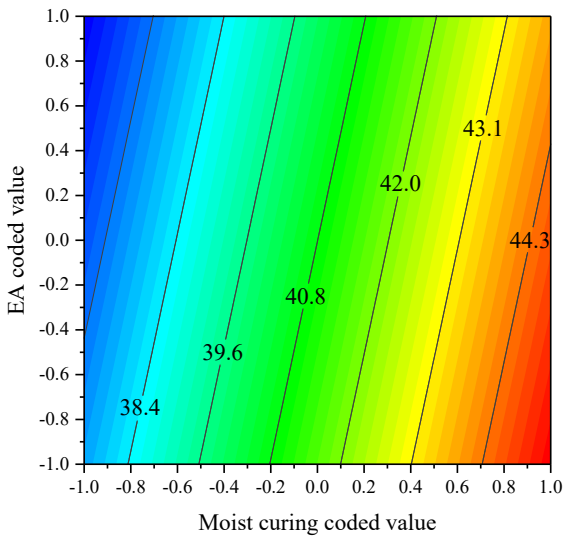


EA, LWS coded values as 0, 0

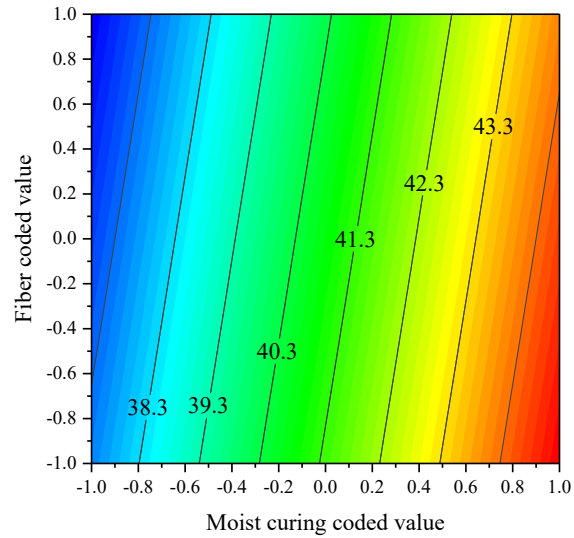


EA, Fiber coded values as -1, -1

### 28-day compressive strength

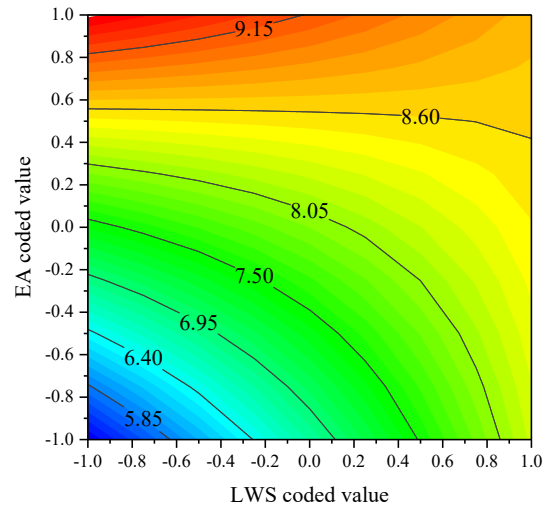
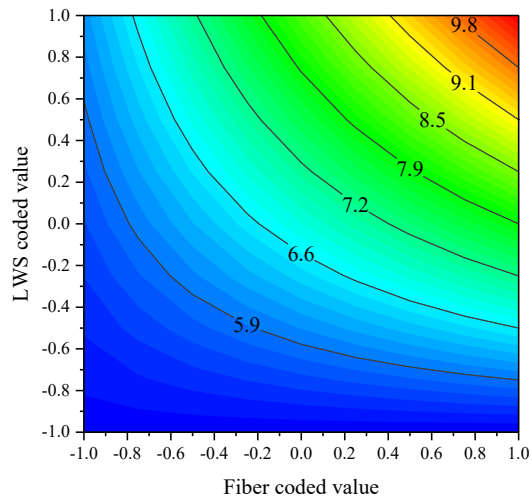
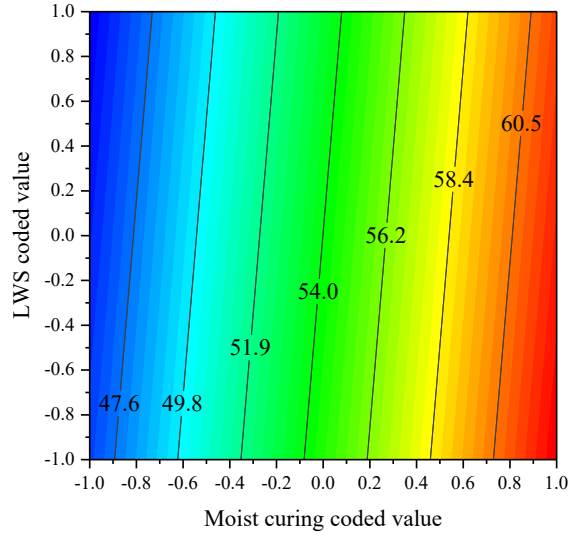
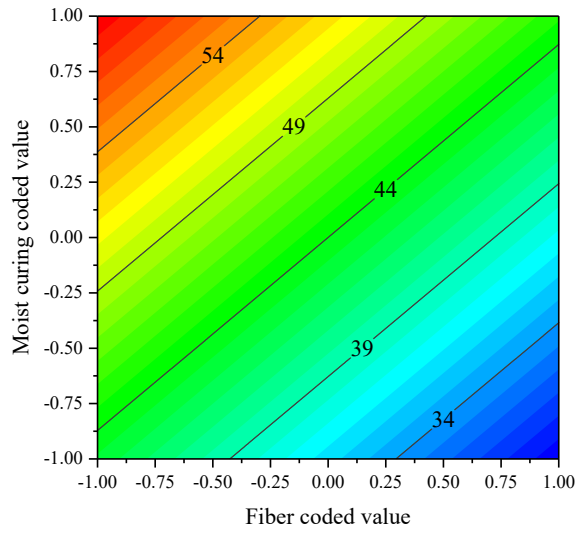


LWS, Fiber coded values as 0, 1



LWS, EA coded values as 0, 1

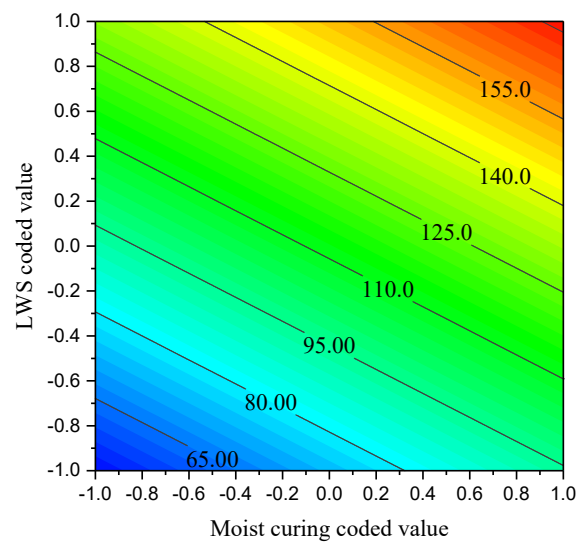
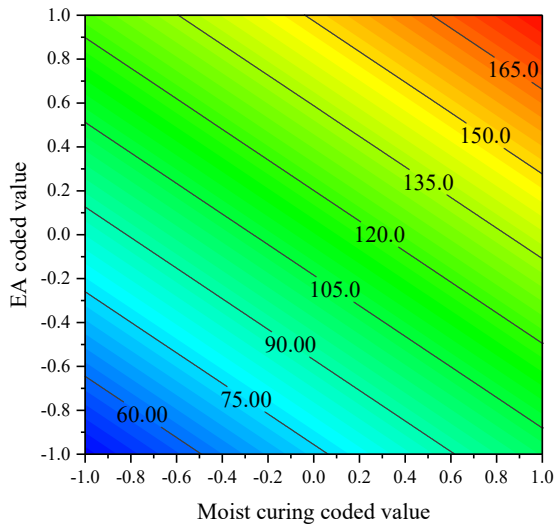
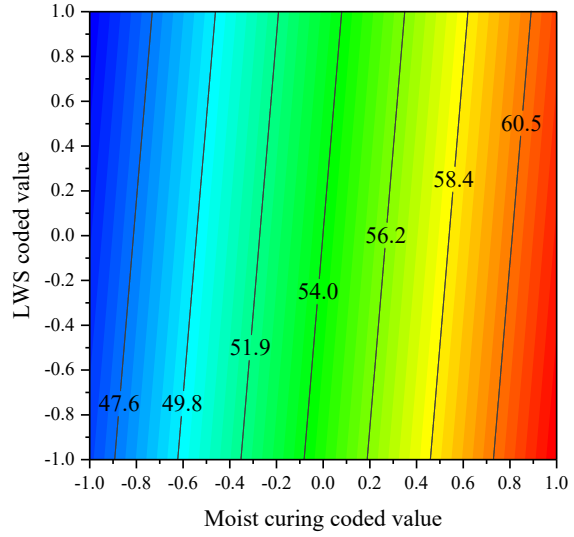
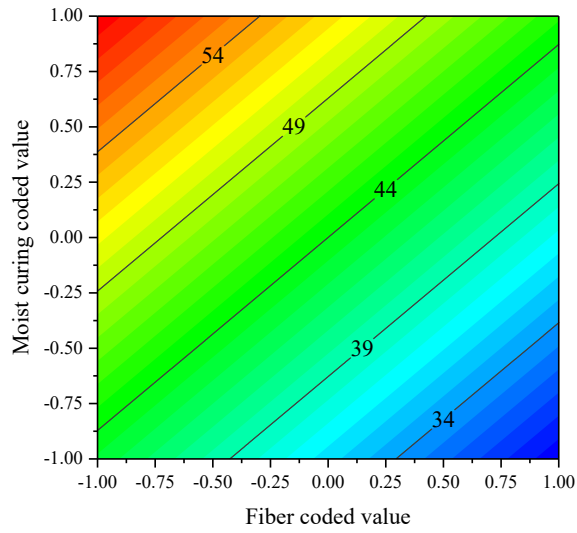
### 56-day compressive strength



EA, Moist curing coded values as -1, -1

Moist curing, Fiber coded values as 0, 0

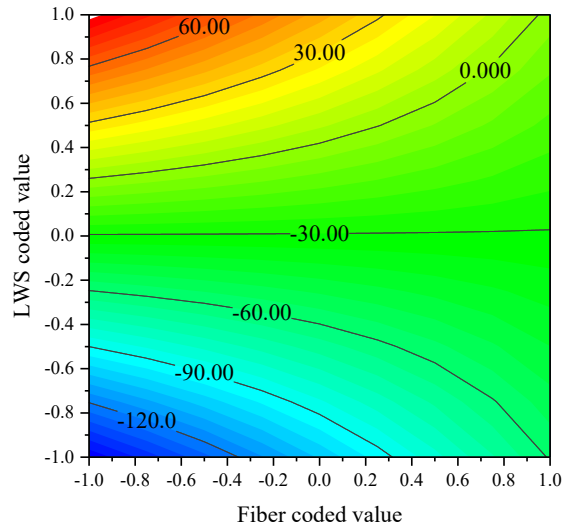
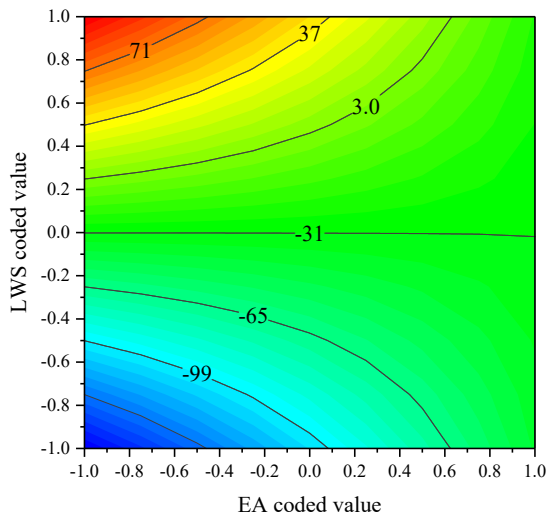
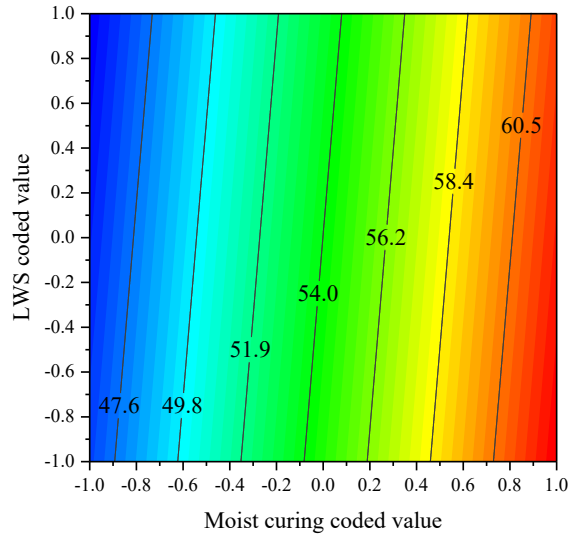
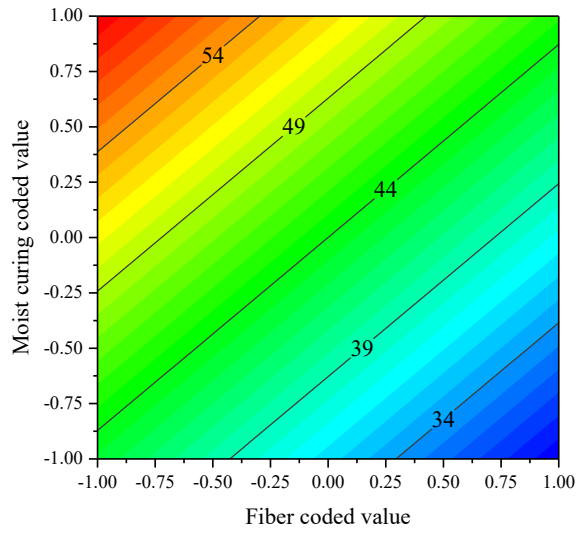
56-day flexural strength



LWS, Fiber coded values as 0, 0

EA, Fiber coded values as 0, 0

7-day drying shrinkage

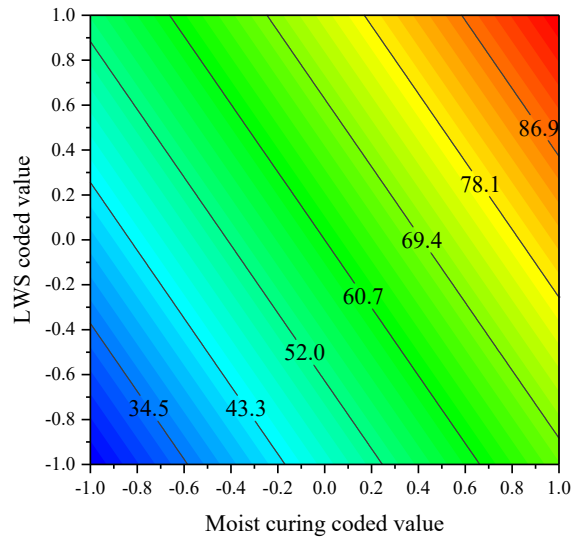
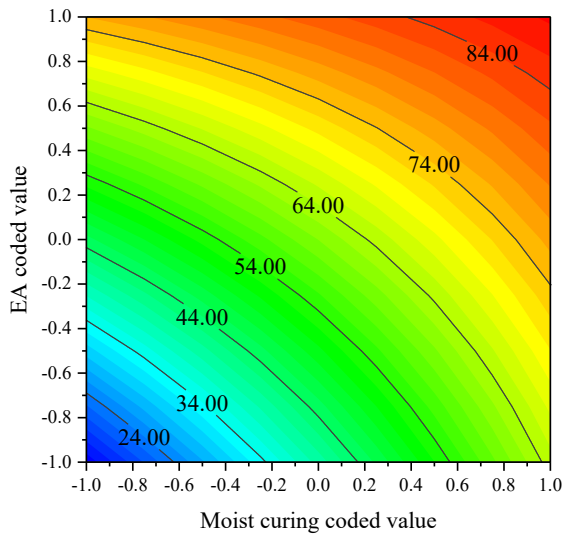
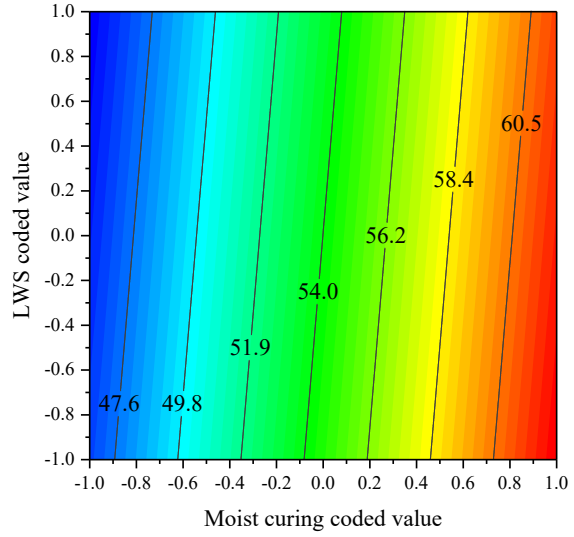
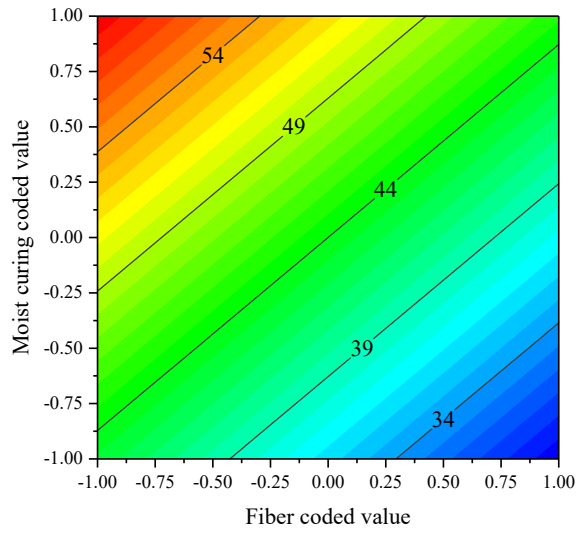


Moist curing, Fiber coded values as 0, 0

EA, Moist curing coded values as 0, 0

56-day drying shrinkage

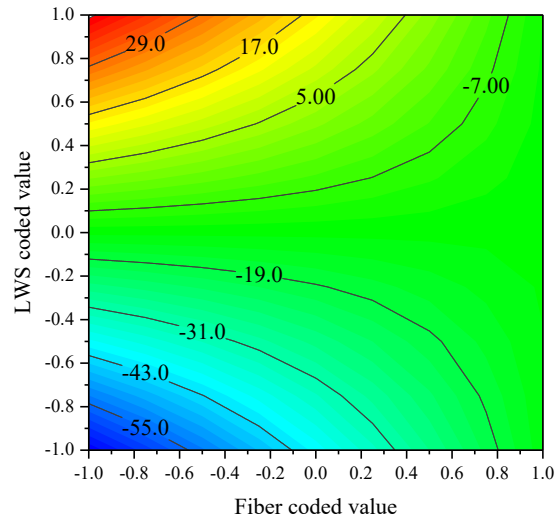
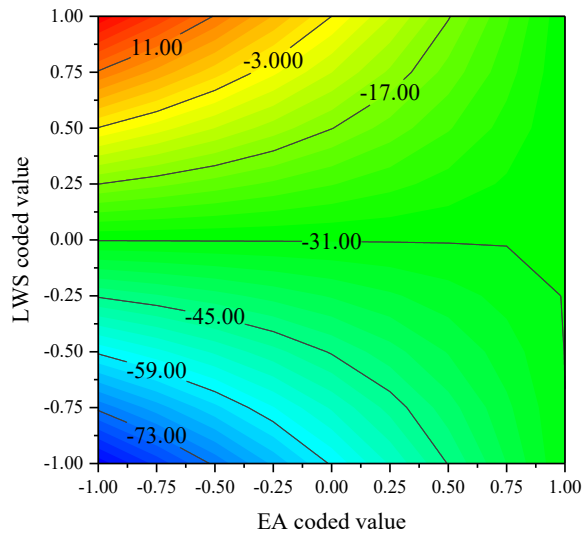
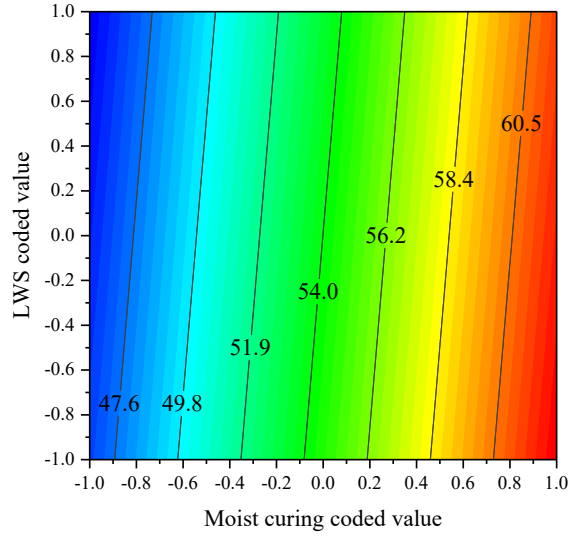
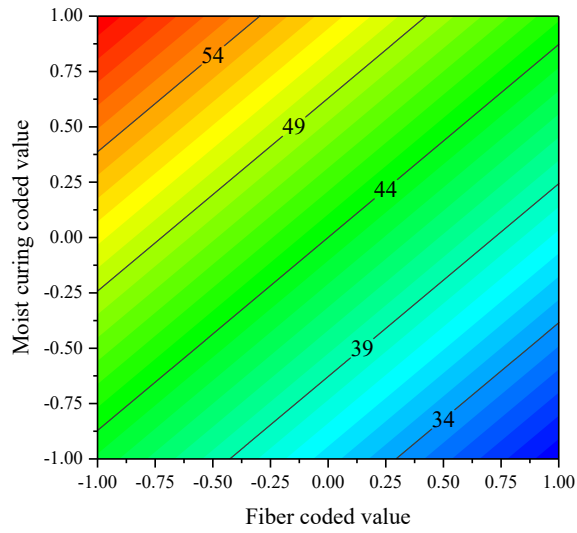




LWS, Fiber coded values as 0, 0

EA, Fiber coded values as 0, -1

7-day restrained expansion



Moist curing, Fiber coded values as 0, 0

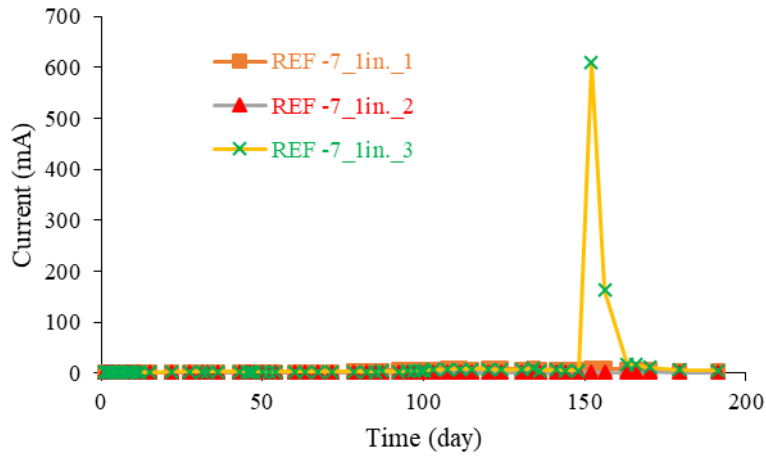
EA, Moist curing coded values as 0, 0

56-day restrained expansion

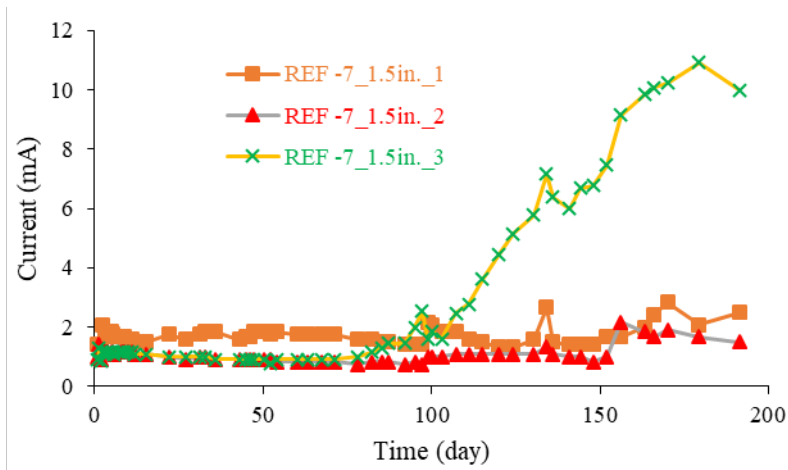
**Figure B-1 – Contour diagrams based on statistic model**

## Appendix-C

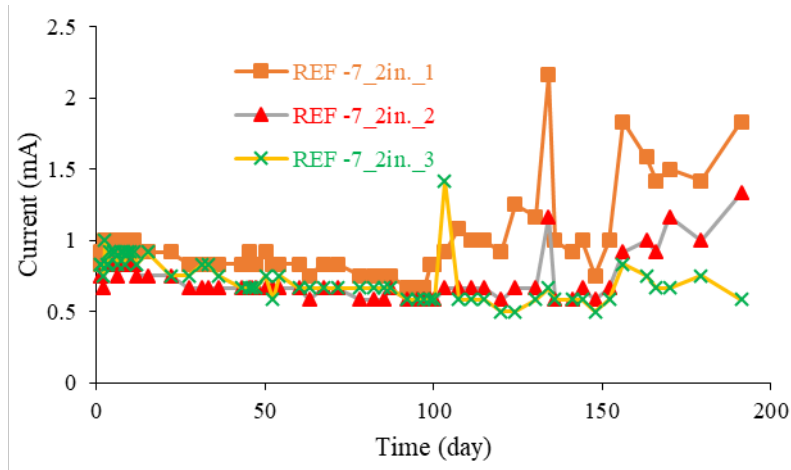
### Task I-C: Corrosion resistance of reinforcing bars in optimized Eco-Bridge-Crete mixtures



(a)

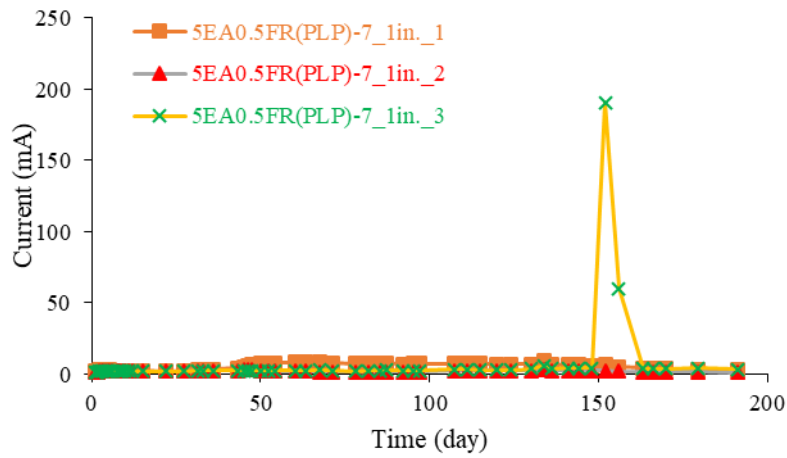


(b)

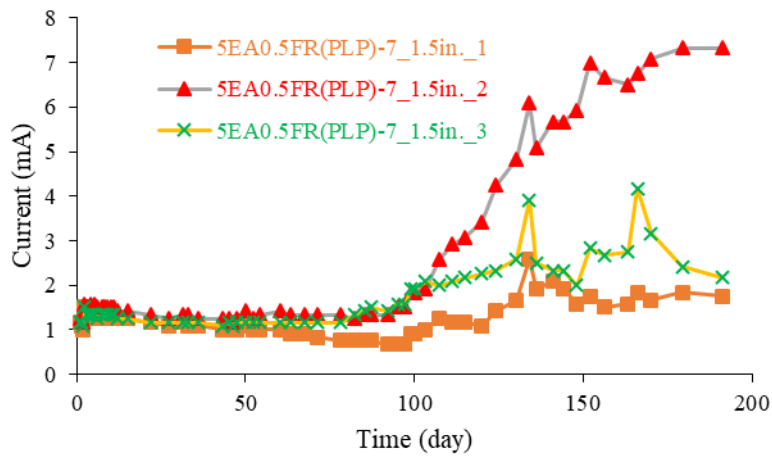


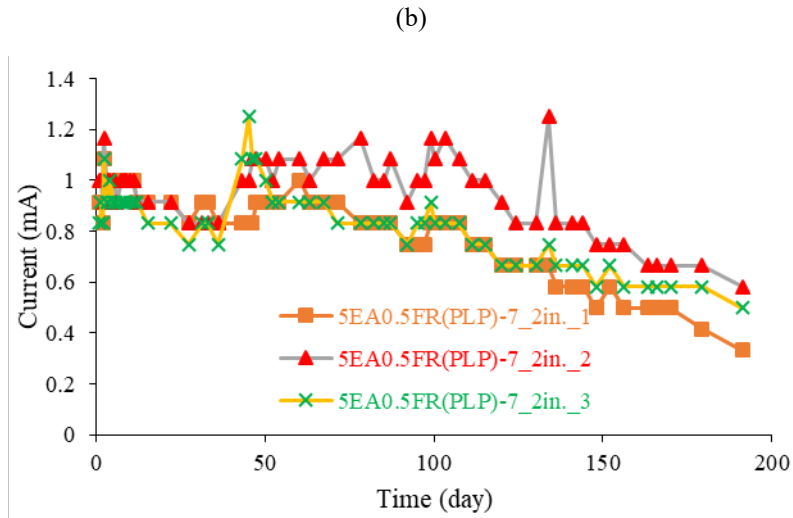
(c)

**Figure C-1 – Current variation with exposure to chlorides for REF-7 mixture with reinforcing bars at cover depths at (a) 1 in. (b) 1.5 in. and (c) 2 in.**



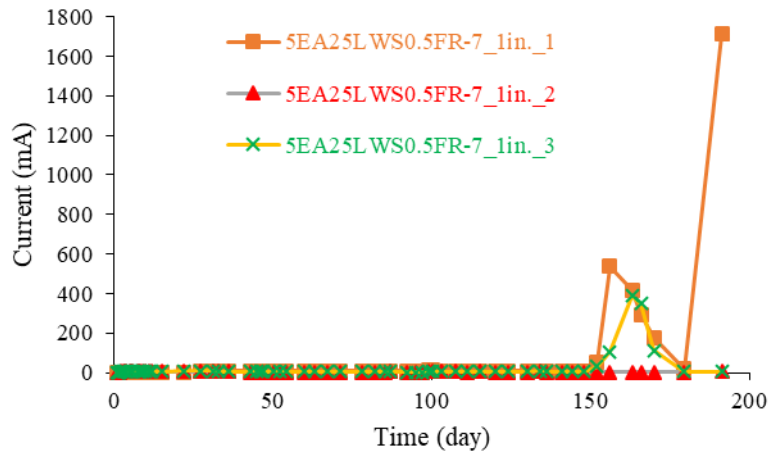
(a)



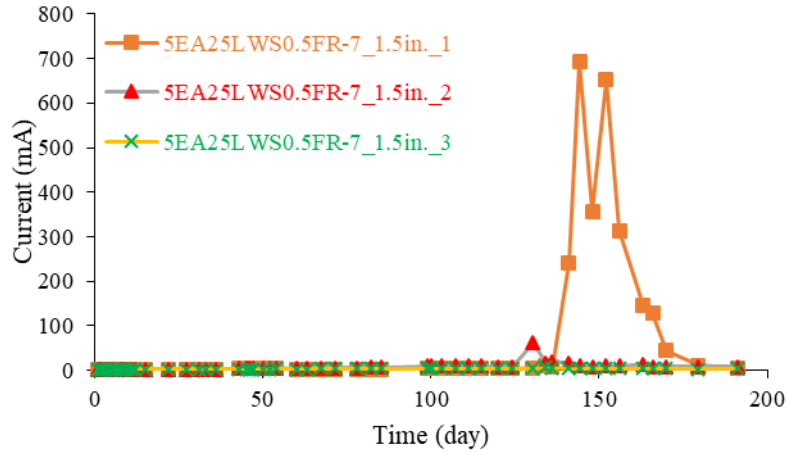


(c)

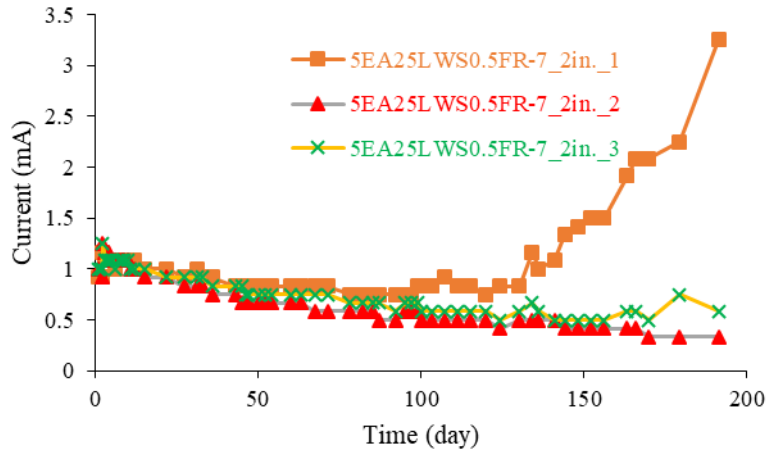
**Figure C-2 – Current variation with exposure to chlorides for 5EA0.5FR(PLP)-7 mixture with reinforcing bars at cover depths at (a) 1 in. (b) 1.5 in. and (c) 2 in.**



(a)

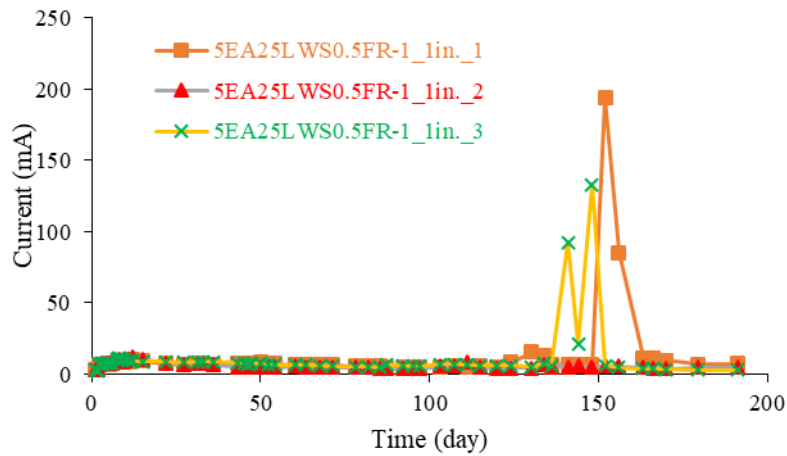


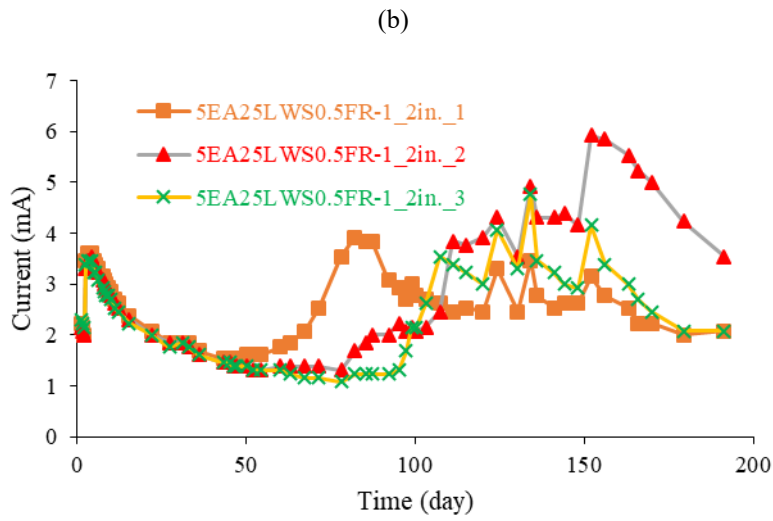
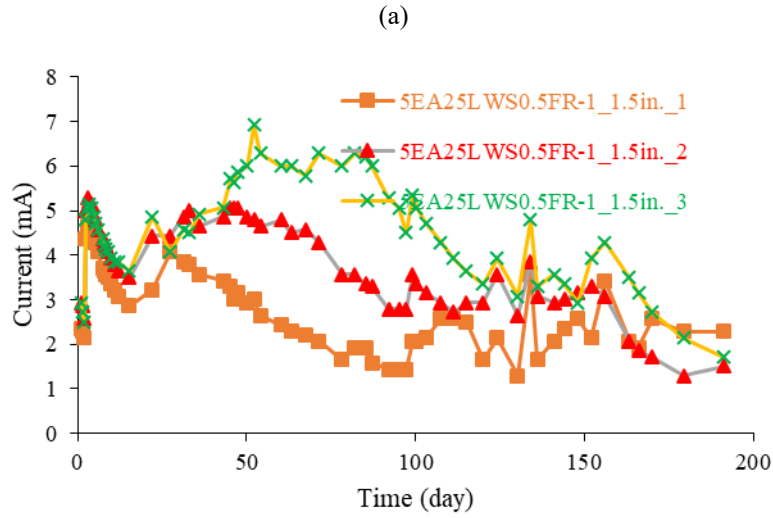
(b)



(c)

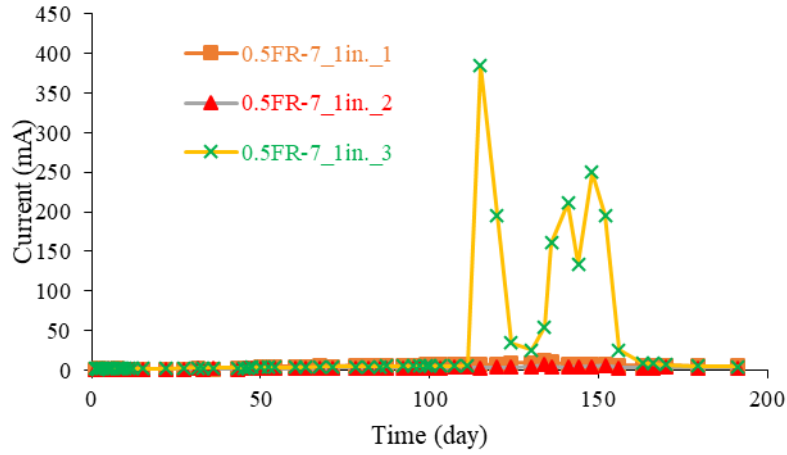
**Figure C-3 – Current variation with exposure to chlorides for 5EA25LWS0.5FR-7 mixture with reinforcing bars at cover depths at (a) 1 in. (b) 1.5 in. and (c) 2 in.**



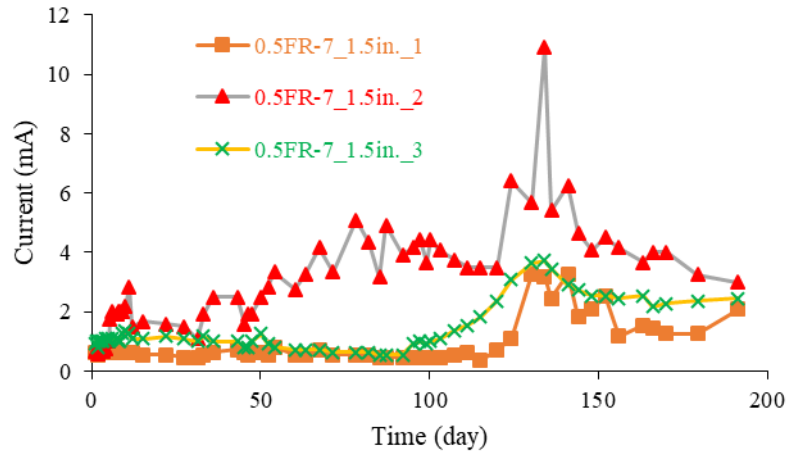


(c)

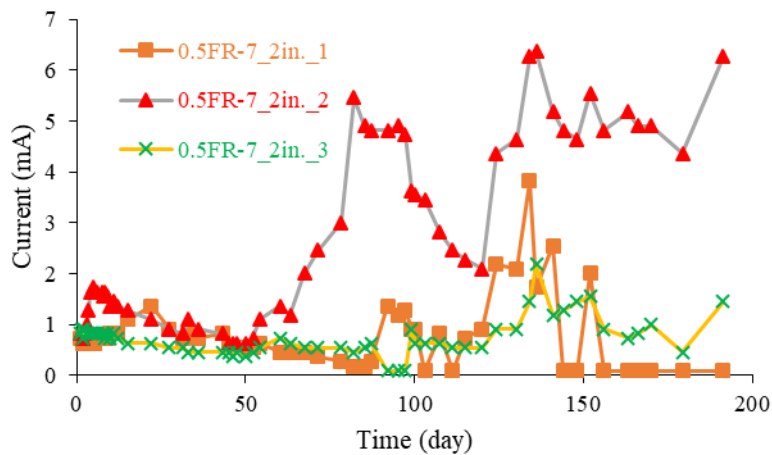
**Figure C-4 – Current variation with exposure to chlorides for 5EA25LWS0.5FR-1 mixture with reinforcing bars at cover depths at (a) 1 in. (b) 1.5 in. and (c) 2 in.**



(a)



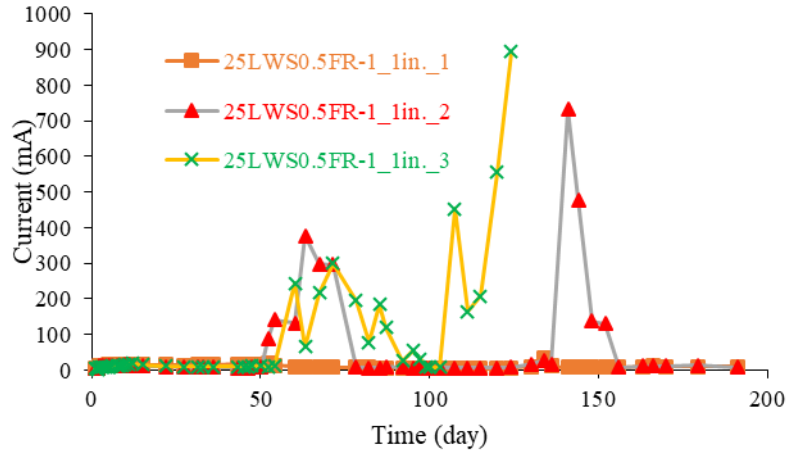
(b)



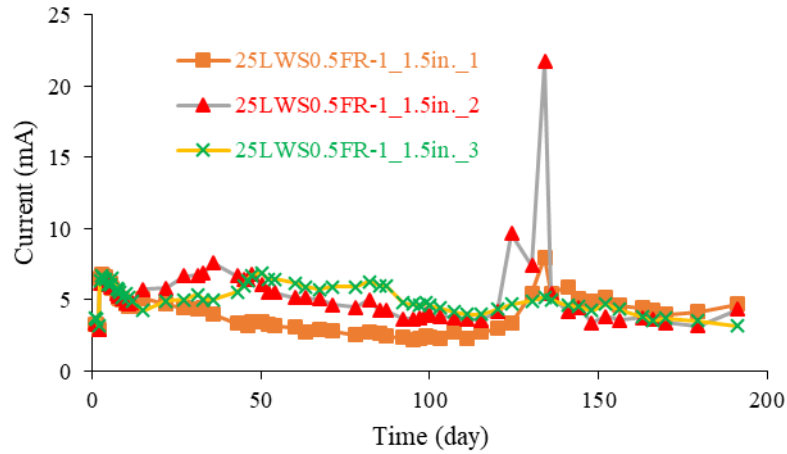
(c)

**Figure C-5 – Current variation with exposure to chlorides for 0.5FR-7 mixture with reinforcing bars at cover depths at (a) 1 in. (b) 1.5 in. and (c) 2 in.**

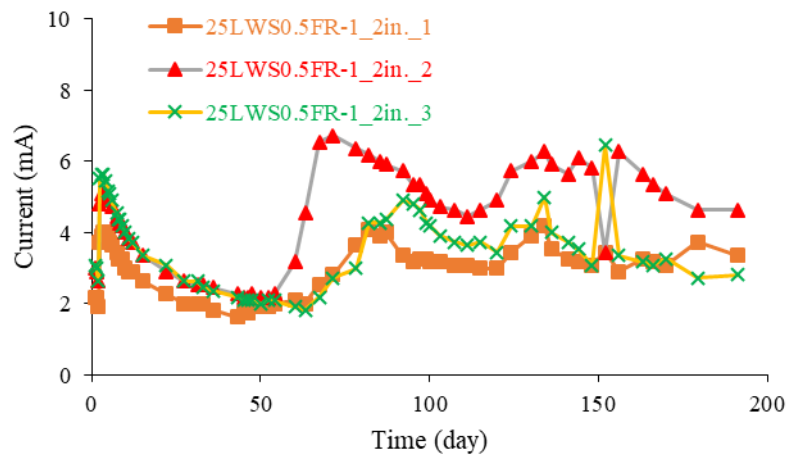




(a)

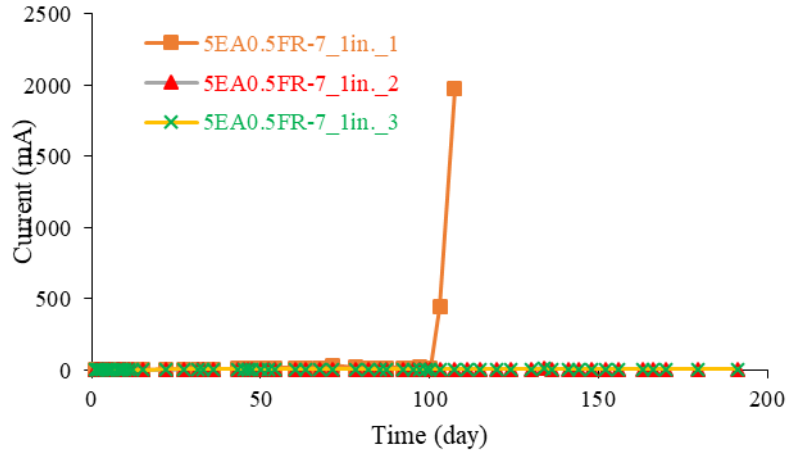


(b)

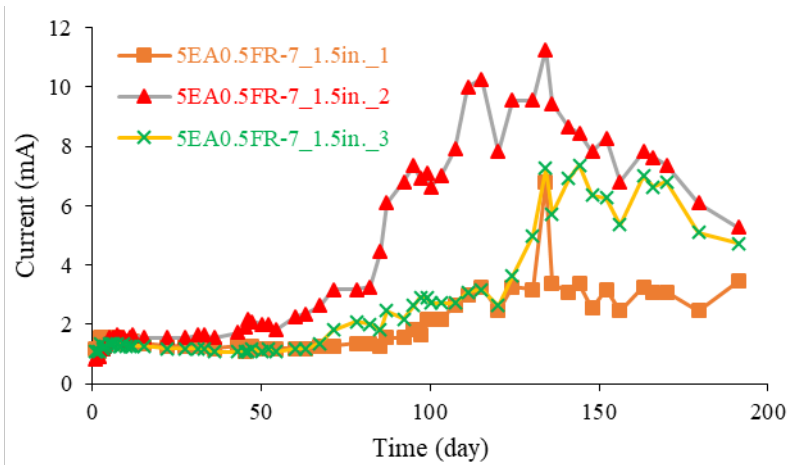


(c)

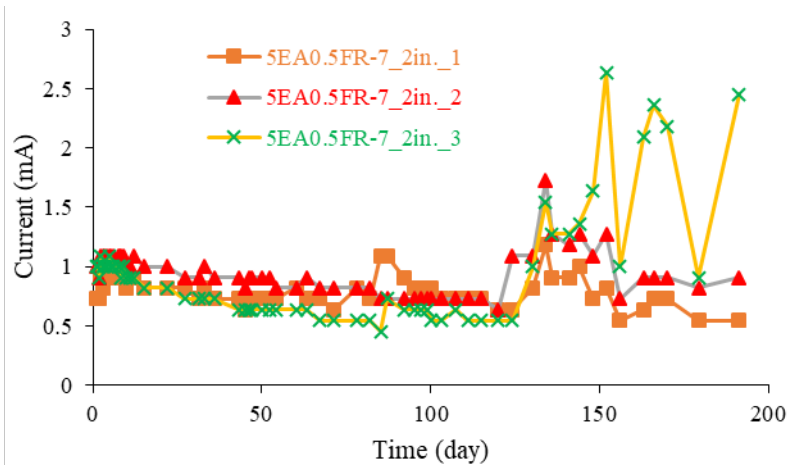
**Figure C-6 – Current variation with exposure to chlorides for 25LWS0.5FR-1 mixture with reinforcing bars at cover depths at (a) 1 in. (b) 1.5 in. and (c) 2 in.**



(a)

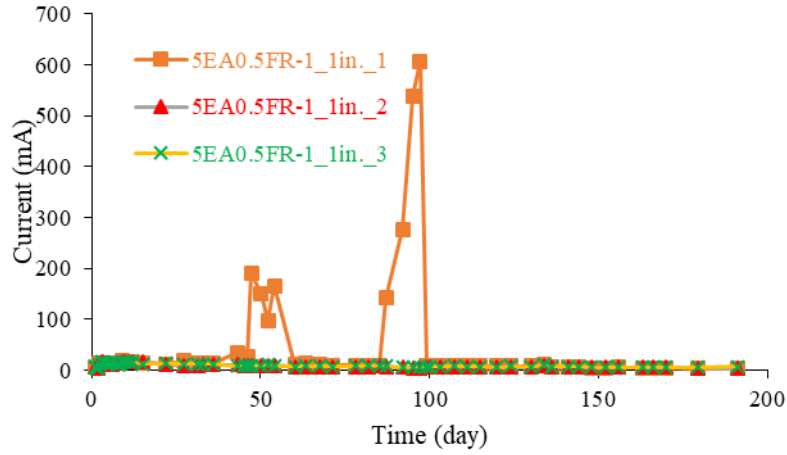


(b)

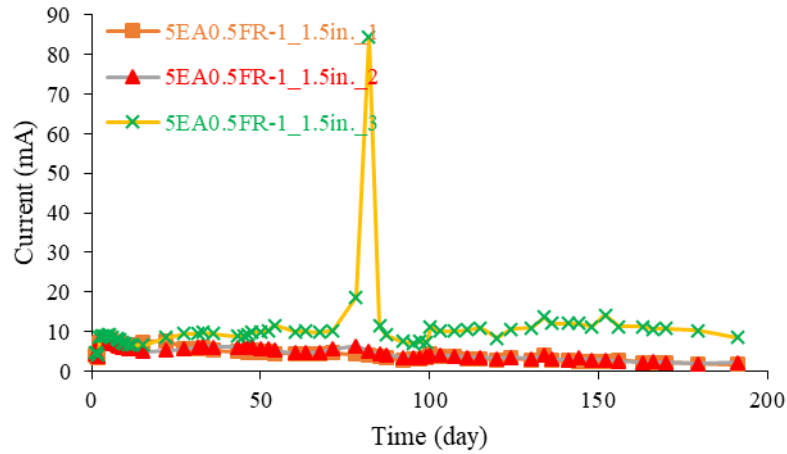


(c)

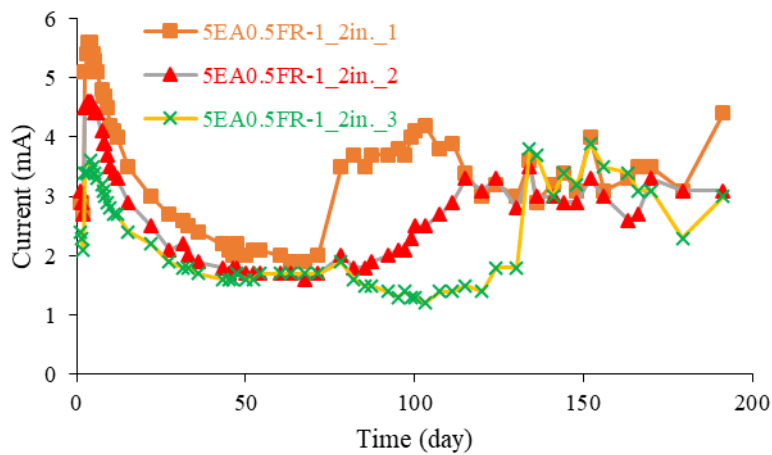
**Figure C-7 – Current variation with exposure to chlorides for 5EA0.5FR-7 mixture with reinforcing bars at cover depths at (a) 1 in. (b) 1.5 in. and (c) 2 in.**



(a)



(b)



(c)

**Figure C-8 – Current variation with exposure to chlorides for 5EA0.5FR-1 mixture with reinforcing bars at cover depths at (a) 1 in. (b) 1.5 in. and (c) 2 in.**